ENERGY AND EXERGY ANALYSIS OF GAX AND GAX HYBRID ABSORPTION REFRIGERATION SYSTEMS

By

MANOJ DIXIT

2K10/THR/05

Mechanical Engineering Department

Submitted

In partial fulfillment of the requirement for the award of the Degree of

Master of Technology
In
Thermal Engineering

To The

Department of Mechanical Engineering,

Delhi Technological University, Delhi

June 2012

CERTIFICATE

I hereby declare that the work which is being presented in the thesis entitled ***"Energy and exergy analysis of GAX and GAX hybrid absorptions refrigeration systems"*** in partial fulfillment for the award of degree of **Master of Technology** with specialization in **"Thermal Engineering"** submitted to **Delhi Technological University**, is authentic record of my own work carried out under the supervision of **Dr. Akhilesh Arora,** Department of Mechanical Engineering, Delhi Technological University. I have not submitted the matter in this dissertation for the award of any other Degree or Diploma or any other purpose whatever.

Date: July 02, 2012

Manoj Dixit

2K10/THR/05

This is to certify that above statement made by the candidate is true to the best of my knowledge and belief.

Dr. Akhilesh Arora

Asstt. Professor

Department of Mechanical Engineering

Delhi Technological University, Delhi

ACKNOWLEDGEMENT

It is a matter of distinct pleasure for me to express deep sense of gratitude and indebtedness to my learned supervisor **Dr. Akhilesh Arora**, Assistant Professor in the Department of Mechanical Engineering, Delhi Technological University, Delhi, for his invaluable expert guidance and patient review. His continuous inspiration has made me complete this major dissertation.

I would also like to extend my sincere thanks to all faculty members and staff of library for their moral support and encouragement.

I am thankful to my friends and classmates for their unconditional support and motivation during the project.

Manoj Dixit

2k10/THR/05

ABSTRACT

In this work GAX and GAX hybrid aqua-ammonia absorption refrigeration cycles are studied and compared from the viewpoint of first and second laws of thermodynamics. The effect of generator temperature on COP, heat transfer rates in various components, exergetic efficiency and exergy destruction rates are evaluated. The effects of degassing range and approach temperature on COP and exergetic efficiency are studied. Comparison of hybrid and conventional GAX cycle is done and it is found that the GAX hybrid cycle has an average of 27% higher value of COP than the conventional GAX cycle. Exergy analysis is performed in order to calculate the total exergy destruction rate and to calculate the contribution of different components to the total exergy destruction. The generator temperature has more effect on exergetic efficiency than on COP for both GAX and hybrid cycles. The maximum exergy destruction occurs in desorber and absorber (as a unit component) of both the cycles while the lowest contribution belongs to the expansion valve 2. The required COP can be obtained in lower degassing range in the GAX hybrid cycle as compared to the simple GAX cycle. Therefore, GAX hybrid can operate successfully utilizing low temperature energy sources. The exergetic efficiency, like COP, attains a maximum value for a particular degassing range. Thus, increase in degassing range, always does not cause increase in COP and second law efficiency. The study shows that GAX hybrid systems are more promising than simple GAX systems.

TABLE OF CONTENTS

LIST OF FIGURES

LIST OF TABLES

List of Symbols

COP	Coefficient of Performance
D_x	Degassing range
$\dot{E}_d$	Exergy destruction rate (kW)
EV	Expansion valve
GAX	Generator Absorber Heat Exchanger
GAX A	Generator Absorber Heat Exchanger Absorber
GAX D	Generator Absorber Heat Exchanger Desorber
h	Specific enthalpy (kJ/kg)
$\dot{m}$	Mass flow rate (kg/s)
P	Pressure (kPa)
$\dot{Q}$	Heat transfer rate (kW)
RHX	Condensate pre-cooler
s	Entropy (kJ/kg. K)

T	Temperature (ºC or K)
v	Specific volume (m^3/kg)
$\dot{w}$	Work (kW)
x	Concentration (kg of absorbent/kg of solution)
Y	Exergy destruction ratio

Greek Symbols

Ƞ	Efficiency
∈	Effectiveness
$\boldsymbol{\psi}$	Exergy flow (kJ/kg)

Subscripts

0	Dead state
1, 2, 3…	State points in the system
a, abs	Absorber
abs & des	Absorber and desorber (as a unit)
av	Available
avg	Average

c, cond	Condenser
comp	Compressor
des	Desorber
e, evap	Evaporator
exv	Expansion valve
g, gen	Generator
gax	Generator absorber heat exchanger
i	Inlet
max	Maximum
o	Outlet
p, pump	Pump
r	Refrigerant
rq	Required
rect	Rectifier
rev	Reversible
sp	Specific pump
th	Thermal
u	Useful

CHAPTER -1
INTRODUCTION

Most of industrial process uses a lot of thermal energy by burning fossil fuel to produce steam or heat for the purpose. After the processes, heat is rejected to the surrounding as waste. This waste heat can be converted to useful refrigeration by using a heat operated refrigeration system, such as an absorption refrigeration cycle. In this way, electricity purchased from utility companies for conventional vapor compression refrigerators can be reduced. The use of heat operated refrigeration systems helps in reducing problem related global warming due to CO_2 emission from the combustion of fossil fuels in utility power plants.

Another difference between absorption systems and conventional vapor compression systems is the working fluid used. Most vapor compression systems commonly use chlorofluorocarbon refrigerants (CFCs), because of their favourable thermo-physical properties. It is through the restricted use of CFCs, due to depletion of the ozone layer that will make absorption systems more prominent. However, although absorption systems seem to provide many advantages, vapor compression systems still dominate all market sectors. In order to promote the use of absorption systems, further development is required to improve their performance and reduce cost.

In recent years, absorption refrigeration systems have been paid more attention because of environmental and energy consumption concerns of conventional vapour compression systems. As these systems can utilize solar, geothermal and biomass energy sources as well as waste heat from thermal systems [1], they challenge the vapor compression cycles in spite of their relatively lower COP values. In addition, working fluids in absorption refrigeration systems are ozone layer friendly and have no impact on the global warming [2].

Though cooling by absorption was known for more than hundred years, it was a little investigated after its invention. The early development of an absorption cycle dates back to the 1700's. It was known that ice could be produced by an evaporation of pure water from a vessel contained within an evacuated container in the presence of sulfuric acid [2, 16]. In 1810, ice could be made from water in a vessel, which was connected to another vessel containing sulfuric acid. As the acid absorbed water vapor, causing a reduction of temperature, layers of ice were formed on the water surface. The major problems of this system were corrosion and leakage of air into the vacuum vessel.

In 1859, Ferdinand Carre introduced a novel machine using water/ammonia as the working fluid. This machine was patented in US in 1860. Machines based on this patent were used to make ice and store food. It was used as a basic design in the early age of refrigeration development. In the 1950's, a system using lithium bromide/water as the working fluid was introduced for industrial applications. A few years later, a double-effect absorption system was introduced and has been used as an industrial standard

for a high performance heat-operated refrigeration cycle. In sixties, absorption technology reappeared with application in air conditioning. These systems used Ammonia-water and Lithium-Bromide as working fluid [3].

The possibility of recovering internal heat in the basic absorption cycle was first described by Altenkirch [4]. Further studies in this field led to the development of a new generation of cycles including the GAX cycle. The GAX cycle is a system that provides the highest coefficient of performance (COP) of any single effect absorption cycle [5]. GAX stands for generator/absorber heat exchanger. It is also called DAHX which stands for desorber/absorber heat exchanger. The GAX cycle is a very elegant way of achieving higher effect performance with a cycle configuration that essentially appears to be a single-stage configuration. The system consists of two single-effect cycles working in a parallel manner. The concept of GAX is to simplify this two stage- double-effect absorption cycle but still produce the same performance. Thus GAX allows the recovery of heat from the absorber and supply it to the generator, thereby, reducing the required heat in the generator from the external source. When a compressor is introduced at the absorber inlet of the GAX cycle, it is referred to as GAX HYBRID cycle. The use of compressor at the absorber inlet can produce relatively higher pressure and temperature. A low value of the absorber temperature in the absorption cycle is a disadvantage as the cooling of the absorber will require a cooling medium other than ambient air. To overcome this problem an ejector or a compressor can be used between evaporator and absorber. The use of ejector does not require any electrical energy input, but compressor requires external work input.

The greatest advantage of the absorption system is found in a decrease of the electrical energy consumption, to use waste heat, to increase the efficiency of the cogeneration system by producing simultaneously electricity, heating and cooling, environmental protection and economic benefits to users. At present the cost of the absorption system is double the cost of the mechanical vapour compression system of the same capacity [12]. Moreover, the operation costs are not low enough to compensate the difference in the initial investment. So, if we want to have a greater commercial success, it is necessary to develop units with smaller equipment cost.

SCOPE

In this work detailed and comprehensive energy and exergy analysis of ammonia water GAX and GAX hybrid absorption refrigeration cycles have been carried out. GAX and GAX hybrid absorption refrigeration cycles are studied from the point of view of both the first and second laws of thermodynamics. In each component of both the cycle thermal load and exergy destruction are calculated from thermodynamic properties of the working fluid at various operating conditions using the Engineering Equation Solver (EES) software. The effect of generator temperature, evaporator temperature, condenser temperature, approach temperature, degassing range on the first and second law performances of both the cycles are carried out using parametric study.

CHAPTER – 2
LITERATURE REVIEW

2.1. Summarization of various authors work

In this chapter a comprehensive literature survey has been done on GAX and GAX hybrid absorption systems. Work of various authors has been presented as follows.

Pongsid et al. [10] provided a literature review on absorption refrigeration technology. Various types of absorption refrigeration systems have been studied. Research on working fluids has been carried out and various methods of improvement of absorption processes are discussed. They further compared various absorption cycles. They found that currently double-effect absorption systems using lithium bromide/water seem to be the only high performance system which is available commercially. Current research and development efforts on multi-effect cycles show considerable promise for future application. A combined ejector-absorption system described by aphornratana [11] is another possible option. This system can provide COP as high as a double-effect system with little increase in system complexity. They further analyzed that diffusion absorption refrigeration system is the only true heat-operated refrigeration cycle which has been widely used as a domestic refrigerator. However, it is only available with small cooling capacity and its COP is low (0.1 to 0.2).

Kang et al. [7] developed four different advanced hybrid GAX cycles using ammonia-water by combining absorption and vapour compression cycles. Four different cycles are: Type A (performance improvement), Type B (Low temperature applications), Type C (reduction of desorption temperature) and type D (Hot water temperature applications). In Type A and Type B a compressor is placed between the evaporator and the absorber while in Type C and Type D compressor is placed between the desorber and the condenser. The COP of Type A can be 24% higher than the standard GAX cycle. In Type B, the evaporation temperature of as low as -80ºC can be achieved with COP of 0.58 – 0.3. The maximum desorption temperature in Type C can be reduced down to 168ºC and therefore the problem of corrosion, which becomes severe at higher temperature of 200ºC, can be completely removed. The COP of HGAX – Type C increases as high as1.19, which is 19% higher than the COP of standard GAX, by controlling the desorber pressure. In Type D, the hot water temperature of as high as 106ºC could be obtained and thus HGAX (Type D) can be applied for space heating and floor heating applications.

Yari et al. [8] studied the GAX and GAX hybrid absorption refrigeration cycles from the viewpoint of both first and second law of thermodynamics. Energy and exergy analysis were performed using EES software. Thermal load, inlet and outlet exergy and exergy destructions were calculated. From the data obtained at various operating conditions, COP, total exergy destruction and exergetic efficiency of both the cycles were calculated. To investigate the effects of generator temperature, evaporator temperature, condenser temperature, absorber pressure on the first and second law performances, parametric studies were conducted. They found that the COP and exergetic efficiencies

of GAX and GAX hybrid cycles were maximum at a particular generator temperature. The value of generator temperature corresponding to maximum exergetic efficiency is slightly higher for GAX hybrid than for the simple GAX cycle. Second law efficiencies of both the cycles are greatly affected by the generator temperature while the COP of both the cycles is less affected by the generator temperature. They further observed an increase of about 75% in the second law efficiency of the GAX cycle as the generator temperature are varied from 400K to 440K, whereas, the corresponding increase in the COP of GAX cycle was around 5%. From the exergy destruction point of view, in the cycles, the desorber and absorber as a unit component has the highest contribution. The lowest contribution belongs to second expansion valve. In this work the range of evaporator temperature is limited to 5ºC to 9ºC. Similarly, the variation of condenser temperature is limited to 37ºC to 40ºC. The degassing range is fixed to 0.3 which can be varied and its effects on the COP and exergetic efficiency can be analyzed. The effect of variation of approach temperature on various entities, like COP, was not studied.

Kang et al. [9] developed an advanced GAX cycle for utilization of waste heat (WGAX) and performed a parametric analysis to study the effects of the waste heat source temperature (T_w) and the outlet temperature of a gas fire desorber (GFD), $T_g$on the cycle performance. They introduced and compared three different WGAX cycles, Type A, Type B and Type C from the viewpoint of performance improvement. They found that the effect of the waste heat source temperature T_w on COPs was negligible for a given GFD temperature T_g. It was further established that COP_α of the WGAX cycles is always greater than the COP of the standard GAX cycle, SGAX. The GFD outlet temperature

could be reduced down to 172ºC with a higher COP_{β} of the WGAX cycle than the COP of the SGAX cycle and hence the corrosion problem in the SGAX cycle at higher T_g than 200ºC can be solved. It was further found that Type A had a merit from the viewpoint of the GAX effect, which was dominant for a lower temperature than 181ºC. Type B had a merit from the view point of the effect of exergy loss, which was dominant for a temperature higher than 181ºC. It was concluded that the SHD should be placed below the GAXD to improve the cycle performance in the WGAX cycles. They concluded that COP_{α} strongly depends on the variation of Q_{GAX} while it is not much affected by the variation of Q_{WHX}. They recommended that there should be a subcooling effect to improve the COP of the WGAX cycles as the subcooling of the weak solution results in a higher GAX effect and the reduction of exergy loss in the GAXA.

Velazquez et al. [12] proposed a relatively simple way to study the operative performance of a Solar-GAX cycle and to find the best working conditions for a particular design. They showed that it is possible to use a hybrid source of energy in an advanced absorption cycle. They found that the decrease in the efficiency of the Solar-GAX cycle, being air cooled, was not severe, even though air at 40ºC and 24% relative humidity was considered. A COP of 0.86 for cooling and 1.86 for heating together with a circulation ratio of 1.43 shows that it can be an interesting option considering the cost and the problems related to the operation of a cooling tower are eliminated. They further analyzed that the efficiency of the Solar-GAX system decreases with the increase in the temperature difference between the condenser and the evaporator. For small air conditioning purposes the proposed cycle with a temperature lift of 46ºC is an excellent

option. For a unit with cooling capacity of 10.6 kW, an internal integration of 16.9 kW was obtained which is 37% more than the energy that is supplied to the generator.

Park et al. [13] developed an ammonia GAX absorption cycle with combined cooling and hot water supply modes. They proposed new multi modes GAX cycles which function in three different modes (Case 1, Case 2 and Case 3) of cooling and hot water supply with one hardware. They finds the best cycle for performance improvement by the parametric analysis. For cooling mode COP_C values for case1, case 2 and case 3 are 60%, 42% and 87% higher than the corresponding standard GAX cycle respectively. Case 1 gives the best performance from the viewpoint of hot water supply, however, when the cooling mode is the primary purpose rather than the hot water supply then case 3 becomes the most desirable cycle. They also recommended that the optimum design values of UA_{SCA} and UA_{HCA} for case 3 should be less than those for case 1.

Gomez et al. [14] performed a theoretical and experimental analysis of an indirect-fired GAX Prototype Cooling System (GAX-PCS) using ammonia-water as the working fluid. The experimental tests were used to validate the simulation model and to evaluate the performance operated with thermal oil. The cooling load of system was 10.6 kW. The theoretical COP obtained was 0.58 with the generator temperature of 192.5ºC. An internal heat recovery of about 55% with respect to the total heat supplied in the generator was obtained. It was integrated to a micro gas turbine (MGT) to form a

cogeneration system. Over all efficiencies from 29% to 49% were obtained for cooling loads from 5kW to 20kW.

Kang and Kashiwagi [15] developed an environmentally friendly GAX cycle and compared it with single effect cycle for panel heating. The total coefficient of performance COP_{TOT} of the PGAX cycle is higher than that of the PSE cycle due to the internal heat recovery in the GAX component. They concluded that the effect of *UA* ratio is more prominent on COP_{TOT} of the PGAX cycle than that of the PSE cycle because the absorption performance in the *HCA* components is more sensitive to the coolant temperature than the *SCA*. The panel heating COP is more significantly affected by the absorber UA variation than the space heating COP. The also found that there is an optimum ratio of absorber UAs to provide the highest total COP for given split ratio of the coolant mass flow rate in the PGAX cycle. They found that the optimum UA values of the absorbers for the split ratio of 0.87.

Garimella et al. [16] modeled and studied GAX heat pump for heating as well as cooling modes. They showed that in the actual cooling mode COP of about 0.925 can be achieved at 95ºF. The heating mode COP at 47ºF is about 1.51and stays at values greater than 1.0 for ambient temperatures as low as -22ºF. In the cold ambient heating mode a small liquid heat exchanger between the solution- heated desorber and the solution-cooled desorber offers significant performance benefits.

Sabir et al. [17] analyzed and described the performance of a novel heat driven GAX-R refrigeration cycle, which is a combination of the vapour resorption and the GAX cycle. They showed that the performance was very critical and sensitive to certain parameters like heat effectiveness, mass effectiveness, inlet temperature of the chilled water etc. It

was shown that the performance of GAX-R is better than typical absorption and resorption cycles, but below that of GAX cycles.

Kumar and Udayakumar [18] theoretically analyzed a hybrid GAX cycle for an aqua ammonia absorption air conditioning system. They found that the maximum COP occurs at the mean value of the degassing ratio of 0.4 with the variation of 0.05. As the absorber pressure increases the COP increases. The increase in generator temperature results in increase in COP. The COP initially increases and then decreases with the degassing range. Comparison of hybrid and conventional GAX cycle was conducted and they found that the hybrid GAX cycle has an average of 30% higher value of COP than the conventional GAX cycle. They also concluded that the circulation ratio varies inversely with the degassing range. At constant degassing range, increasing the generator temperature increases the circulation ratio. Circulation ratio is not affected by the variation of absorber pressure. They further founded that required COP can be attained in lower degassing ranges in the hybrid cycle and it can operate successfully using low temperature energy sources.

Jawahar and Saravanan [19] performed an experimental investigation on the performance of an air-cooled modified generator absorber heat exchange (GAX) absorption cooling system of 10.5 kW capacity. They observed that at a low evaporator temperature of -5ºC was achieved at the sink temperature of 35ºC, under no load conditions. The internal heat recovery of about 15 kW was obtained for the set operating conditions. Their system yielded the fuel COP of 0.61 at the generator and evaporator temperatures of 120ºC and 2ºC respectively and a maximum cooling capacity of 9.5 kW. The introduction of high pressure GAX, low pressure GAX, solution

heat exchanger 2, condensate pre-cooler and the solution cooler recovers about 30-40% of the total heat recovered, there by reducing the generator heat input and improve the performance of the system.

Kaushik and Arora [20] presented the energy and exergy analysis of single effect and series flow double effect water-lithium bromide absorption systems. The analysis involved the determination of effects of generator, absorber and evaporator temperatures on the energetic and exergetic performance of these systems. The effects of pressure drop between the evaporator and the absorber and the effectiveness of heat exchangers were also investigated.

2.2. Conclusion of Literature Survey

Undoubtedly, so much research work has been done on the performance characteristics of ammonia water GAX and GAX hybrid cycles from the view point of first law of thermodynamics, very little is known about their performance from the view point of second law of thermodynamics. It is a known fact that exergy analysis provides more substantial and useful information when energy conversion systems are analyzed. Second law analysis helps in identifying the locations, magnitudes and sources of thermodynamic inefficiencies in energy conversion systems. Not only this, information obtained by exergetic analysis helps us in comparing various systems from the view point of thermo-economic and environ-economic aspects.

2.3. Gaps

A little research work has been done on second law analysis of GAX and GAX hybrid absorption systems. Whatever work has been done, it is restricted to either heat pumps or air conditioning applications. No effort has been made to analyze the GAX and GAX hybrid absorption systems for refrigeration applications of temperature below 0ºC. Further, the effect of degassing range on exergy analysis is not done. Also, the effect of approach temperature on second law analysis is neglected.

2.4. Objective of Present work

In this work, detailed and comprehensive energy and exergy analysis of aqua-ammonia GAX and GAX hybrid absorption refrigeration cycles have been carried out. The coefficient of performance (COP) and exergetic efficiencies are calculated at various conditions to study the effect of generator temperature, condenser temperature and evaporator temperature on them. The effect of absorber pressure on first and second law analysis of GAX hybrid system has also been studied. The analysis of effects of degassing range and approach temperature on first and second law efficiency is carried out in detail. The exergy analysis is performed in order to observe the irreversibility within the systems and contribution of different components to the exergy destruction in the cycles.

CHAPTER – 3
THERMODYNAMIC ANALYSIS

3.1. System description

Fig.3.1.illustrates the main components of the GAX ammonia water absorption refrigeration cycle. The saturated solution is assumed to leave the absorber (1) and the generator (3), and saturated ammonia liquid is assumed to leave the condenser (8). The condensate pre-cooler (RHX) sub-cools the refrigerant the leaves the condenser by pre-heating the vapour entering the absorber (12).

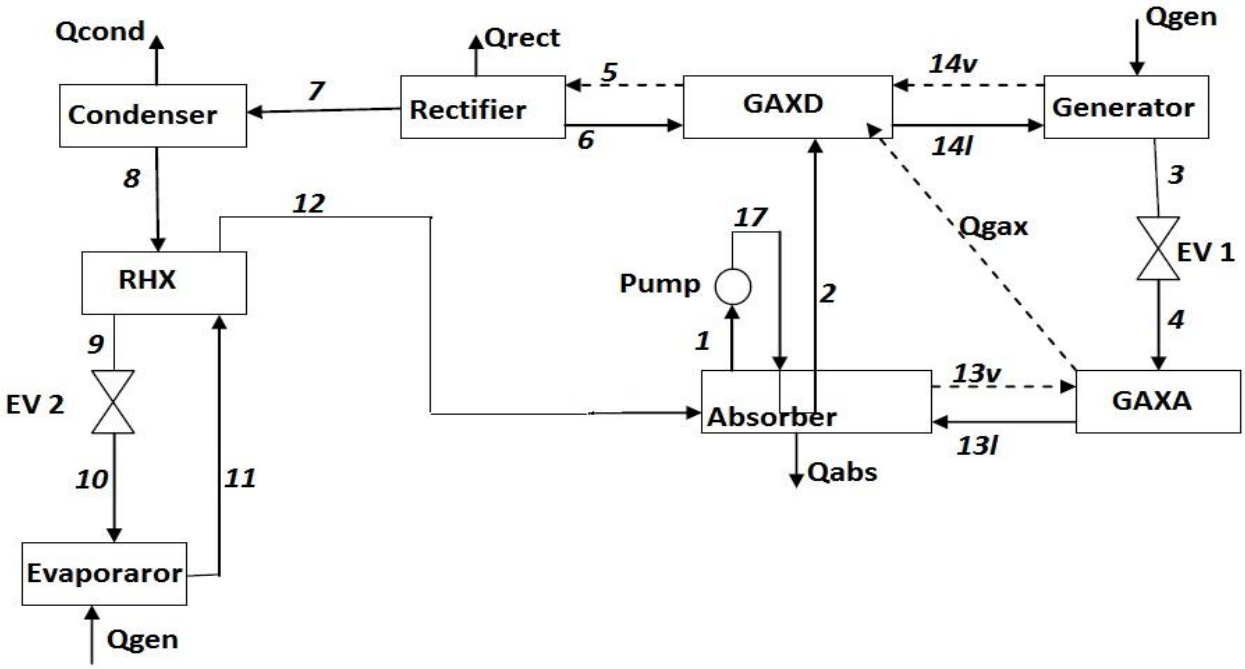

Fig.3.1. Schematic diagram of GAX absorption refrigeration cycle [8]

The high pressure cooled liquid refrigerant (8) from the condensate pre-cooler (9) enters the evaporator (10) through an expansion valve that reduces the pressure of the refrigerant to the evaporator pressure. This low pressure liquid refrigerant (10) vaporizes in the evaporator by absorbing heat from the room being cooled, and passes to the absorber (12) through the condensate pre-cooler. In the absorber, the refrigerant vapour is absorbed by the weak solution coming from the generator (3) through an expansion vale (4) and forms the strong solution (1). The term “strong solution” refers to the solution strong in refrigerant (NH_3) while “weak solution” refers to the solution that is weak in refrigerant. The strong solution (1) pumped to the generator pressure (17) is introduced into the high temperature part of the absorber, where it receives heat from the absorber and the refrigerant in it is boiled off in the generator. The remaining solution (3) flows back to the absorber and thus completes the cycle. There is partial overlapping in generator and absorber temperature which allows the heat of the absorber to be transferred to the generator. The line of Q_{gax} represents the heat exchange between the absorber and generator.

Fig.3.2. represents the schematic diagram of the GAX hybrid ammonia-water absorption refrigeration cycle. A compressor is added in between the evaporator and the absorber, which differentiate it from the simple GAX cycle. The existence of compressor causes the absorber to work at comparatively higher pressure and temperature. This allows more heat to be transferred from the absorber to the generator and thus greater internal heat recovery is there in GAX hybrid cycles as compared to the standard GAX cycle.

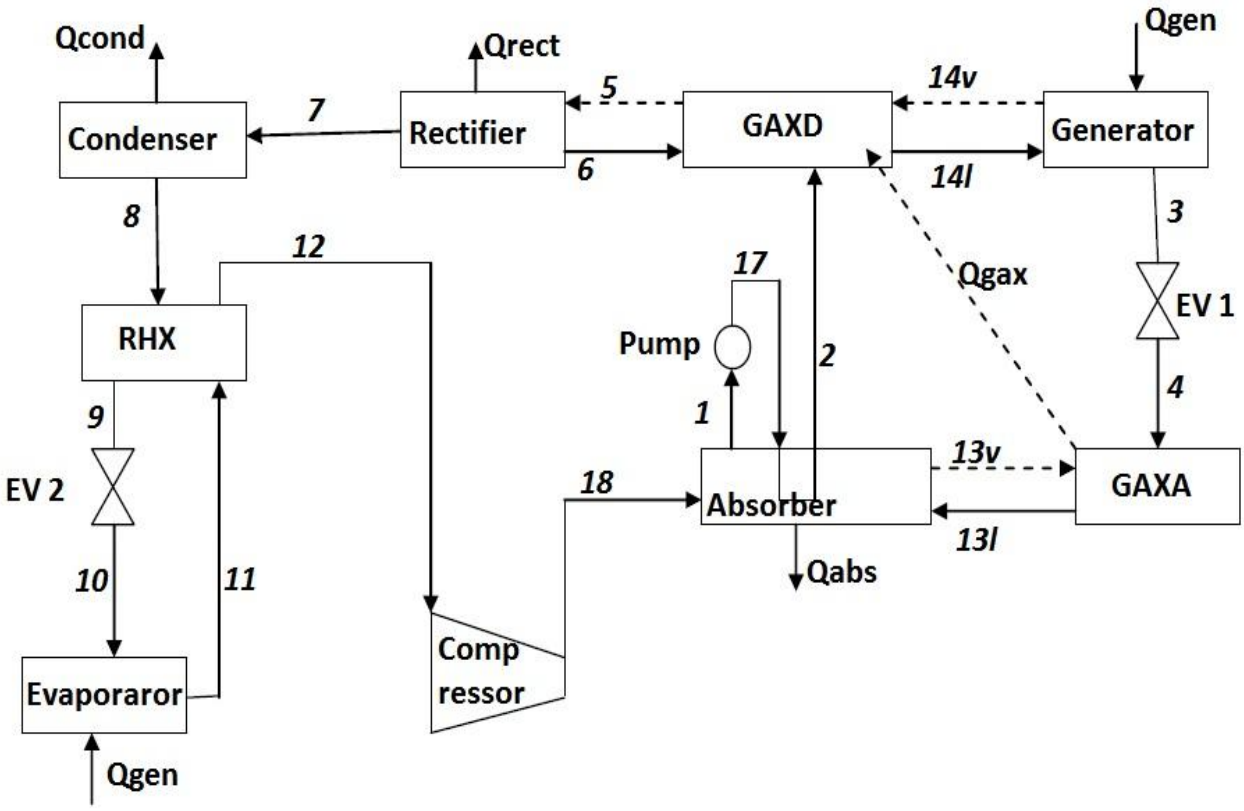

Fig.3.2. Schematic diagram of GAX hybrid absorption refrigeration cycle [8]

3.2. GAX cycle analysis

3.2.1. Introduction

To carry out the thermodynamic analysis, each component of the system is considered as a control volume. The principles of mass and material balance, first and second laws of thermodynamics are applied to each component of the system.

3.2.2. Mass and Material Balances

By conservation of mass, if there is no accumulation of mass within the control volume, the sum of the mass flow rate entering must equal mass flow rate leaving. Similarly rate of material entering must be equal to the rate of material leaving. Here, mass fraction of ammonia is considered

$$\sum \dot{m}_i - \sum \dot{m}_o = 0 \quad (1)$$

$$\sum \dot{m}_i x_i - \sum \dot{m}_o x_o = 0 \quad (2)$$

Mass and Material balance in different components of GAX system is as follows:

Desorber

$$\dot{m}_2 + \dot{m}_6 = \dot{m}_5 + \dot{m}_3 \quad (3)$$

$$\dot{m}_2 x_2 + \dot{m}_6 x_6 = \dot{m}_5 x_5 + \dot{m}_3 x_3 \quad (4)$$

GAX desorber

$$\dot{m}_2 + \dot{m}_6 + \dot{m}_{14v} = \dot{m}_5 + \dot{m}_{14l} \quad (5)$$

$$\dot{m}_2 x_2 + \dot{m}_6 x_6 + \dot{m}_{14v} x_{14v} = \dot{m}_5 x_5 + \dot{m}_{14l} x_{14l} \quad (6)$$

Absorber

$$\dot{m}_1 + \dot{m}_2 = \dot{m}_{12} + \dot{m}_4 + \dot{m}_{17} \quad (7)$$

$$\dot{m}_1 x_1 + \dot{m}_2 x_2 = \dot{m}_{12} x_{12} + \dot{m}_4 x_4 + \dot{m}_{17} x_{17} \quad (8)$$

GAX absorber

$$\dot{m}_{13l} = \dot{m}_{13v} + \dot{m}_4 \quad (9)$$

$$\dot{m}_{13l} x_{13l} = \dot{m}_{13v} x_{13v} + \dot{m}_4 x_4 \quad (10)$$

Rectifier

$$\dot{m}_5 = \dot{m}_6 + \dot{m}_7 \quad (11)$$

$$\dot{m}_5 x_5 = \dot{m}_6 x_6 + \dot{m}_7 x_7 \quad (12)$$

Pump

$$\dot{m}_1 = \dot{m}_{17} \quad (13)$$

$$x_1 = x_{17} \quad (14)$$

Expansion valve 1 (EV 1)

$$\dot{m}_3 = \dot{m}_4 \quad (15)$$

$$x_3 = x_4 \quad (16)$$

Expansion valve 2 (EV 2)

$$\dot{m}_9 = \dot{m}_{10} \quad (17)$$

$$x_9 = x_{10} \quad (18)$$

Condensate Pre-cooler (RHX)

$$\dot{m}_9 = \dot{m}_8 \; and \; \dot{m}_{11} = \dot{m}_{12} \quad (19)$$

$$x_9 = x_8 and \; x_{11} = x_{12} \quad (20)$$

Condenser

$$\dot{m}_7 = \dot{m}_8 \quad (21)$$

$$x_7 = x_8 \quad (22)$$

Evaporator

$$\dot{m}_{10} = \dot{m}_{11} \quad (23)$$

$$x_{10} = x_{11} \quad (24)$$

3.2.3. Energy Analysis

The first law of thermodynamics yields the energy balance of the system specified by the following Steady Flow Energy Equation.

$$\left[\sum(\dot{m}h)_i - \sum(\dot{m}h)_o\right] + \left[\sum \dot{Q}_i - \sum \dot{Q}_o\right] + \left[\sum \dot{W}_i - \sum \dot{W}_o\right] = 0 \quad (25)$$

Energy balance in different components of GAX system is as follows:

Desorber

$$\dot{m}_2 h_2 + \dot{m}_6 h_6 + \dot{Q}_{gen} = \dot{m}_5 h_5 + \dot{m}_3 h_3 \quad (26)$$

GAX desorber

$$\dot{m}_2 h_2 + \dot{m}_6 h_6 + \dot{m}_{14v} h_{14v} + \dot{Q}_{required} = \dot{m}_5 h_5 + \dot{m}_{14l} h_{14l} \quad (27)$$

Absorber

$$\dot{m}_1 h_1 + \dot{m}_2 h_2 + \dot{Q}_{absorber} = \dot{m}_{12} h_{12} + \dot{m}_4 h_{14} + \dot{m}_{17} h_{17} \quad (28)$$

GAX absorber

$$\dot{m}_{13l} h_{13l} + \dot{Q}_{available} = \dot{m}_{13v} h_{13v} + \dot{m}_4 h_4 \quad (29)$$

Rectifier

$$\dot{m}_5 h_5 = \dot{m}_6 h_6 + \dot{m}_7 h_7 + \dot{Q}_{rect} \quad (30)$$

Pump

$$\eta_p = \frac{\dot{w}_{sp}}{\dot{w}_p}, \qquad \dot{w}_{sp} = \dot{m}_1 v_1 (P_{17} - P_1), \qquad \dot{w}_p = \dot{m}_1 (h_{17} - h_1) \quad (31)$$

EV 2

$$h_9 = h_{10} \quad (32)$$

Condenser

$$\dot{Q}_{cond} = \dot{m}_8 (h_8 - h_7) \quad (33)$$

RHX

$$\dot{m}_9(h_9 - h_8) = \dot{m}_{12}(h_{11} - h_{12}) \quad (34)$$

$$\in = \frac{Q_{actual}}{Q_{max}} \quad (35)$$

Evaporator

$$\dot{Q}_{evap} = \dot{m}_{11}(h_{11} - h_{10}) \quad (36)$$

EV 1

$$h_4 = h_3 \quad (37)$$

Coefficient of Performance (COP)

It is defined as the ratio of useful heat to work. Here, useful heat is taken as the refrigerating effect. Considering the first law of thermodynamics, the performance of GAX cycle is evaluated using COP, which is expressed as follows:

$$COP = \frac{\dot{Q}_{evap}}{\dot{Q}_{gen} + \dot{w}_p} \quad (38)$$

where, $\dot{Q}_{evap}$ is the refrigerating effect, $\dot{Q}_{gen}$ is heat input in generator and $\dot{w}_p$ is pump work.

3.2.4. Exergy Analysis

The exergy of a system is defined as the maximum shaft work that could be done by the composite of the system and a specified reference environment that is assumed to be infinite, in equilibrium and ultimately enclosing all other systems. This represents the *useful Work potential* of the system at the specified state. It represents the upper limit

on the amount of work a device can deliver without violating any thermodynamic laws. Exergy is a property of the system environment combination and not of the system alone. The following are some terms found in the literature that is equivalent to exergy: available energy, essergy, utilizable energy, available work, availability.

The rate of exergy destruction for a component is given for a control volume undergoing steady state process is expressed as:

$$\dot{E}_d = \sum \dot{m}_i \psi_i - \sum \dot{m}_o \psi_o + \left[\sum \left(\dot{Q} \left(1 - {}^{T_0}/_{T} \right) \right)_i - \left(\dot{Q} \left(1 - {}^{T_0}/_{T} \right) \right)_o \right] \pm \sum \dot{W} \qquad (39)$$

Exergy Destruction in different components of GAX system is as follows:

Desorber

$$\dot{E}_{d,gen} = \dot{m}_{14l}(h_{14l} - T_o s_{14l}) - \dot{m}_{14v}(h_{14v} - T_o s_{14v}) - \dot{m}_3(h_3 - T_o s_3) + \dot{Q}_{gen} \qquad (40)$$

GAX desorber & GAX absorber

$$\dot{E}_{d,gax} = \dot{m}_2(h_2 - T_o s_2) + \dot{m}_4(h_4 - T_o s_4) + \dot{m}_6(h_6 - T_o s_6) + \dot{m}_{13v}(h_{13v} - T_o s_{13v}) + \dot{m}_{14v}(h_{14v} - T_o s_{14v}) - \dot{m}_{14l}(h_{14l} - T_o s_{14l}) - \dot{m}_{13l}(h_{13l} - T_o s_{13l}) - \dot{m}_5(h_5 - T_o s_5) \qquad (41)$$

Absorber

$$\dot{E}_{d,abs} = \dot{m}_{12}(h_{12} - T_o s_{12}) + \dot{m}_{17}(h_{17} - T_o s_{17}) + \dot{m}_{13l}(h_{13l} - T_o s_{13l}) - \dot{m}_{13v}(h_{13v} - T_o s_{13v}) - \dot{m}_2(h_2 - T_o s_2) - \dot{m}_1(h_1 - T_o s_1) \qquad (42)$$

Rectifier

$$\dot{E}_{d,rect} = \dot{m}_5(h_5 - T_o s_5) - \dot{m}_6(h_6 - T_o s_6) - \dot{m}_7(h_7 - T_o s_7) \qquad (43)$$

Pump

$$\dot{E}_{d,pump} = T_o \dot{m}_1 (s_{17} - s_1) \quad (44)$$

EV 2

$$\dot{E}_{d,exv2} = T_o \dot{m}_{10} (s_{10} - s_9) \quad (45)$$

Condenser

$$\dot{E}_{d,cond} = T_o \dot{m}_7 \{(h_7 - h_8) - (s_7 - s_8)\} \quad (46)$$

RHX

$$\dot{E}_{d,RHX} = T_o (\dot{m}_9 s_9 + \dot{m}_{12} s_{12} - \dot{m}_8 s_8 - \dot{m}_{11} s_{11}) \quad (47)$$

Evaporator

$$\dot{E}_{d,evap} = \dot{m}_{10}(h_{10} - T_o s_{10}) - \dot{m}_{11}(h_{11} - T_o s_{11}) + \dot{Q}_{evap}\left[1 - \left({T_0}/{T_{evap}}\right)\right] \quad (48)$$

Exergetic Efficiency

The exergy efficiency is an important parameter for measuring the performance of thermal system.

The second law efficiency is a measure of the performance of a device relative to the performance under reversible conditions for the same end states and for heat engines it is given by

$$\eta_{II} = \frac{\eta_{th}}{\eta_{th,rev}} = \frac{W_u}{W_{rev}}$$

For refrigerators, heat pumps and other work producing devices it is given by

$$\eta_{II} = \frac{COP}{COP_{rev}} = \frac{W_{rev}}{W_u}$$

In terms of exergy, second law efficiency can be written as

$$\eta_{II} = \frac{Exergy\ recovered}{Exergy\ supplied}$$

$$\eta_{II} = 1 - \frac{Exergy\ destroyed}{Exergy\ supplied}$$

Second law efficiency is also known as Exergetic efficiency.

It can be expressed on the basis of the second law of thermodynamics as by Gomri [21]:

$$\eta_{II} = \frac{\dot{Q}_{evap}(1-T_0/T_{evap})}{[\dot{Q}_{gen}(1-T_o/T_{avg})+\dot{w}_p]} \quad (49)$$

Total Exergy Destruction

Total exergy destruction rates are the sum of the exergy destruction rate in each component.

$$\dot{E}_{d,total} = \dot{E}_{d,gen} + \dot{E}_{d,gax} + \dot{E}_{d,abs} + \dot{E}_{d,rect} + \dot{E}_{d,cond} + \dot{E}_{d,pump} + \dot{E}_{d,exv2} + \dot{E}_{d,RHX} + \dot{E}_{d,exv1} + \dot{E}_{d,evap} \quad (50)$$

3.3. GAX hybrid cycle analysis

3.3.1. Introduction

The analysis of GAX hybrid system involves the mass and material balance, energy analysis and exergy analysis. Thus, COP is found out and various parameters affecting it are studied. Similarly exergetic efficiency and exergy destruction rates are obtained.

3.3.2. Mass and Material Balances

By conservation of mass, if there is no accumulation of mass within the control volume, the sum of the mass flow rate entering must equal mass flow rate leaving. This is expressed same as in equations 1 and 2.

Mass and Material balance in different components of GAX hybrid system is same as that for standard GAX cycle mentioned earlier. Additional equations are as follows:

Compressor

$$\dot{m}_{12} = \dot{m}_{18} \quad (51)$$

$$x_{12} = x_{18} \quad (52)$$

3.3.3. Energy Analysis

The first law of thermodynamics yields the energy balance of the system specified by the following Steady Flow Energy Equation.

$$\left[\sum(\dot{m}h)_i - \sum(\dot{m}h)_o\right] + \left[\sum \dot{Q}_i - \sum \dot{Q}_o\right] + \left[\sum \dot{W}_i - \sum \dot{W}_o\right] = 0$$

Energy balance in different components of GAX hybrid system is same as that for the simple GAX cycle. The additional equation for compressor is as follows:

Compressor

$$\dot{w}_{comp} = \dot{m}_{12}(h_{18} - h_{12}) \quad (53)$$

where, $\dot{w}_{comp}$ is compressor work

Coefficient of Performance

Considering the first law of thermodynamics, the performances of GAX hybrid cycles are evaluated using COP, which is defined as follows:

$$COP = \frac{\dot{Q}_{evap}}{\dot{Q}_{gen} + \dot{w}_p + \dot{w}_{comp}} \quad (54)$$

3.3.4. Exergy Analysis

The rate of exergy destruction for a component for a control volume undergoing steady state process is same as mentioned earlier for GAX cycle.

Exergy Destruction in different components of GAX hybrid system is expressed in a same way as for the simple GAX cycle. The additional equation for compressor is as follow:

Compressor

$$s_{12} = s_{18} \tag{55}$$

Exergetic Efficiency

It can be expressed on the basis of the second law of thermodynamics as by Gomri [21]:

$$\eta_{II} = \frac{\dot{Q}_{evap}(1-T_0/T_{evap})}{[\dot{Q}_{gen}(1-T_o/T_{avg})+\dot{w}_p+\dot{w}_{comp}]} \tag{56}$$

Where T_{evap} and T_{avg} are the thermodynamic mean temperatures ($T = \int {Tds}/{\Delta s}$) of evaporator and generator respectively.

Total Exergy Destruction

Total exergy destruction rates are the sum of the exergy destruction rate in each component.

$$\dot{E}_{d,total} = \dot{E}_{d,gen} + \dot{E}_{d,gax} + \dot{E}_{d,abs} + \dot{E}_{d,rect} + \dot{E}_{d,cond} + \dot{E}_{d,pump} + \dot{E}_{d,exv2} + \dot{E}_{d,RHX} +$$

$$\dot{E}_{d,exv1} + \dot{E}_{d,evap} + \dot{E}_{d,comp} \quad (57)$$

Exergy Destruction Ratio

It is defined as ratio of exergy destruction rate in a component to the total exergy destruction rate in the cycle [34]. It is expressed as follows:

$$\dot{Y}_{d,i} = \frac{\dot{E}_{d,i}}{E_{d,total}} \quad (58)$$

where $\dot{E}_{d,i}$ is the exergy destruction rate in a component.

Degassing Range

It is defined as the difference in the strong and the weak solution concentration. It is expressed with reference to fig.3.1 as

$$D_x = x_2 - x_3 \quad (59)$$

Approach temperature

It is defined as the difference in temperature at inlet of hot fluid and exit of cold fluid and vise versa in a heat exchanger (counter flow).

3.4. Assumptions

The analysis of the system is based on the following assumptions.

1. The system is operating under steady conditions.
2. The refrigerant is saturated at the exits of the condenser and the evaporator.
3. The solutions are at equilibrium at the exits of the generator and the absorber and they are at the corresponding device temperature.
4. Pressure drops within the cycle can be neglected except through the expansion valves.
5. The approach temperature is assumed to be 0 K at either end of the GAX heat exchanger.
6. Compression is isentropic in compressor.

3.5. Input Parameters

Parameters 1, 2, 3 and 7 are taken from Yari et al. [8]

1. The efficiency of the solution pump is 0.5.
2. The effectiveness of the heat exchanger (RHX) is 0.8.
3. The Degassing value is assumed to be 0.3.
4. Evaporator temperature is varied from -5^{0}C to 5^{0}C.
5. Condenser temperature varies between 35^{0}C to 45^{0}C.
6. Generator temperature varies between 130^{0}C to 175^{0}C.
7. Absorber pressure for GAX hybrid cycles are 716.8 kP$_a$ and 916.8 kP$_a$.
8. The reference environmental state is at the temperature of $T_o = 25℃$ and the pressure of $P_o = 100\ kP_a$.

3.6. Sample Calculations

The values of temperature, pressure, enthalpy, entropy and ammonia concentration etc. are obtained at different state points of the GAX cycle shown in fig.3.1. The values are shown below in the table 3.1. Table 3.2 shows the values of COP, Heat transfer rates, Exergetic efficiency and total exergy destruction rate of GAX cycle at $T_g = 170℃$, $T_c = 40℃$ and $T_e = 5℃$.

Table.3.1. Various properties at different state points of GAX cycle at $T_g = 170℃$, $T_c = 40℃$ and $T_e = 5℃$

Points	P [kPa]	T [°C]	x	h [kJ/kg]	s [kJ/kg.K]	m [kg/s]	Q	v
1	478.4	52.93	0.4133	4.241	0.6352	0.02939	0	0.001196
2	1548	98.19	0.4133	210.5	1.224	0.02939	0.000114	0.001288
3	1548	170	0.1133	654	2.103	0.01939	0	0.001216
4	478.4	129	0.1133	654	2.131	0.01939	0.09585	0.03779
5	1548	98.19	0.9651	1500	4.772	0.01054	1	0.1076
6	1548	98.2	0.4133	210.7	1.224	0.000543	0.000182	0.001295
7	1548	67.11	0.995	1375	4.421	0.01	1	0.09483
8	1548	40	0.995	187.3	0.6622	0.01	0	0.001726
9	1548	12.2	0.995	53.52	0.215	0.01	-0.001	0.0016
10	478.4	3.064	0.995	53.52	0.2229	0.01	0.03418	0.01044
11	478.4	5	0.995	1198	4.343	0.01	0.94	0.2478
12	478.4	30.16	0.995	1332	4.808	0.01	0.9931	0.292
13	478.4	98.19	NA	NA	NA	NA	NA	NA
14	1548	129	NA	NA	NA	NA	NA	NA
17	1548	53.38	0.4133	6.799	0.6392	0.02939	-0.001	0.001196

Table.3.2. COP, heat transfer rates, exergetic efficiency and total exergy destruction

rate of GAX cycle at $T_g = 170℃$				$T_c = 40℃$ and $T_e = 5℃$				
$\boldsymbol{COP}$	$\boldsymbol{Q_{av}}$ **(kW)**	$\boldsymbol{Q_{rq}}$ **(kW)**	$\boldsymbol{Q_g}$ **(kW)**	$\boldsymbol{Q_a}$ **(kW)**	$\boldsymbol{Q_c}$ **(kW)**	$\boldsymbol{Q_e}$ **(kW)**	$\boldsymbol{\eta_{II}}$ **(%)**	$\boldsymbol{E_{d,total}}$ **(kW)**
0.9454	10.74	10.16	12.03	9.725	11.88	11.44	22.64	2.848

Table 3.3 and 3.5 shows the values of pressure, temperature, ammonia concentration, enthalpy, entropy etc. for GAX hybrid cycle (fig.3.2.) for $P_a = 716.8\ kPa\ and P_a = 916.8\ kPa$ respectively.

Table.3.3. Various properties at different state points for GAX hybrid cycle at $P_a = 716.8\ kPa$, $T_g = 170$℃, $T_c = 40$℃ and $T_e = 5$℃

Points	P [kPa]	T [℃]	x	h [kJ/kg]	s [kJ/kg.K]	m [kg/s]	Q	v
1	716.8	66.94	0.4133	66.95	0.8226	0.02939	0	0.001216
2	1548	98.19	0.4133	210.5	1.224	0.02939	0.000114	0.001288
3	1548	170	0.1133	654	2.103	0.01939	0	0.001216
4	716.8	142.3	0.1133	654	2.116	0.01939	0.0673	0.01869
5	1548	98.19	0.9651	1500	4.772	0.01054	1	0.1076
6	1548	98.2	0.4133	210.7	1.224	0.000543	0.000182	0.001295
7	1548	67.11	0.995	1375	4.421	0.01	1	0.09483
8	1548	40	0.995	187.3	0.6622	0.01	0	0.001726
9	1548	12.2	0.995	53.52	0.215	0.01	-0.001	0.0016
10	478.4	3.064	0.995	53.52	0.2229	0.01	0.03418	0.01044
11	478.4	5	0.995	1198	4.343	0.01	0.94	0.2478
12	478.4	30.16	0.995	1332	4.808	0.01	0.9931	0.292
13	716.8	98.19	NA	NA	NA	NA	NA	NA
14	1548	142.3	NA	NA	NA	NA	NA	NA
17	1548	67.33	0.4133	68.97	0.8257	0.02939	-0.001	0.001216
18	716.8	54.06	0.995	1390	4.808	0.01	1.001	0.2103

Table.3.4. COP, heat transfer rates, exergetic efficiency and total exergy destruction rate of GAX hybrid cycle ($P_a = 716.8\ kPa$) at $T_g = 170$℃, $T_c = 40$℃ and $T_e = 5$℃

COP	Q_{av} (kW)	Q_{rq} (kW)	Q_g (kW)	Q_a (kW)	Q_c (kW)	Q_e (kW)	η_{II} (%)	$E_{d,total}$ (kW)
1.253	13.98	13.70	8.491	6.755	11.88	11.44	25.43	2.444

Table 3.4 shows the calculated values of COP, Heat transfer rates, Exergetic efficiency and total exergy destruction rate of GAX hybrid cycle ($P_a = 716.8\ kPa$) at $T_g = 170$℃, $T_c = 40$℃ and $T_e = 5$℃.

Table.3.5. Various properties at different state points for GAX hybrid at $P_a = 916.8\ kPa$, $T_g = 170$℃, $T_c = 40$℃ and $T_e = 5$℃

Points	P [kPa]	T [°C]	x	h [kJ/kg]	s [kJ/kg.K]	m [kg/s]	Q	v
1	916.8	76.21	0.4133	108.9	0.9437	0.02939	0	0.001232
2	1548	98.19	0.4133	210.5	1.224	0.02939	0.000114	0.001288
3	1548	170	0.1133	654	2.103	0.01939	0	0.001216
4	916.8	150.8	0.1133	654	2.11	0.01939	0.04789	0.01103
5	1548	98.19	0.9651	1500	4.772	0.01054	1	0.1076
6	1548	98.2	0.4133	210.7	1.224	0.000543	0.000182	0.001295
7	1548	67.11	0.995	1375	4.421	0.01	1	0.09483
8	1548	40	0.995	187.3	0.6622	0.01	0	0.001726
9	1548	12.2	0.995	53.52	0.215	0.01	-0.001	0.0016
10	478.4	3.064	0.995	53.52	0.2229	0.01	0.03418	0.01044
11	478.4	5	0.995	1198	4.343	0.01	0.94	0.2478
12	478.4	30.16	0.995	1332	4.808	0.01	0.9931	0.292
13	916.8	98.19	NA	NA	NA	NA	NA	NA
14	1548	150.8	NA	NA	NA	NA	NA	NA
17	1548	76.53	0.4133	110.5	0.946	0.02939	-0.001	0.001232
18	916.8	72.96	0.995	1428	4.808	0.01	1.001	0.1737

Table.3.6. COP, heat transfer rates, exergetic efficiency and total exergy destruction rate of GAX hybrid cycle ($P_a = 916.8\ kPa$) at $T_g = 170$℃, $T_c = 40$℃ and $T_e = 5$℃

COP	Q_{av} (kW)	Q_{rq} (kW)	Q_g (kW)	Q_a (kW)	Q_c (kW)	Q_e (kW)	η_{II} (%)	$E_{d,total}$ (kW)
1.586	16.21	15.99	6.204	4.835	11.88	11.44	28.03	2.14

Table 3.6 shows the calculated values of COP, Heat transfer rates, Exergetic efficiency and total exergy destruction rate of GAX hybrid cycle ($P_a = 916.8\ kPa$) at $T_g = 170$℃, $T_c = 40$℃ and $T_e = 5$℃.

3.6. Model Validation

To validate the simulation model, the results and the parametric profiles are compared with the data available in the literature. Figures 3.3 and 3.4 compare the results obtained from the present work with those obtained by Yari et al. [8] and Kumar et al. [22].

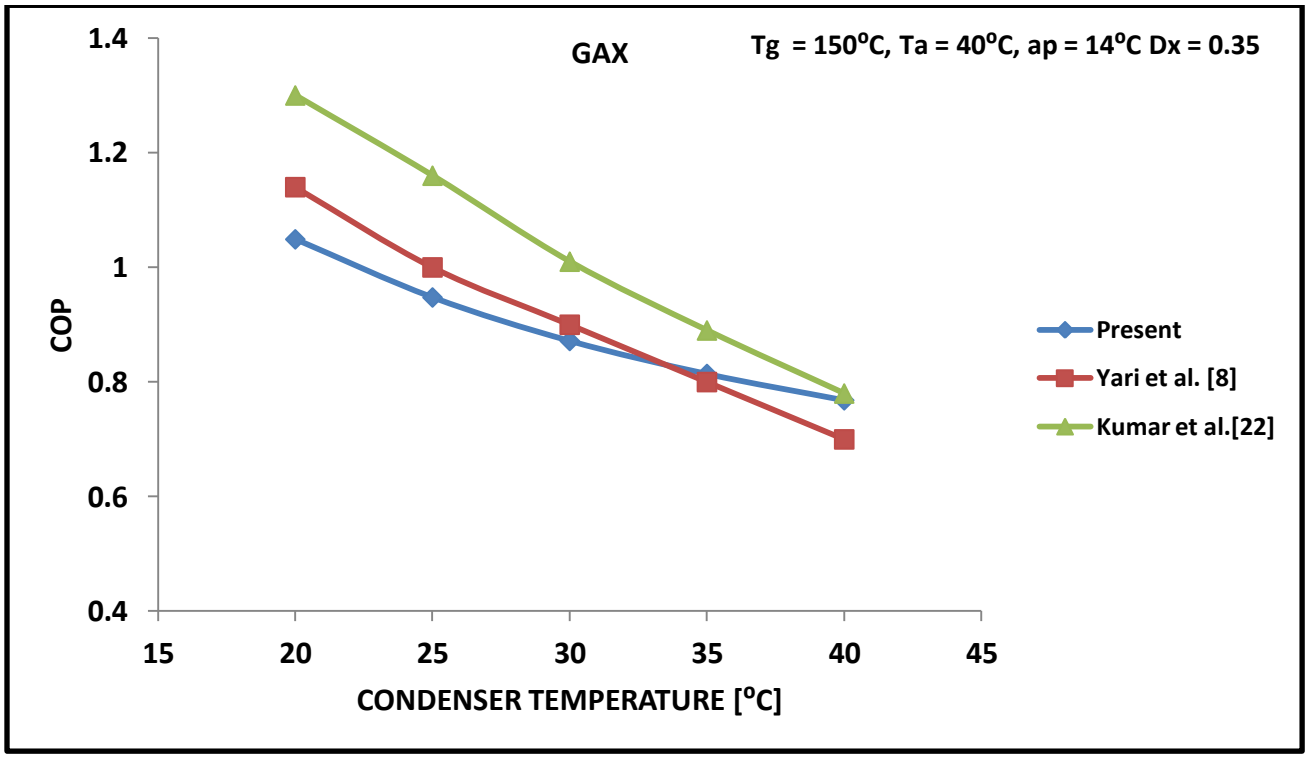

Fig.3.3. Comparison of present work with that of Yari et al. [8] and Kumar et al. [22] for GAX cycle

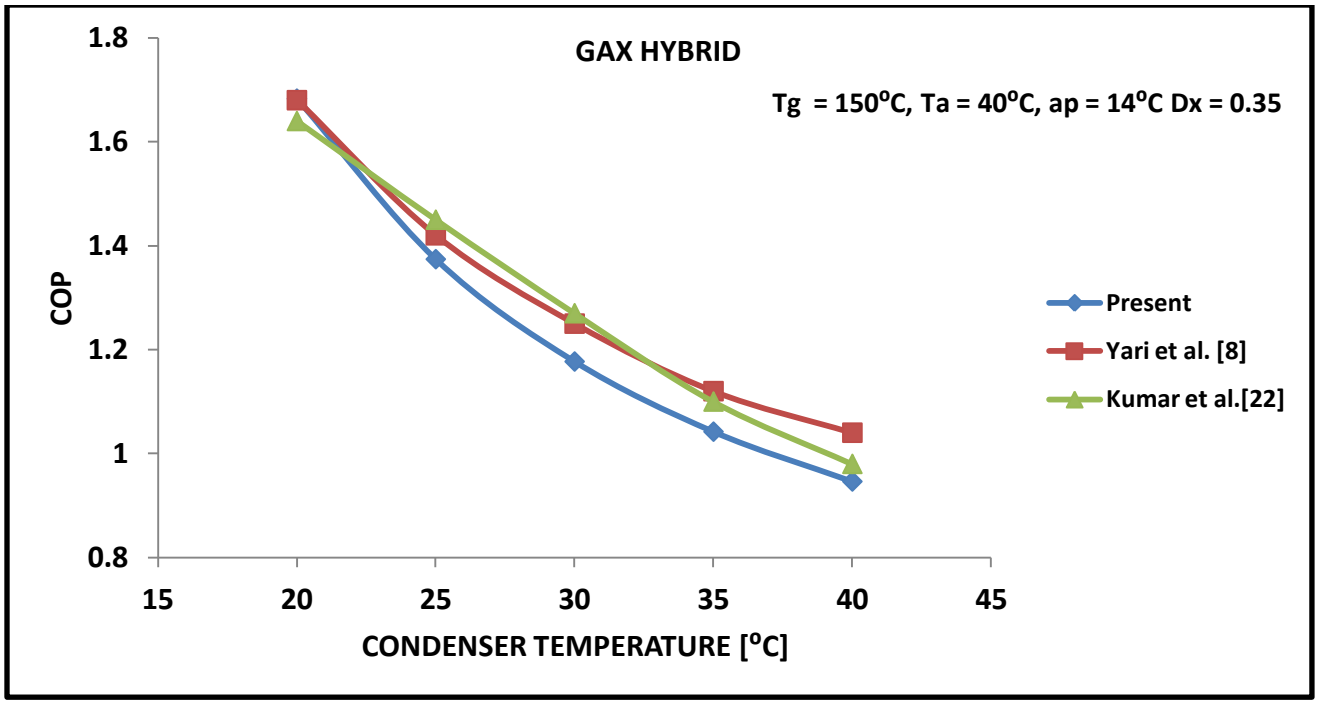

Fig.3.4. Comparison of present work with that of Yari et al. [8] and Kumar et al. [22] for GAX hybrid cycle ($P_a = 916.8\ kPa$)

A comparison among the COPs of GAX cycle calculated in the present work and those reported in the literature [8], [22], [23] is presented in the table 3.7.

Table 3.7.Comparison of COP for GAX cycles

Authors	***COP***	***% difference***	***Operating Parameters***
Present work	1.104	-	T_g =163.3^{0}C,
Yari et al. [8]	1.103	0.09	T_c = 40^{0}C,
Herold et al. [23]	1.10	0.36	T_a = 40^{0}C, T_e = 5^{0}C,
Kumar et al. [22]	1.08	2.22	D_x = 0.35

.

Since the difference between the COP values of the present work and those provided in the literature by Yari et al [8], Herold et al [23] and Kumar et al [22] is less than 5%, it can be concluded that the present model is valid and reliable.

CHAPTER – 4
RESULTS AND DISCUSSION

4.1. Introduction

A computer program to determine the thermodynamic properties of the saturated ammonia water solutions is developed based on the correlations of Patek and Klomfar [24]. The equations for conservation of mass and energy and correlations for ammonia-water solution properties, as well as exergy balance were solved using the EES software [25] for individual components of GAX and GAX hybrid cycles.

4.2. First Law Analysis

4.2.1. Effect of generator temperature on COP

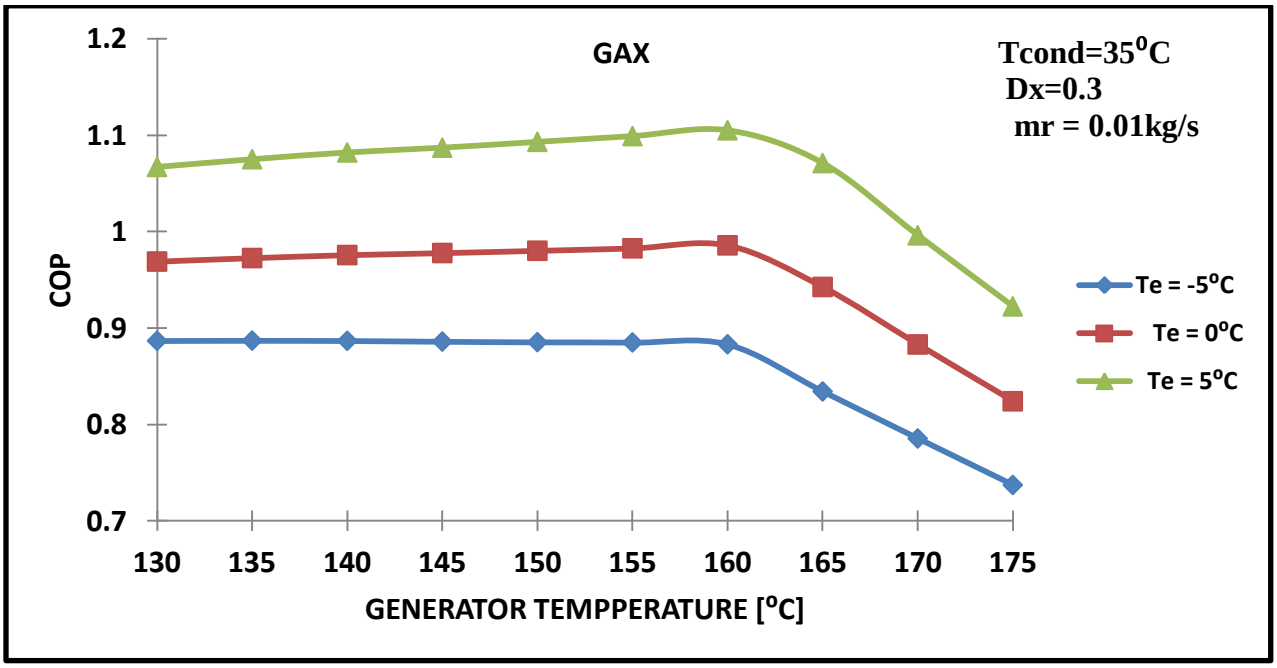

Fig.4.1. Variation of COP with generator temperature T_g for GAX cycle at $T_{cond} = 35^0C$

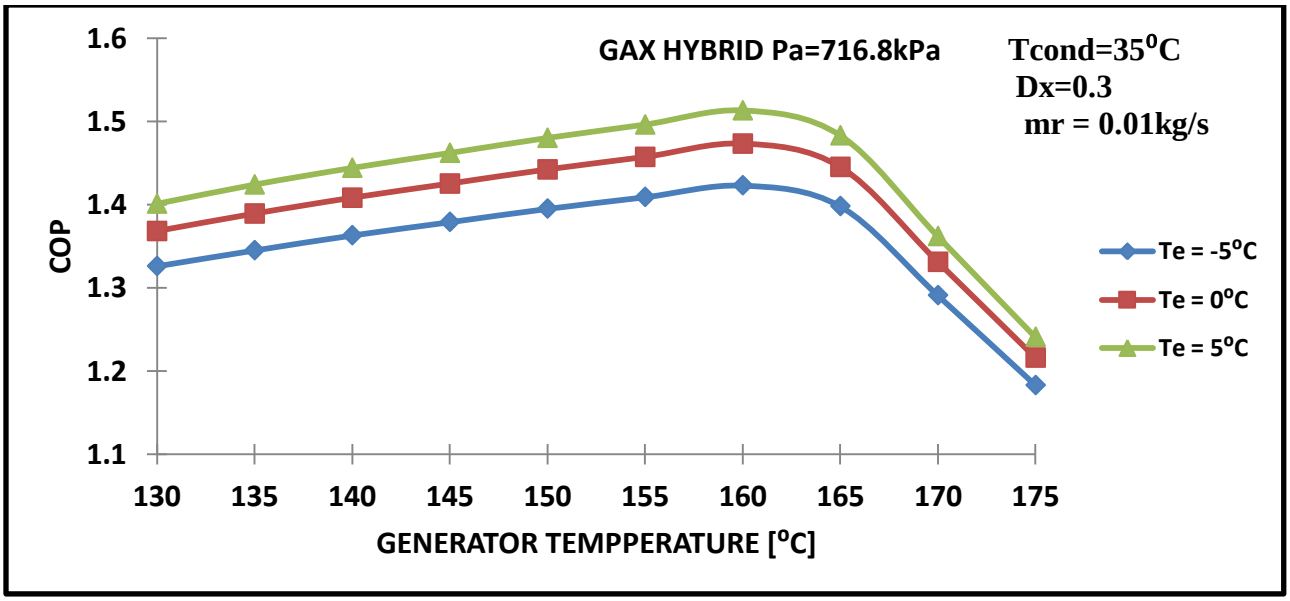

Fig.4.2. Variation of COP with T_g for GAX hybrid cycle $T_{cond} = 35^0C$

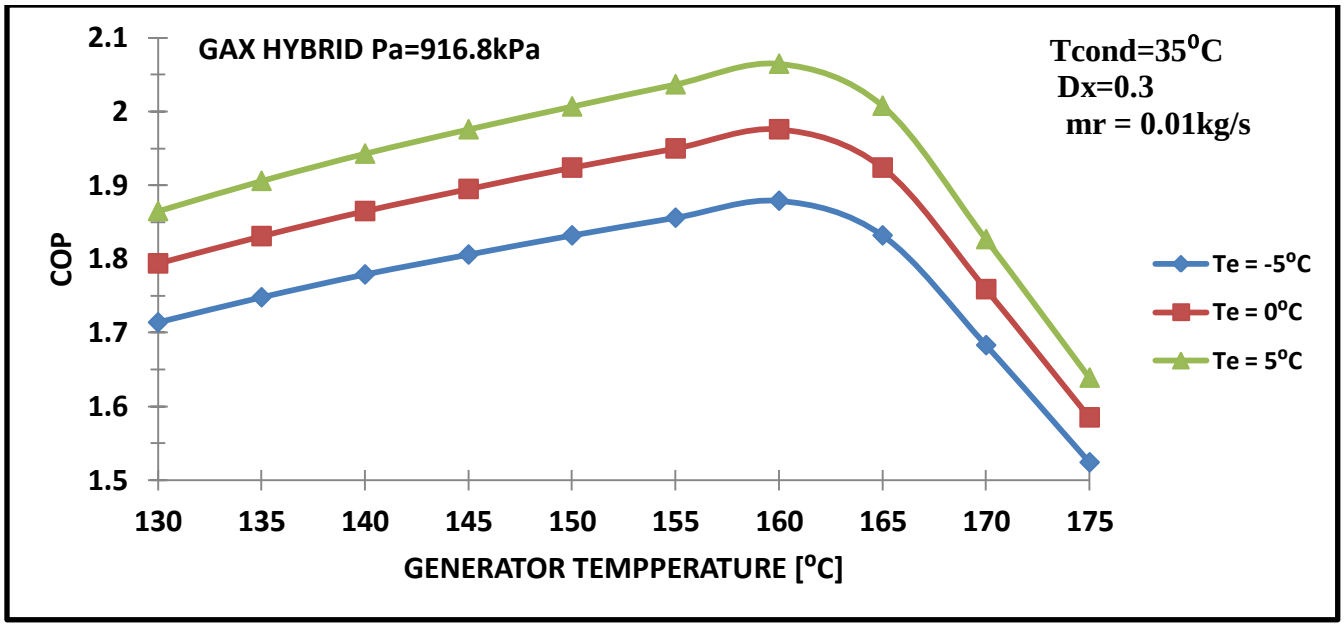

Fig.4.3. Variation of COP with T_g for GAX hybrid cycle at $T_c = 35^0C$

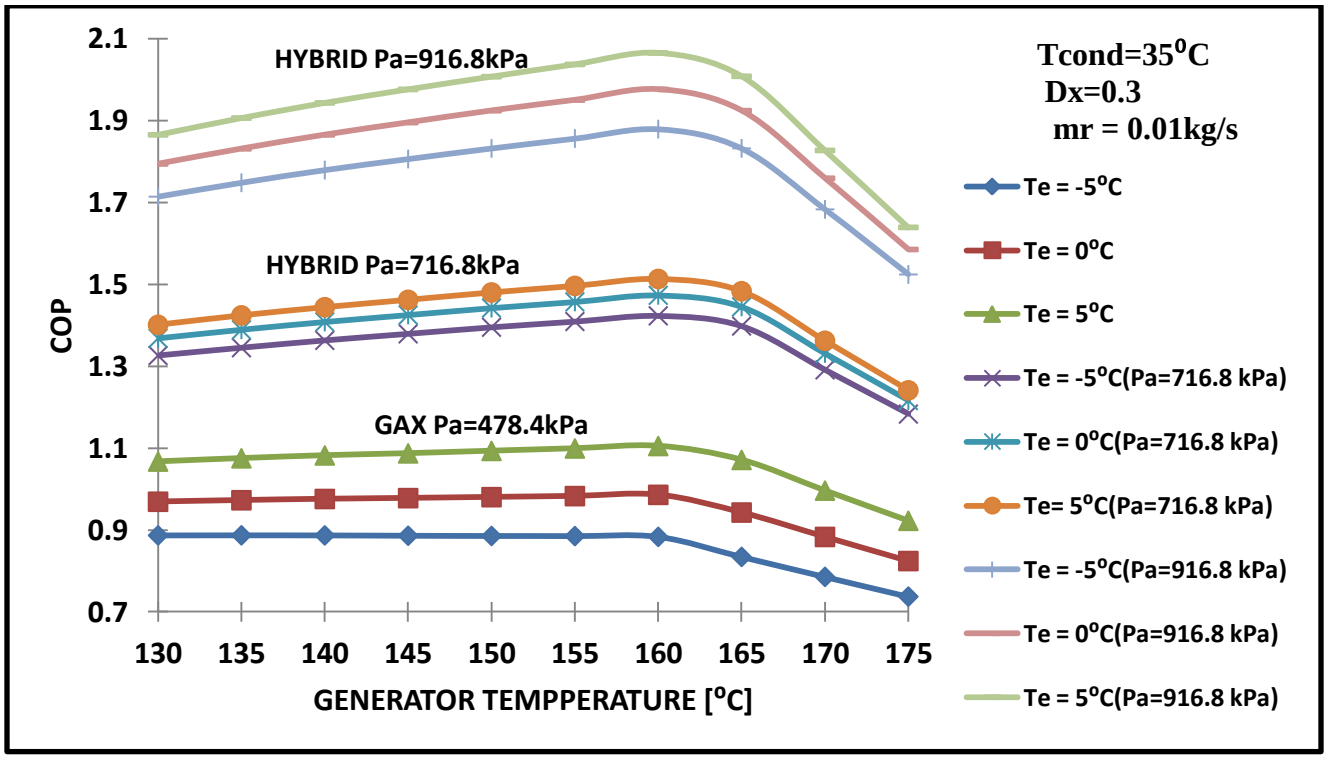

Fig.4.4. COP versus T_g for GAX and GAX hybrid cycles at $T_c = 35^0C$

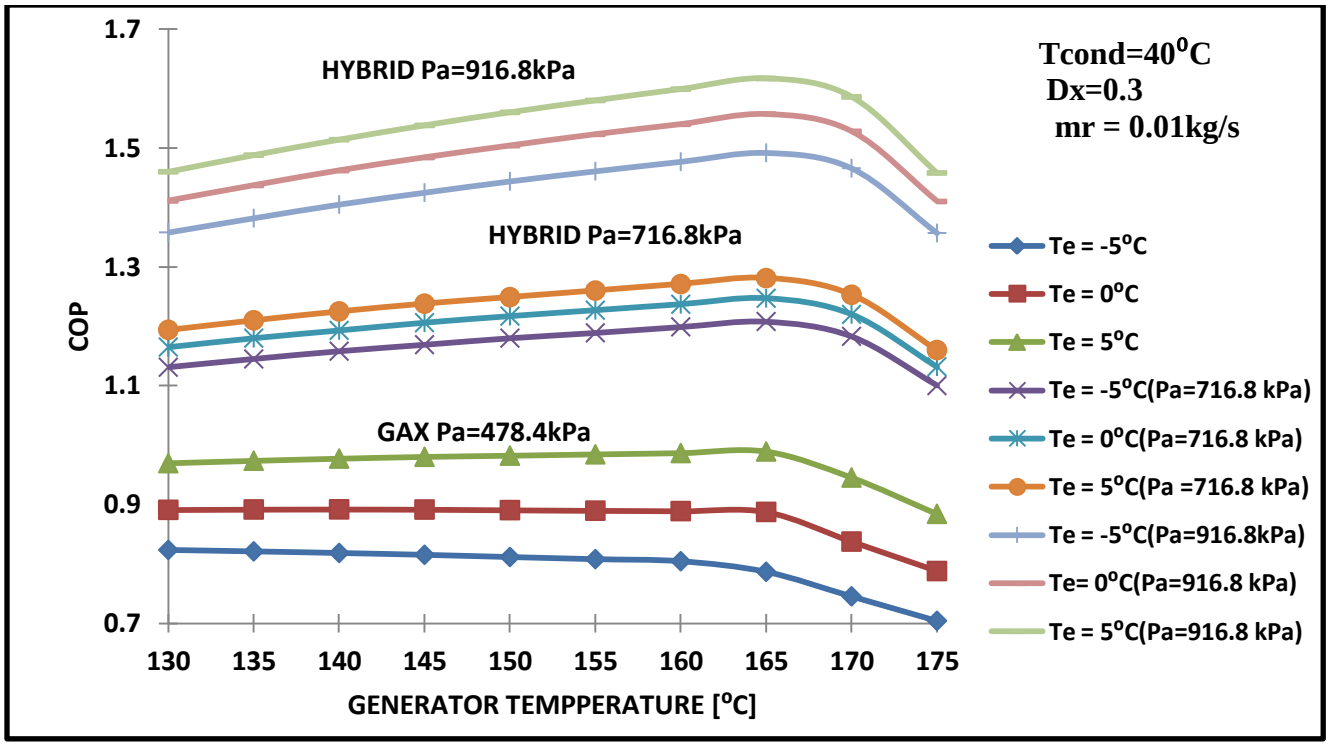

Fig.4.5. COP versus T_g for GAX and GAX hybrid cycles at $T_c = 40^0C$

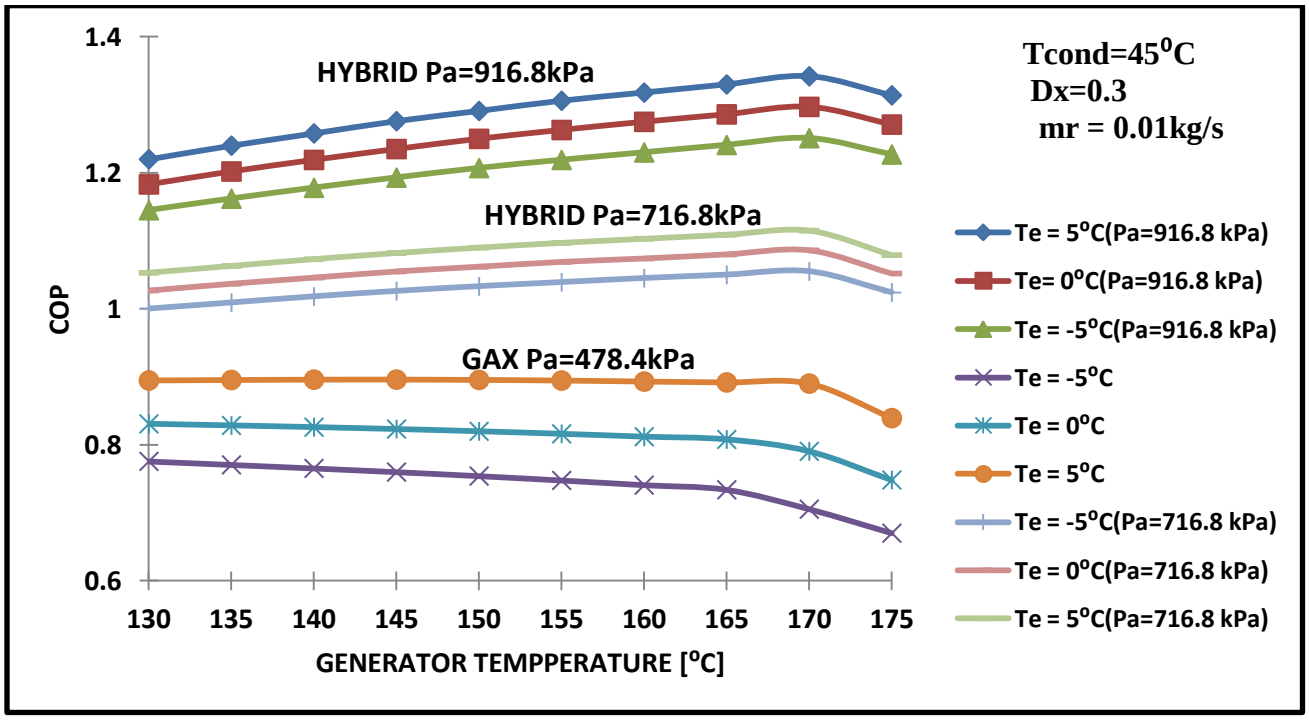

Fig.4.6. COP versus T_g for GAX and hybrid cycles at $T_c = 45^0C$

Fig.4.1 to fig.4.6 show the effects of generator temperature on the coefficient of performance of GAX and GAX hybrid cycles at three condenser temperatures of $T_{cond} = 35^0C$, $T_{cond} = 40^0C$ and $T_{cond} = 45^0C$. The evaporator temperature is varied from $T_{evap} = -5^0C$ to $T_{evap} = 5^0C$. The absorber pressures considered for the study of the GAX hybrid cycle are 716.8 kPa and 916.8 kPa. For the GAX cycle it is 478.4 kPa which is being calculated through program.

From the figures, it is understood that the higher COP values are obtained at higher evaporator temperatures. Higher values of condenser temperatures lead to lower values of COP. Figures also indicates that there is a particular value of the generator temperature at which maximum value of COP is obtained, for a fixed value of evaporator, absorber and condenser temperature. Further, it can be seen that as the condenser temperature increases, the optimum value of generator temperature increases corresponding to maximum value of COP. For GAX hybrid cycles, at condenser temperature of 35^0C, 40^0C and 45^0C, the corresponding maximum COP occurs at generator temperature of 160^0C, 165^0C and 170^0C.

The variation of COP with generator temperature is explained as follows: For a constant cooling load, at a particular evaporator temperature the evaporator mass flow rate is constant. An increase in the generator temperature reduces the weak solution concentration (point3). As the degassing range is assumed to be constant at 0.3, the strong solution concentration also reduces. Hence, for a particular cooling load, the strong solution mass flow rate (point 2) must increase. This increase in mass flow rate and the increase of generator temperature cause the variation of $\dot{Q}_{rq}$ in the GAX

desorber. The $\dot{Q}_{rq}$ increases with the increase in T_g up to an optimum value of generator temperature. The increase in the generator temperature raises the absorber temperature, bringing about a higher available heat in the absorber. For evaporator temperature of $T_{evap} = 5^0C$ and condenser temperature of $T_{cond} = 40^0C$, at generator temperature up to 165ºC, the rate of increase in $\dot{Q}_{av}$ is higher than that of the $\dot{Q}_{rq}$. This leads to the reduction in $\dot{Q}_{gen}$ as the generator temperature increases up to 165ºC where the maximum COP occurs. At this point, the $\dot{Q}_{av}$is equal to $\dot{Q}_{rq}$. At the generator temperatures higher than this value, the $\dot{Q}_{av}$ is greater than the $\dot{Q}_{rq}$ and therefore entire $\dot{Q}_{av}$ is not absorbed in the GAX desorber. This results in higher value of $\dot{Q}_{gen}$ after 165ºC for given conditions and therefore, lower value of the COP.

4.2.2. Effect of generator temperature on heat duty

Q_{rq} is the rate at which heat is needed in the GAX desorber and Q_{av} is the rate at which heat is available from the GAX absorber. Q_{rq} may be less than, greater than or equal to Q_{av}. If Q_{rq} is less than Q_{av} then heat has to be rejected at greater rate from the absorber. On the other hand if $Q_{rq}$is more than Q_{av} then heat has to be supplied at greater rate to the generator

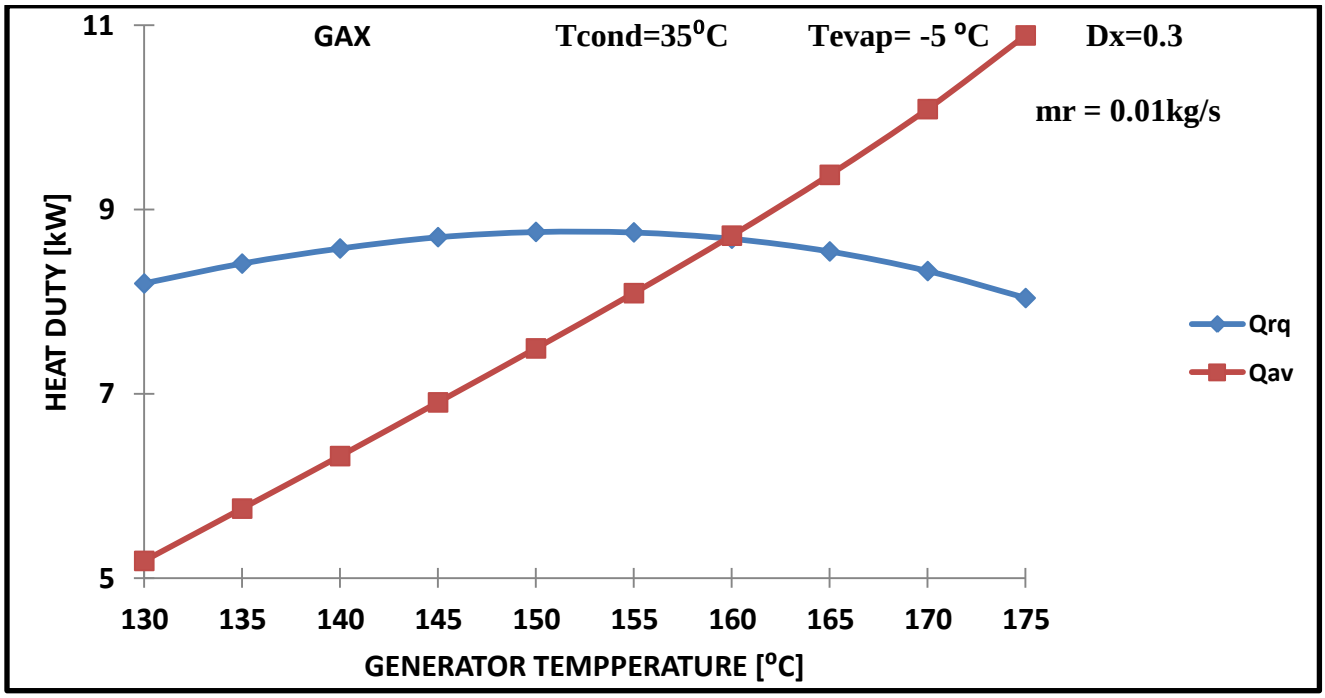

Fig.4.7. Heat duty versus T_g for GAX cycle at $T_c = 35^0C$ and $T_e = -5^0C$

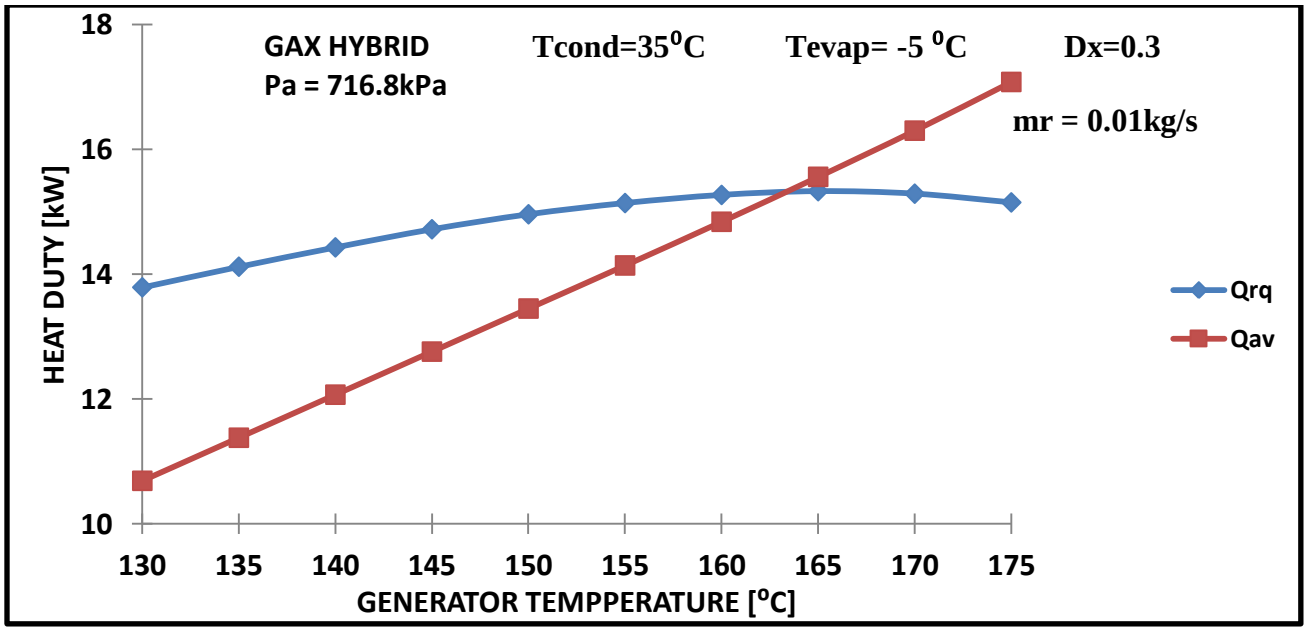

Fig.4.8. Heat duty versus T_g for GAX hybrid (P_a=716.8 kPa) at $T_c = 35^0C$ and $T_e = -5^0\,C$

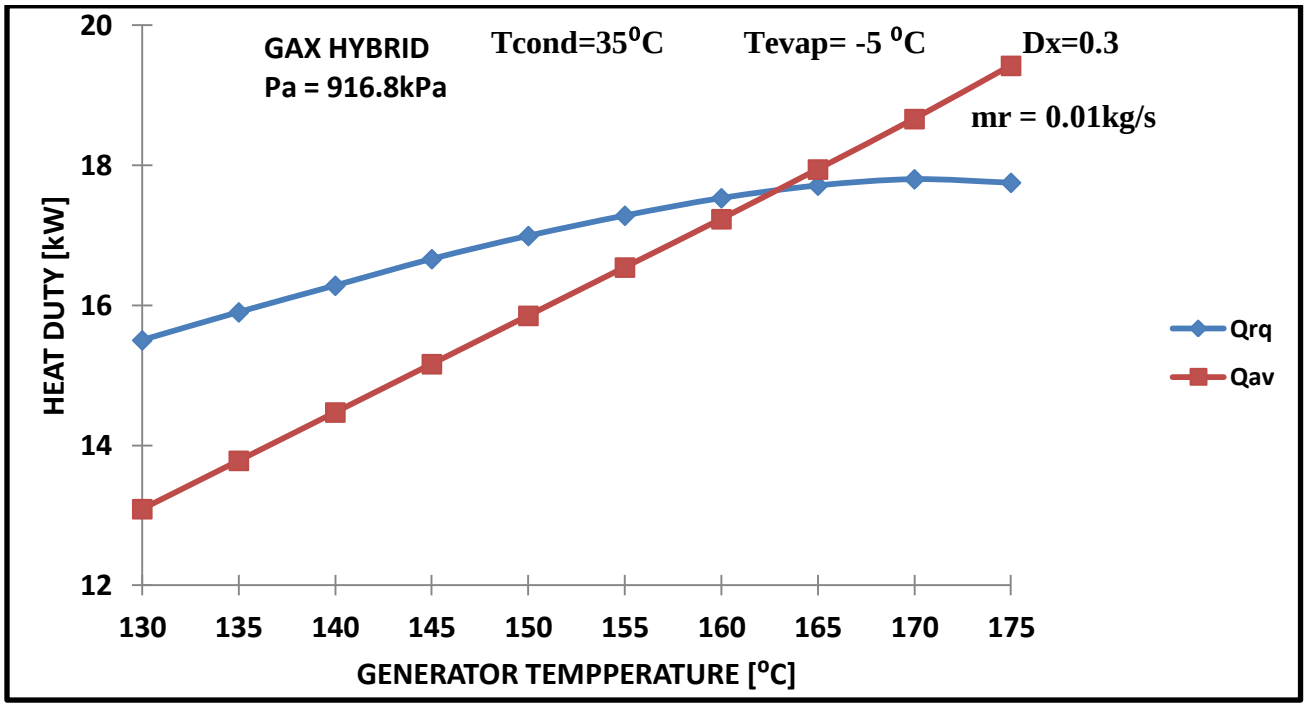

Fig.4.9. Heat duty v/s T_g for GAX hybrid (P_a=916.8 kPa) at $T_c = 35^0C$ and $T_e = -5^0C$

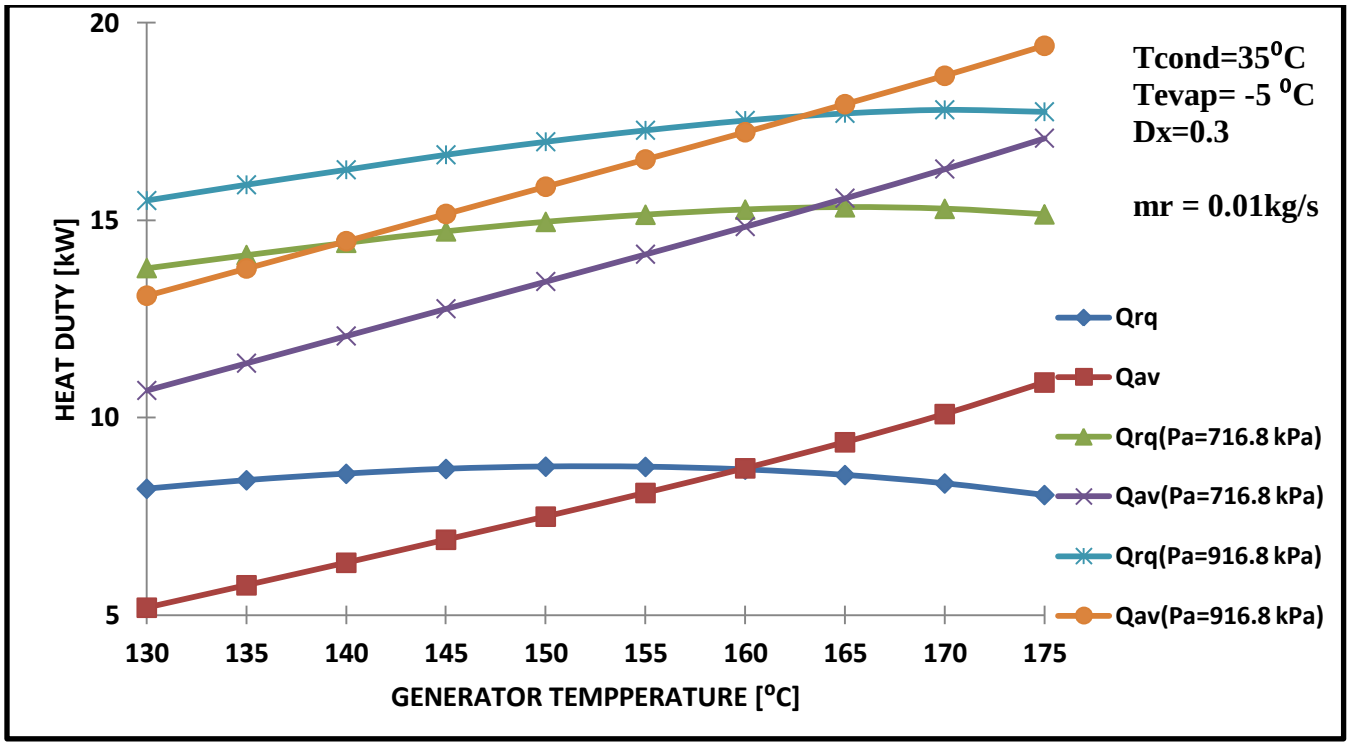

Fig.4.10. Heat duty v/s T_g at $T_c = 35^0C$ and $T_e = -5^0C$ for GAX and GAX hybrid cycles

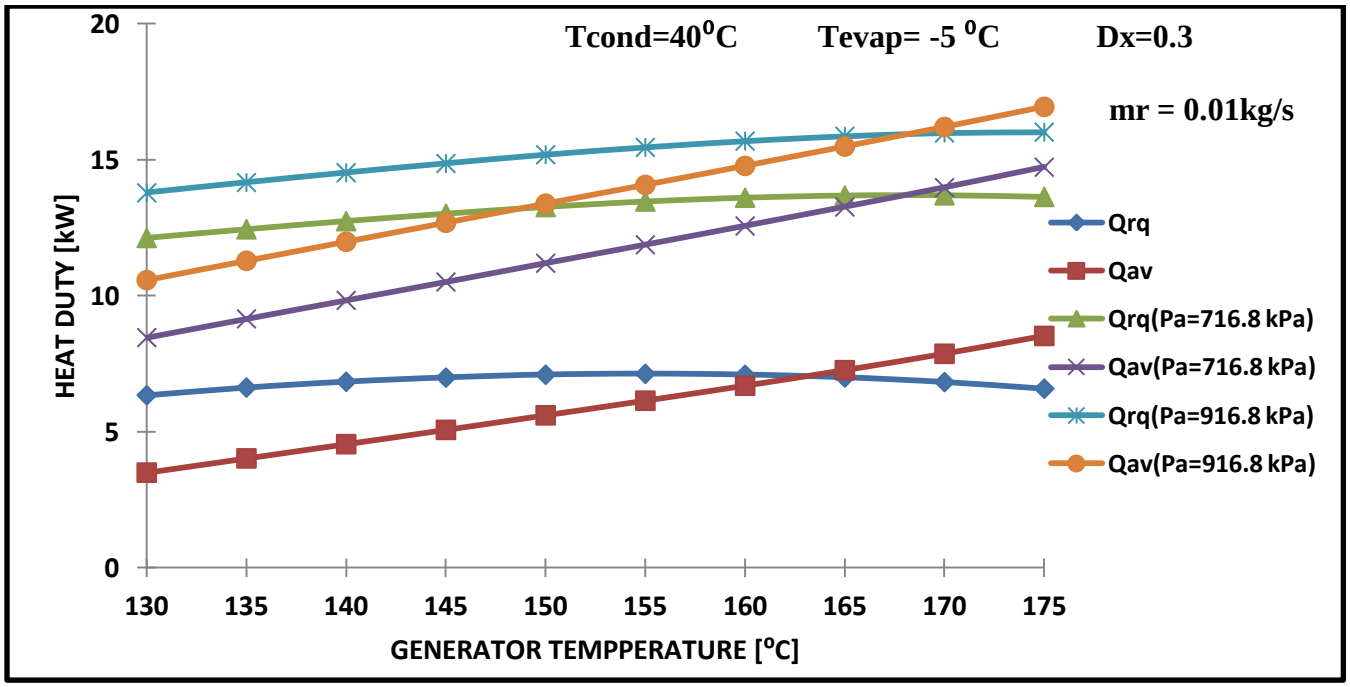

Fig.4.11. Heat duty v/s T_g at $T_c = 40^0C$ and $T_e = -5^0C$ for GAX and GAX hybrid cycles

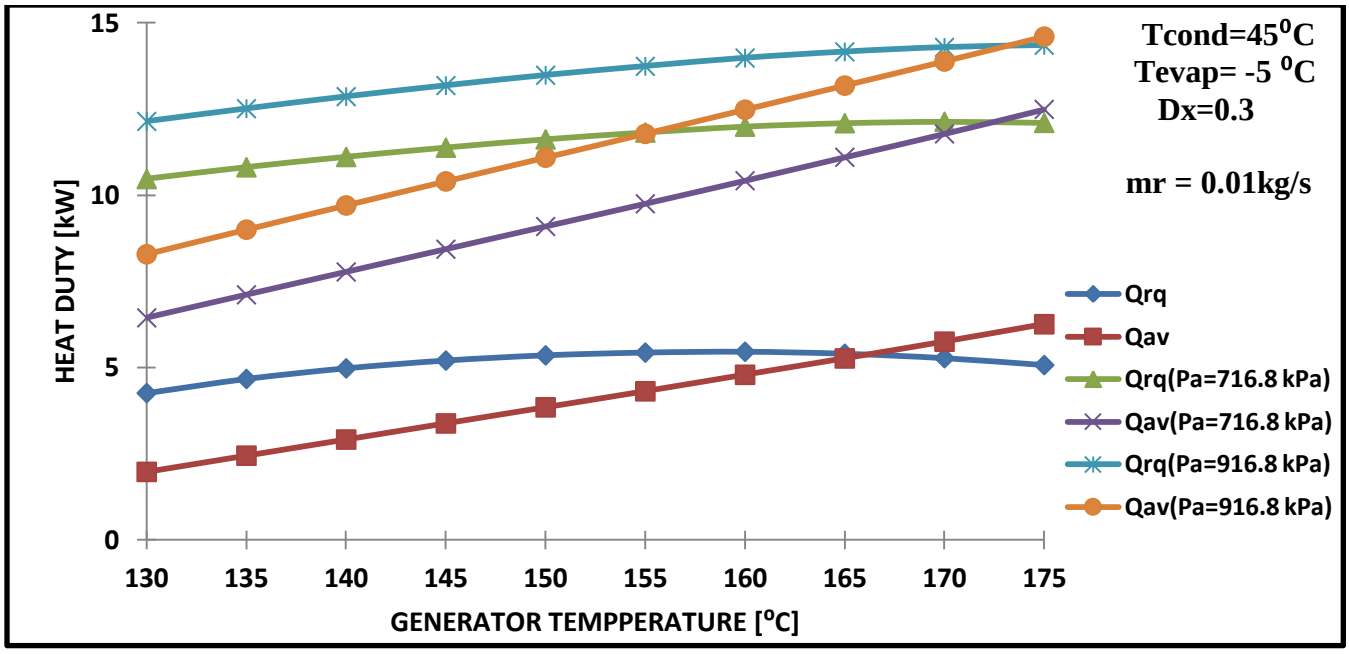

Fig.4.12. Heat duty v/s T_g at $T_c = 45^0C$ and $T_e = -5^0C$ for GAX and GAX hybrid cycles

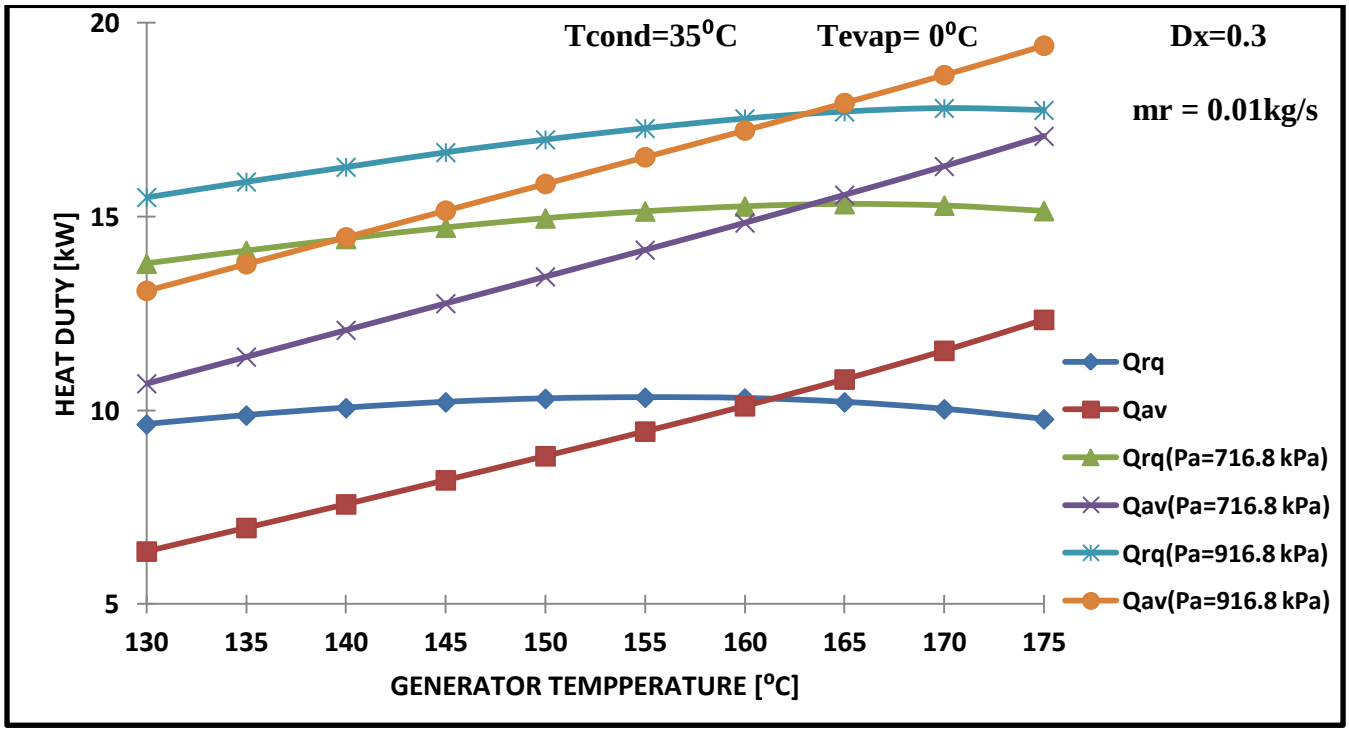

Fig.4.13. Heat duty v/s T_g at $T_c = 35^0C$ and $T_e = 0^0C$ for GAX and GAX hybrid cycles

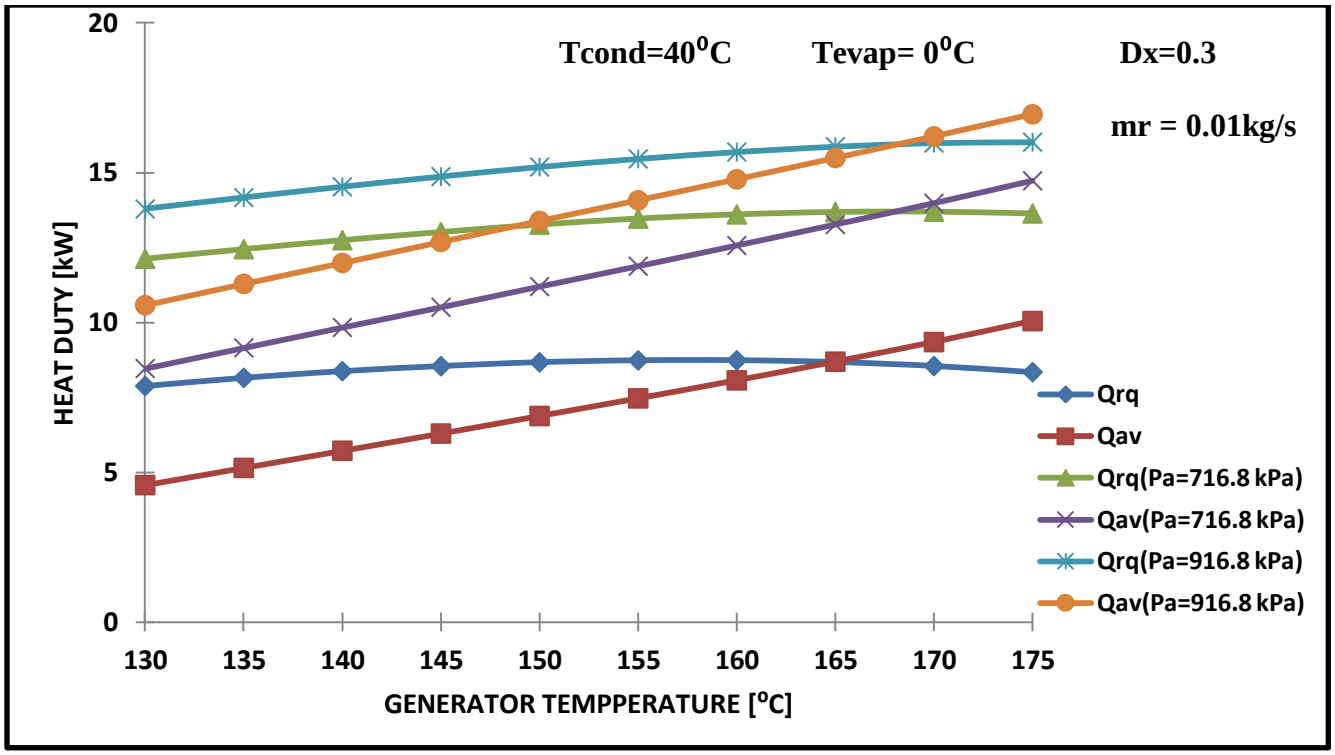

Fig.4.14. Heat duty v/s T_g at $T_c = 40^0C$ and $T_e = 0^0C$ for GAX and GAX hybrid cycles

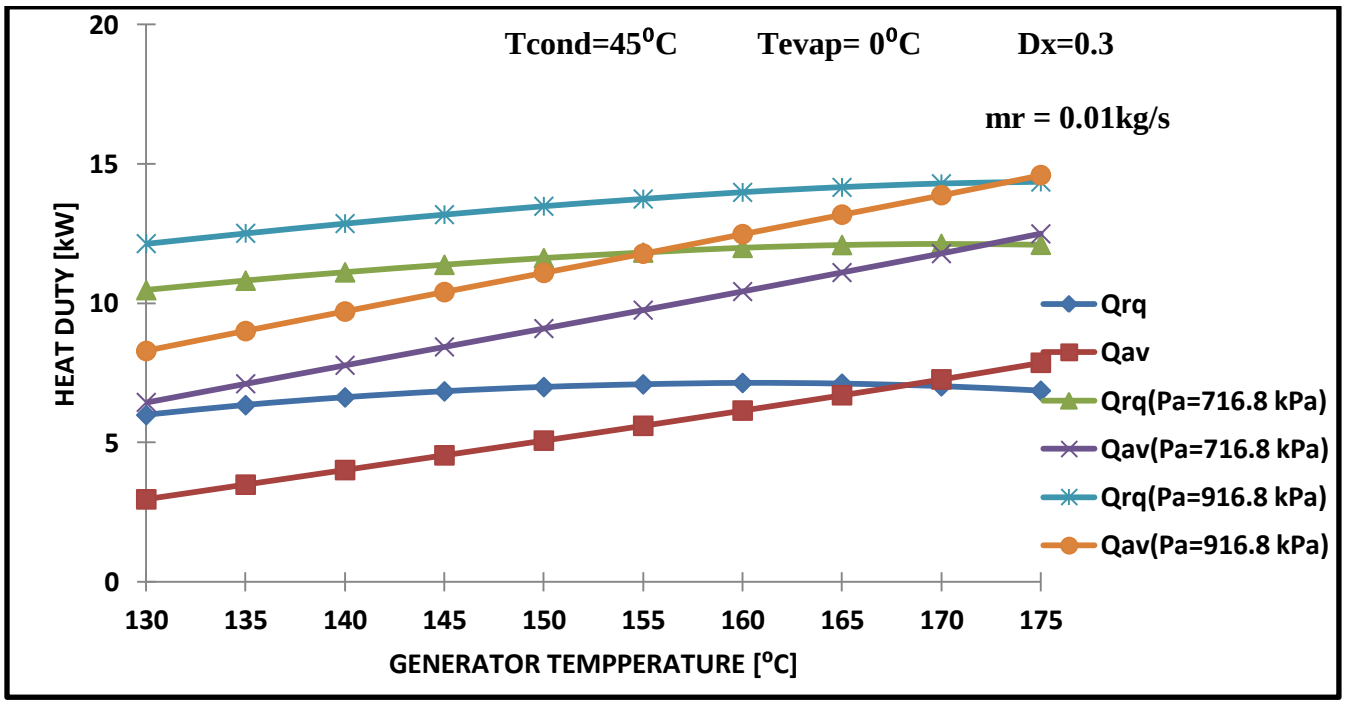

Fig.4.15. Heat duty v/s T_g at $T_c = 45^0C$ and $T_e = 0^0C$ for GAX and GAX hybrid cycles

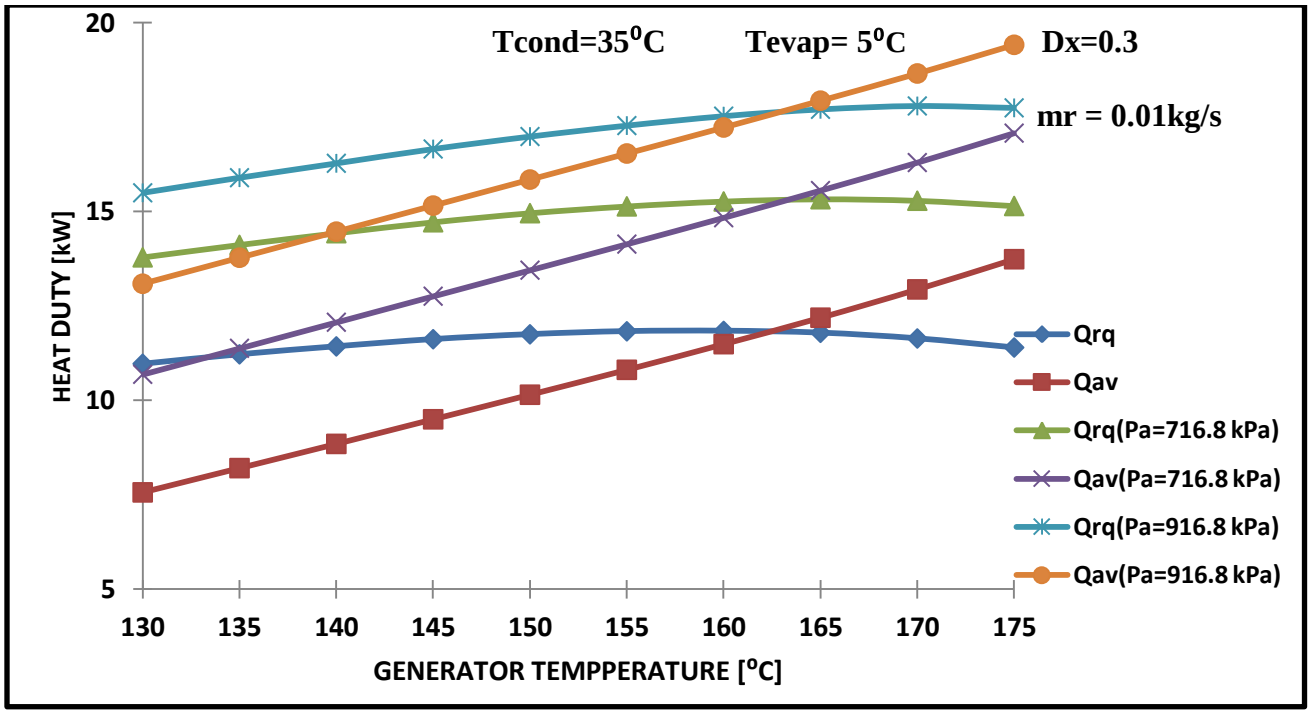

Fig.4.16. Heat duty v/s T_g at $T_c = 35^0C$ and $T_e = 5^0C$ for GAX and GAX hybrid cycles

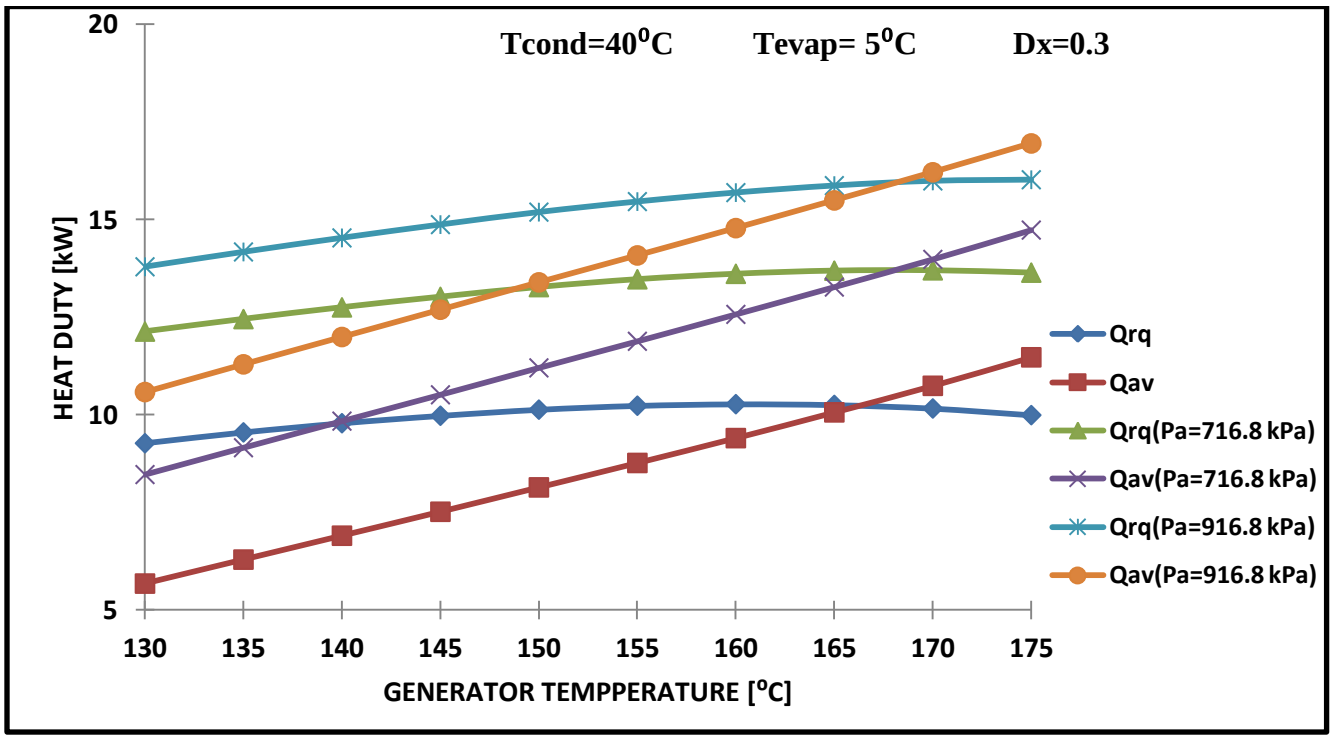

Fig.4.17. Heat duty v/s T_g at $T_c = 40^0C$ and $T_e = 5^0C$ for GAX and GAX hybrid cycles

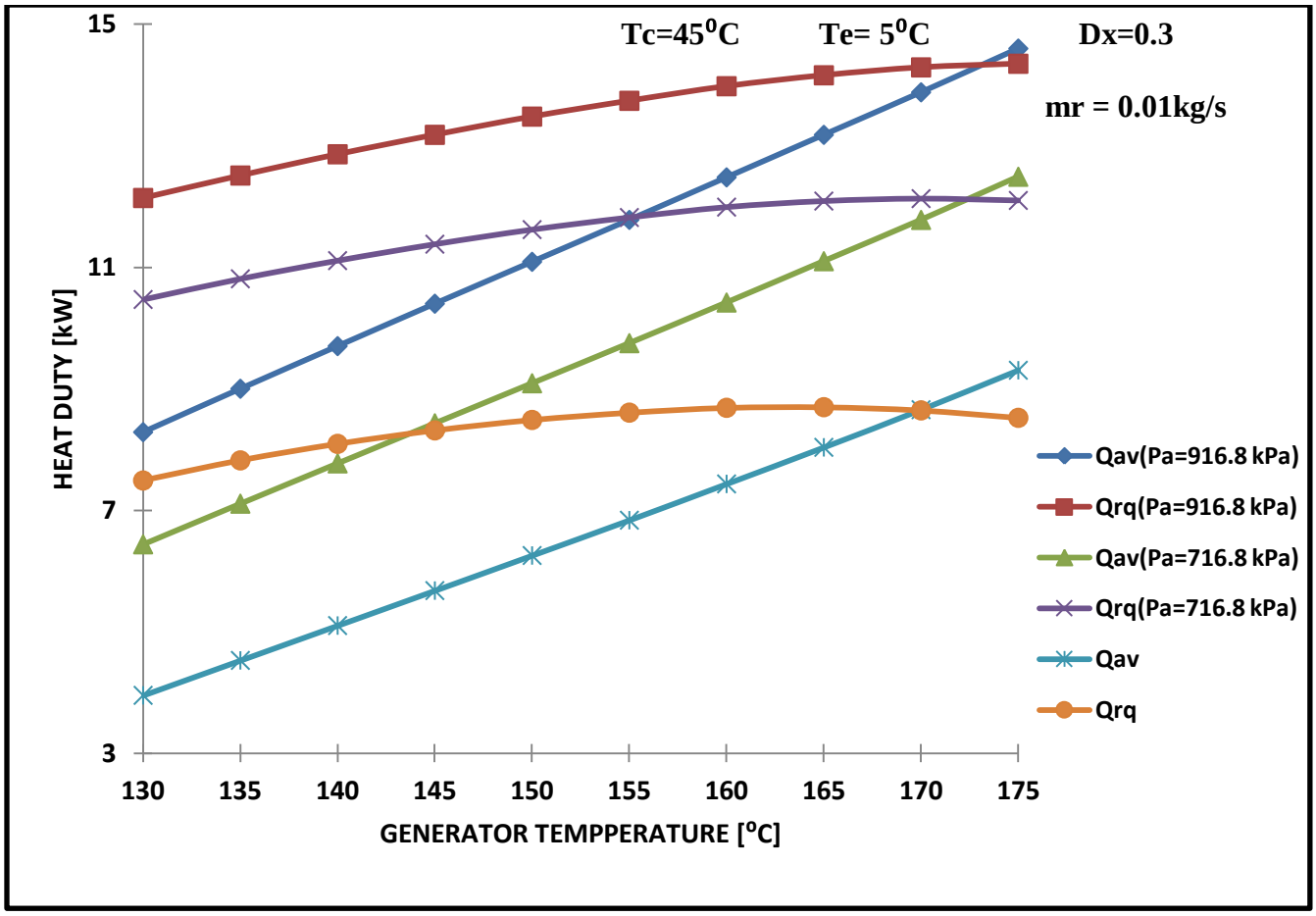

Fig.4.18. Heat duty v/s T_g at $T_c = 45^0C$ and $T_e = 5^0C$ for GAX and GAX hybrid cycles

Figures 4.7 to 4.18 show the variation of available heat in the absorber $\dot{Q}_{av}$ and required heat in the generator $\dot{Q}_{rq}$ with the generator temperature T_g for the GAX and GAX hybrid cycles at different evaporator and condenser temperatures. From the fig.4.18 it is obvious that the required heat in the generator of GAX hybrid cycles is more than that of the GAX cycle. This difference increases with the absorber pressure of GAX hybrid cycle. The average difference is around 5 kW. The variation of available heat with generator temperature reveals that $\dot{Q}_{av}$ increases as T_g increases. It is to be noted that as the total heat rate requirement in desorber for both the cycles is same, the lower values of $\dot{Q}_{av}$ in the case of GAX cycle results in lower values of COP.

4.2.3. Effect of generator temperature on heat transfer rate

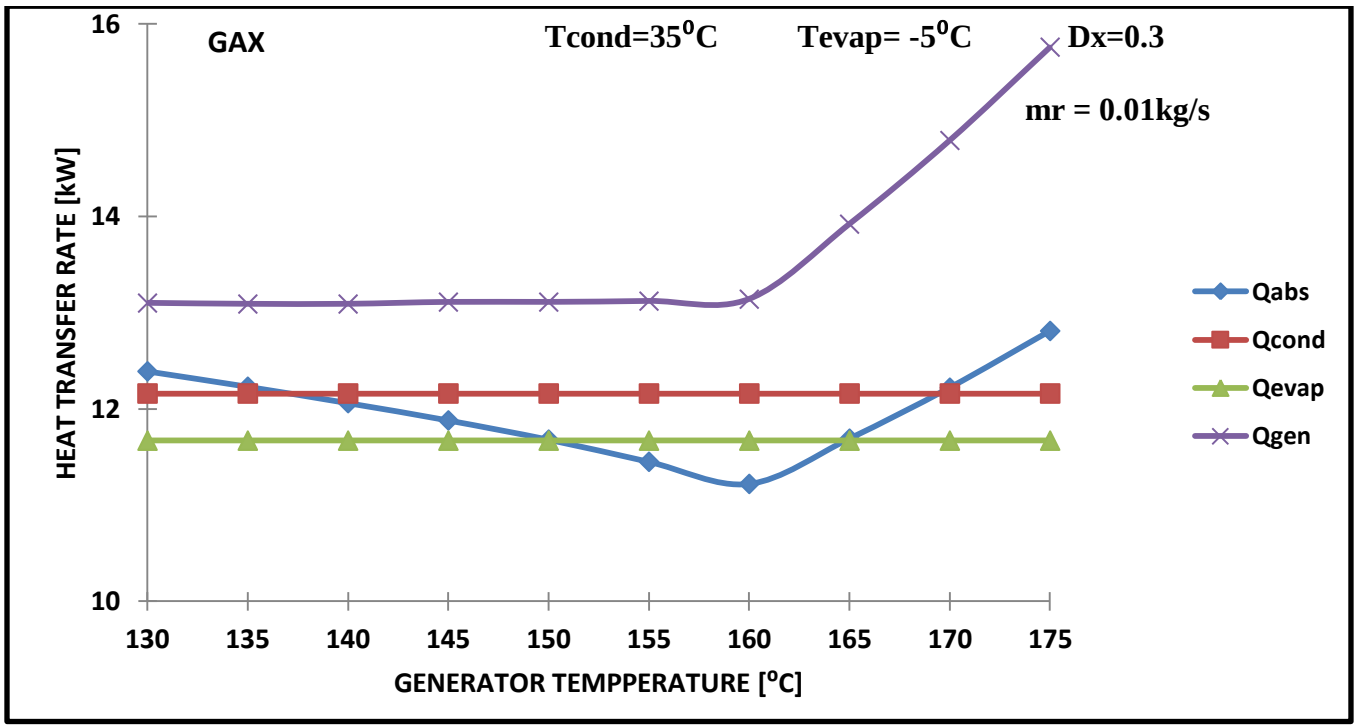

Fig.4.19. Variation of heat transfer rate with T_g at $T_c = 35^0C$ and $T_e = -5^0C$ for GAX cycle

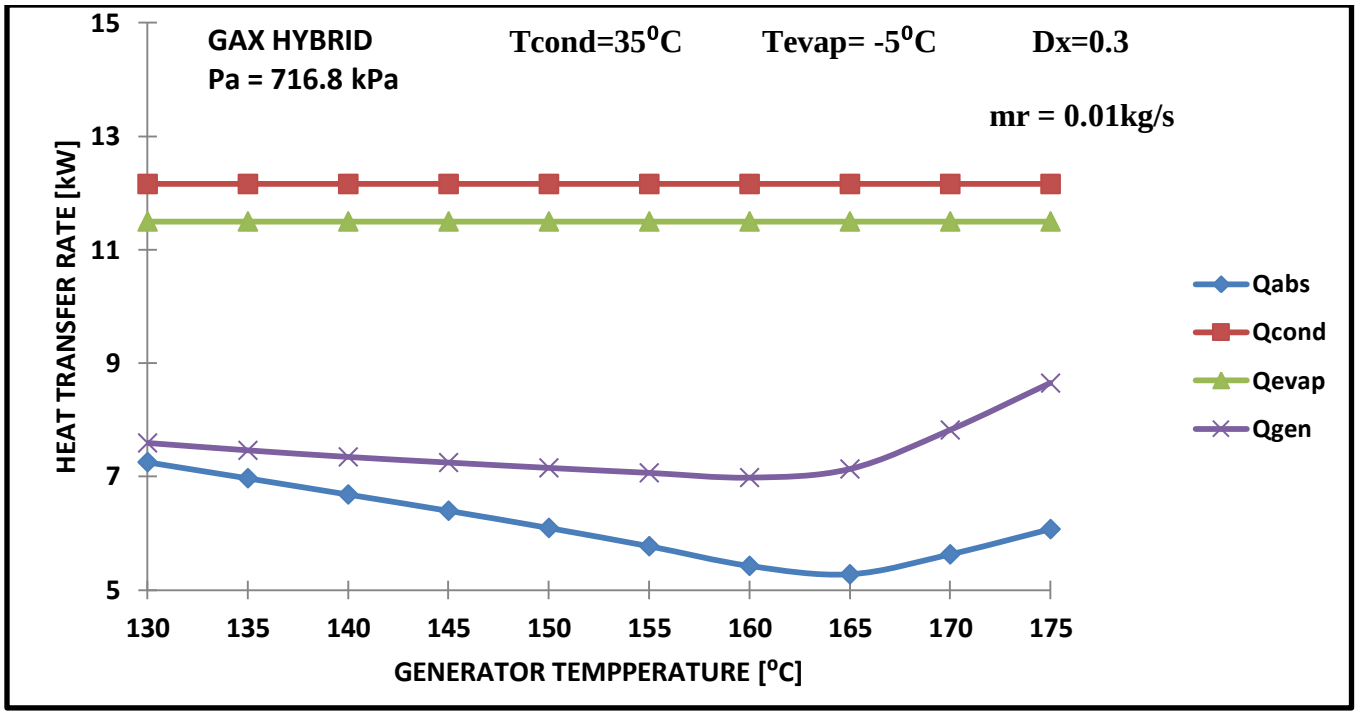

Fig.4.20. Variation of heat transfer rate with T_g at $T_c = 35^0C$ and $T_e = -5^0C$ for GAX hybrid cycle (P_a=716.8 kPa)

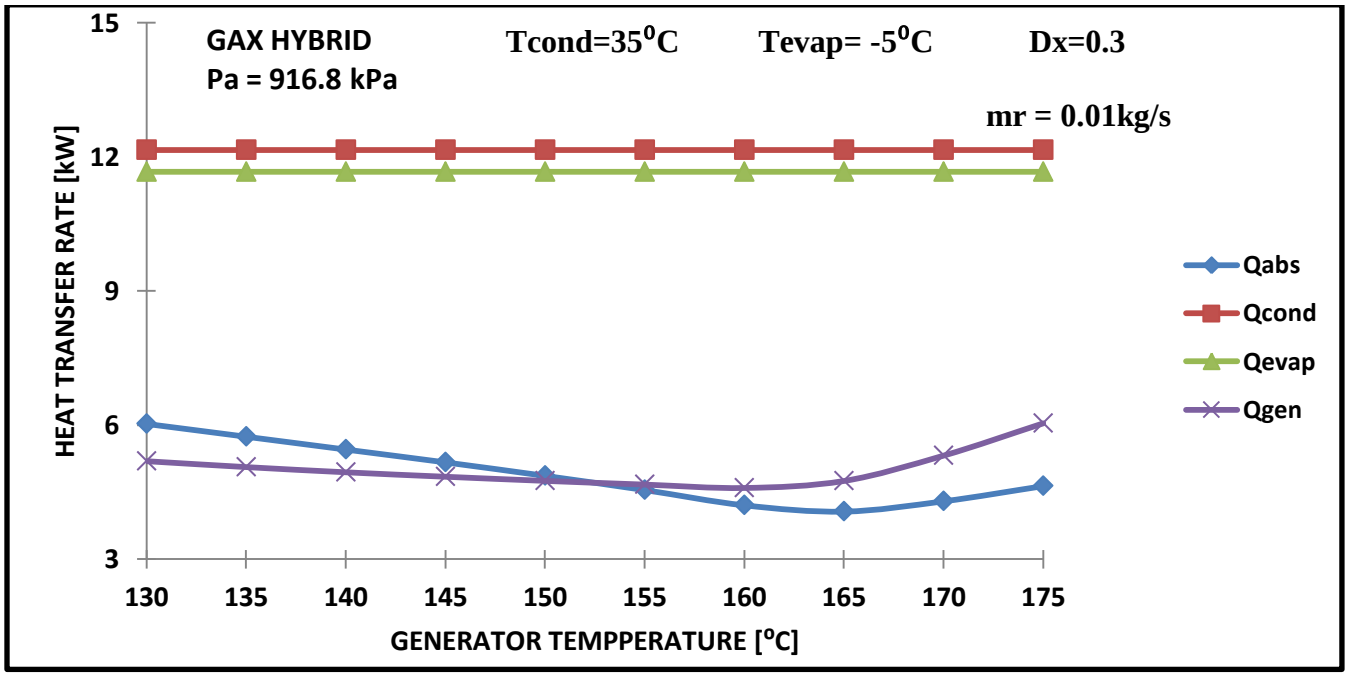

Fig.4.21. Variation of heat transfer rate with T_g at $T_c = 35^0C$ and $T_e = -5^0C$ for GAX hybrid cycle (Pa=916.8 kPa)

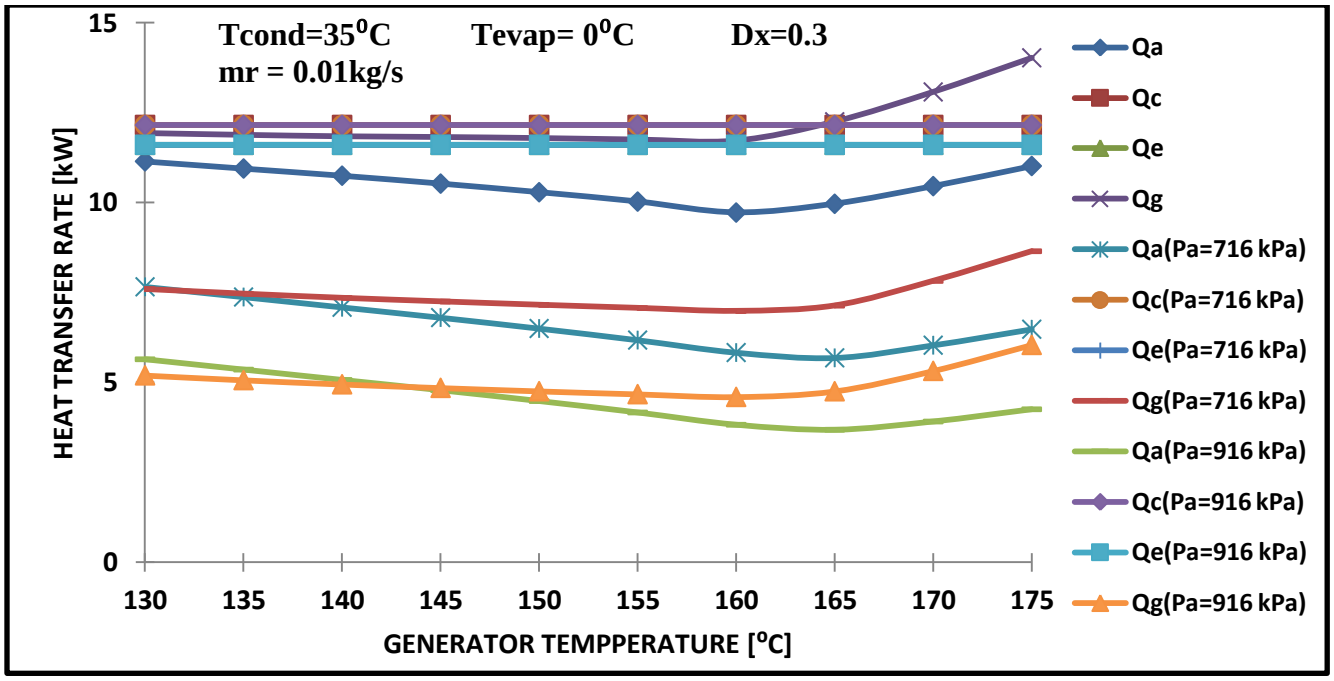

Fig.4.22. Variation of heat transfer rate with T_g at $T_c = 35^0C$ and $T_e = 0^0C$

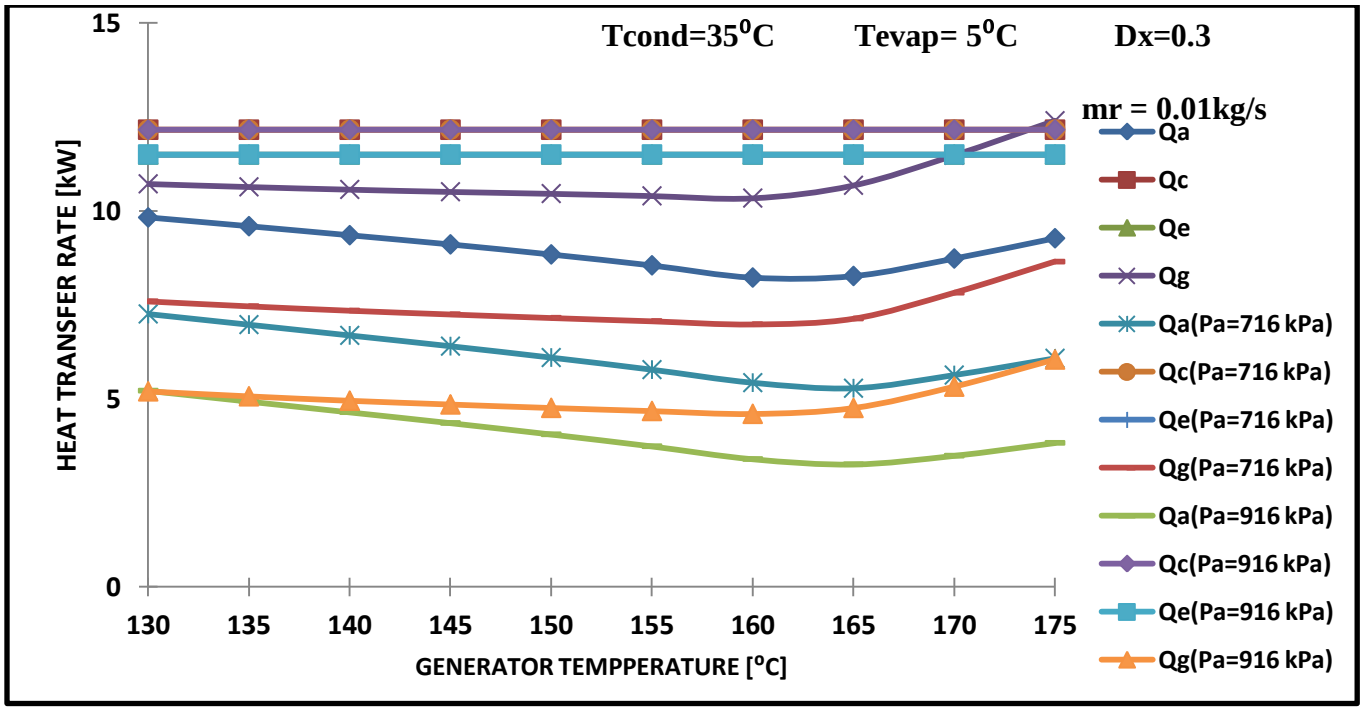

Fig.4.23. Variation of heat transfer rate with T_g at $T_c = 35^0C$ and $T_e = 5^0C$

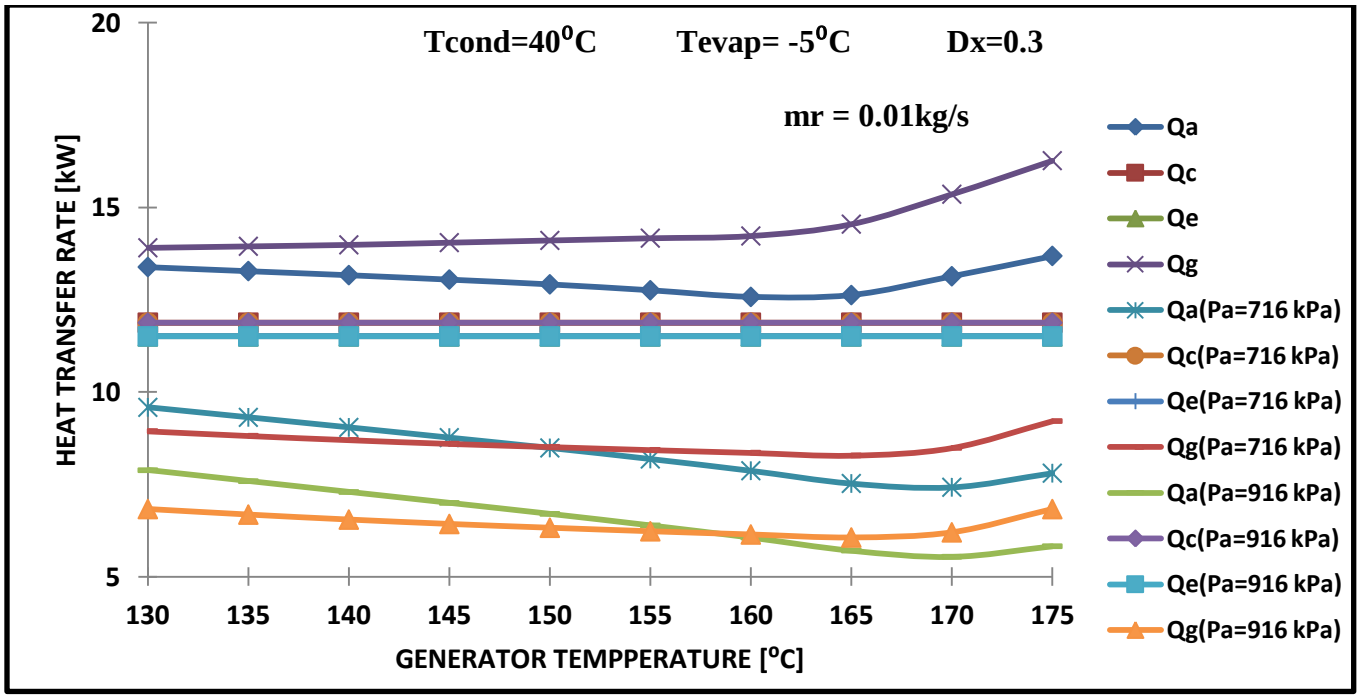

Fig.4.24. Variation of heat transfer rate with T_g at $T_c = 40^0C$ and $T_e = -5^0C$

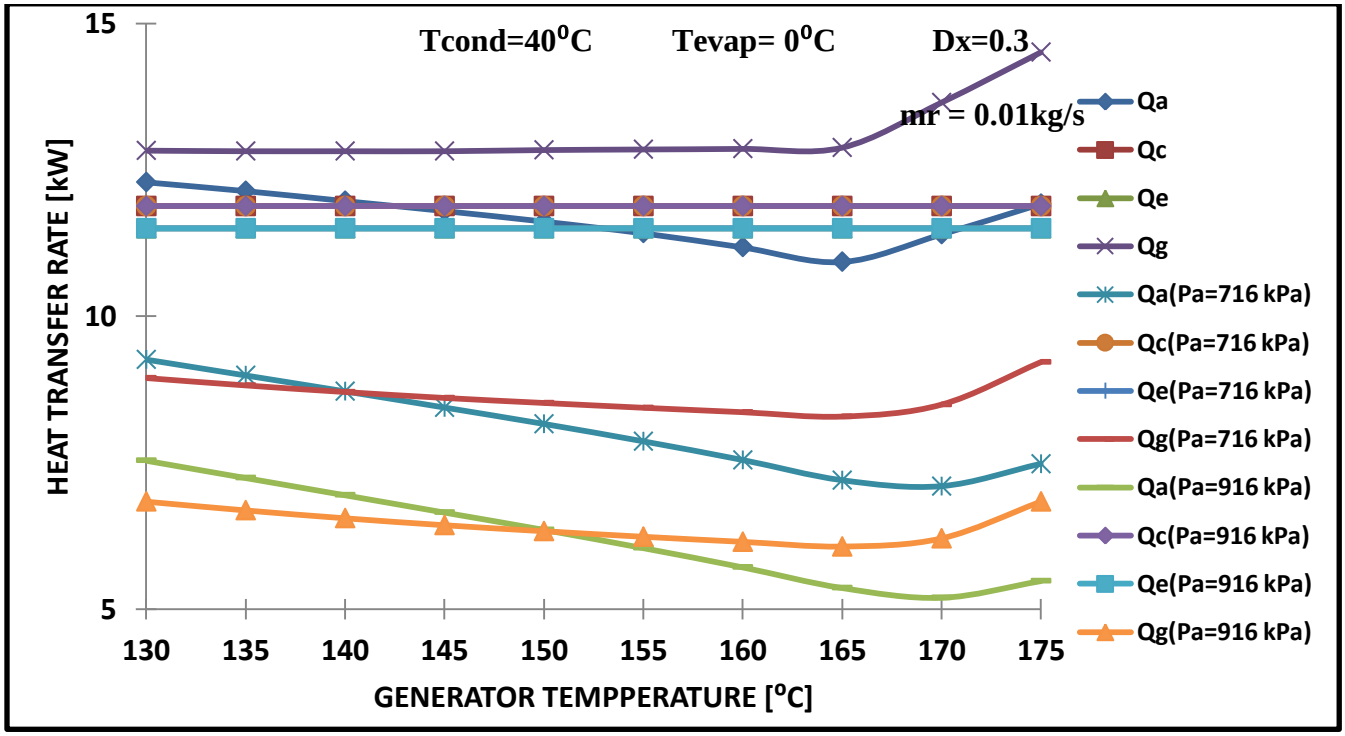

Fig.4.25. Variation of heat transfer rate with T_g at $T_c = 40^0C$ and $T_e = 0^0C$

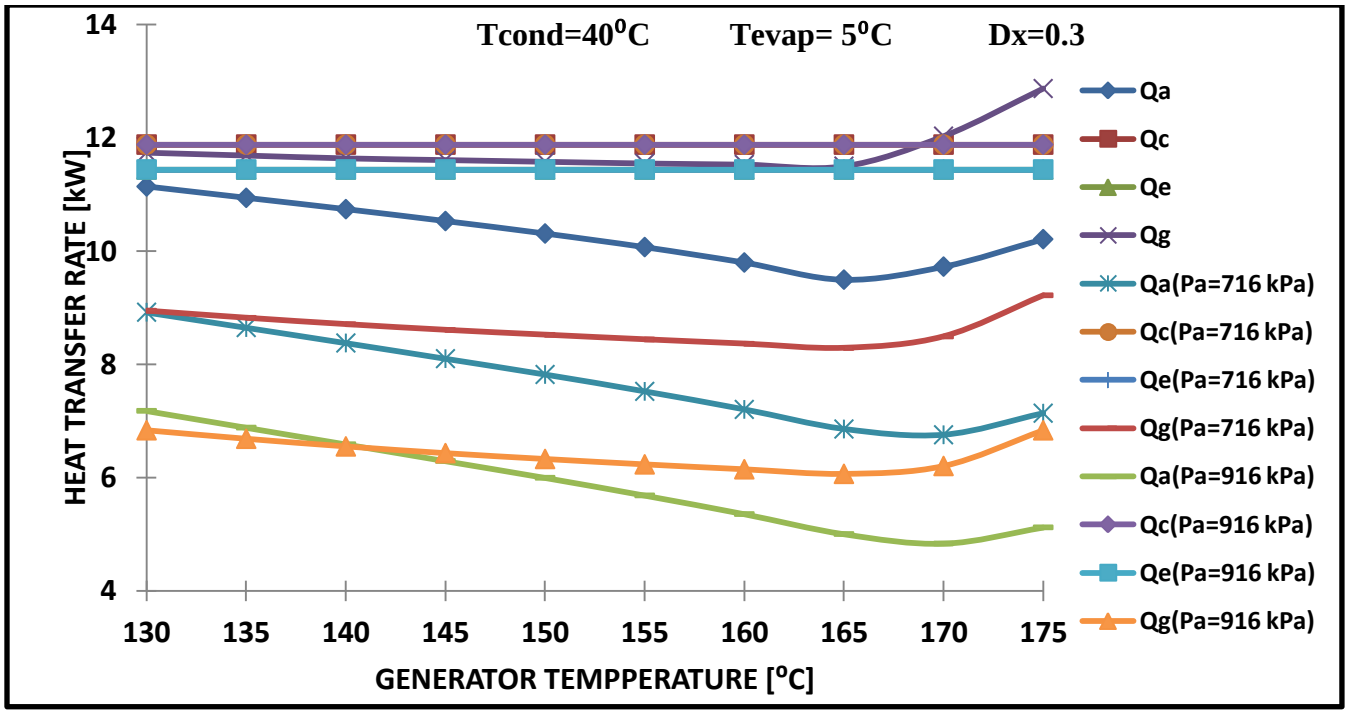

Fig.4.26. Variation of heat transfer rate with T_g at $T_c = 40^0C$ and $T_e = 5^0C$

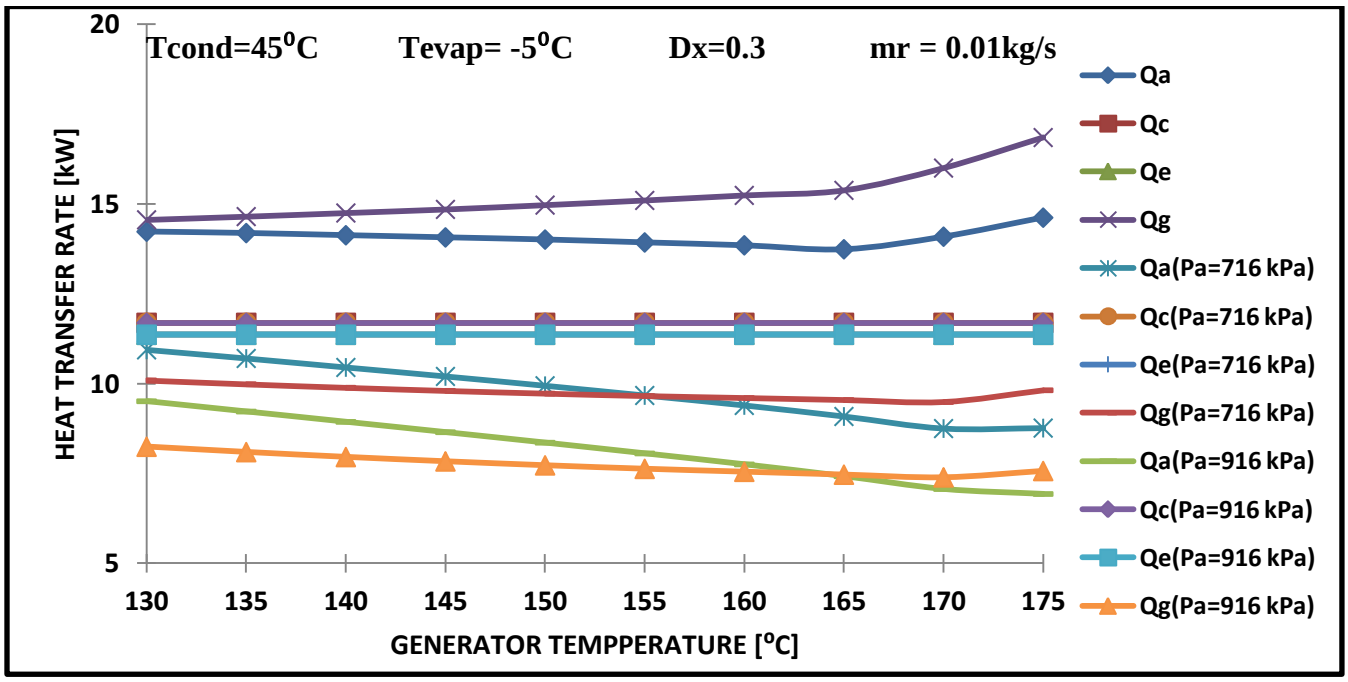

Fig.4.27. Variation of heat transfer rate with T_g at $T_c = 45^0C$ and $T_e = -5^0C$

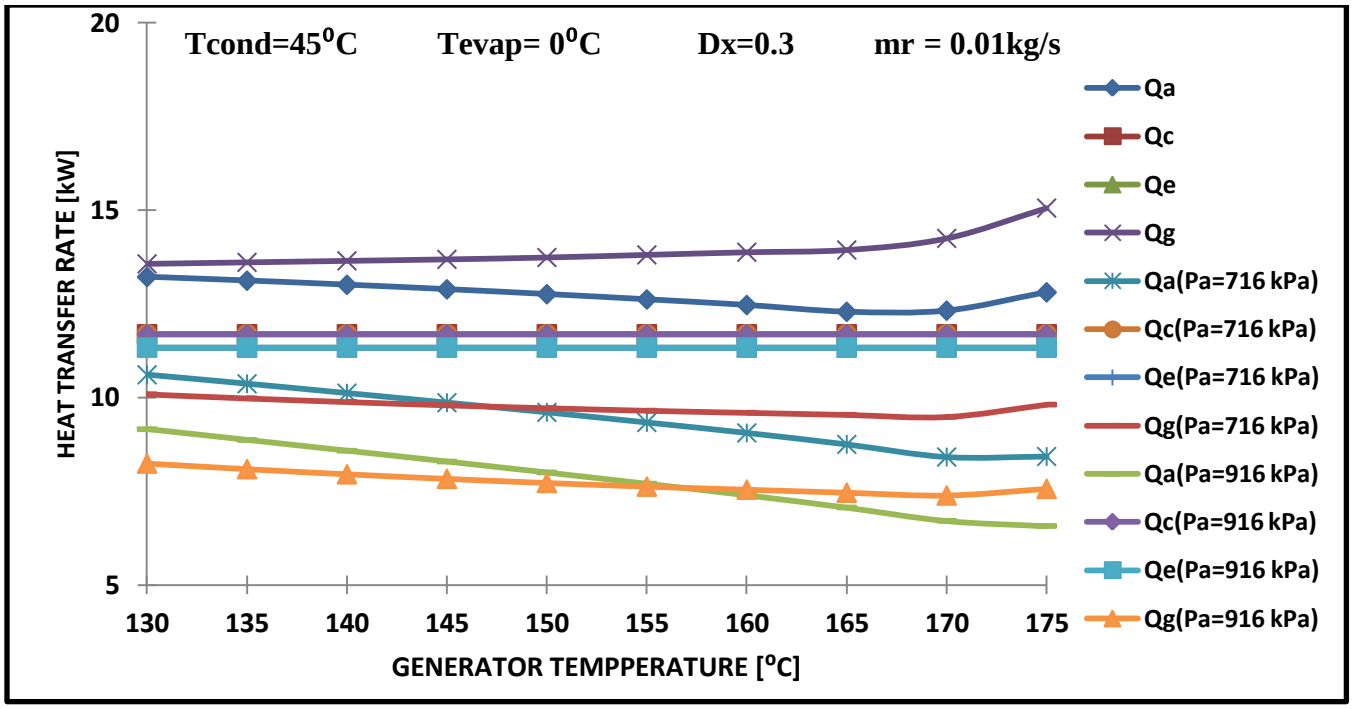

Fig.428. Variation of heat transfer rate with T_g at $T_c = 45^0C$ and $T_e = 0^0C$

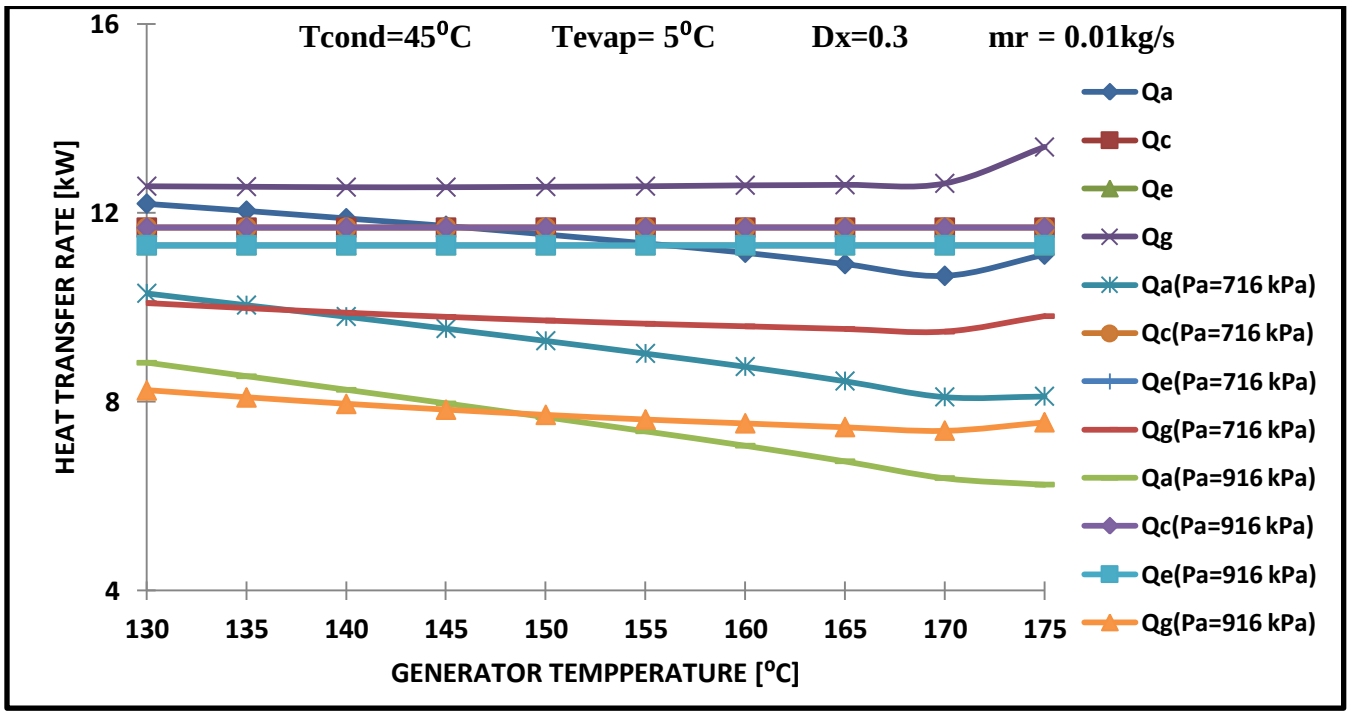

Fig.4.29. Variation of heat transfer rate with T_g at $T_c = 45^0C$ and $T_e = 5^0C$

Figures 4.19 to 4.29 show the variation of heat transfer rate in absorber $\dot{Q}_a$, condenser $\dot{Q}_c$, evaporator $\dot{Q}_e$, generator $\dot{Q}_g$ with generator temperature T_g. In all cases as the generator temperature increases, the evaporator thermal load $\dot{Q}_e$ and condenser thermal load $\dot{Q}_c$ remain constant.

As shown in these figures, when generator temperature increases, the absorber thermal load $\dot{Q}_a$and generator thermal load $\dot{Q}_g$ decreases. There is a particular value of generator temperature T_g at which $\dot{Q}_g$and $\dot{Q}_a$are minimum resulting in the better performance. Gomri [21] reported the similar results for single and double effect refrigeration cycles. These figures also reveal that increase in condenser temperature results in increase in the generator and absorber thermal loads. However, the variation of condenser temperature causes negligible change in condenser and evaporator thermal loads.

The figures show that generator thermal load $\dot{Q}_g$ for GAX cycle is higher than that for the GAX hybrid cycle. For the GAX hybrid cycles, higher absorber pressure results in lower $\dot{Q}_g$ that is $\dot{Q}_g$ is higher at lower absorber pressure.

4.2.4 Effect of degassing range on COP

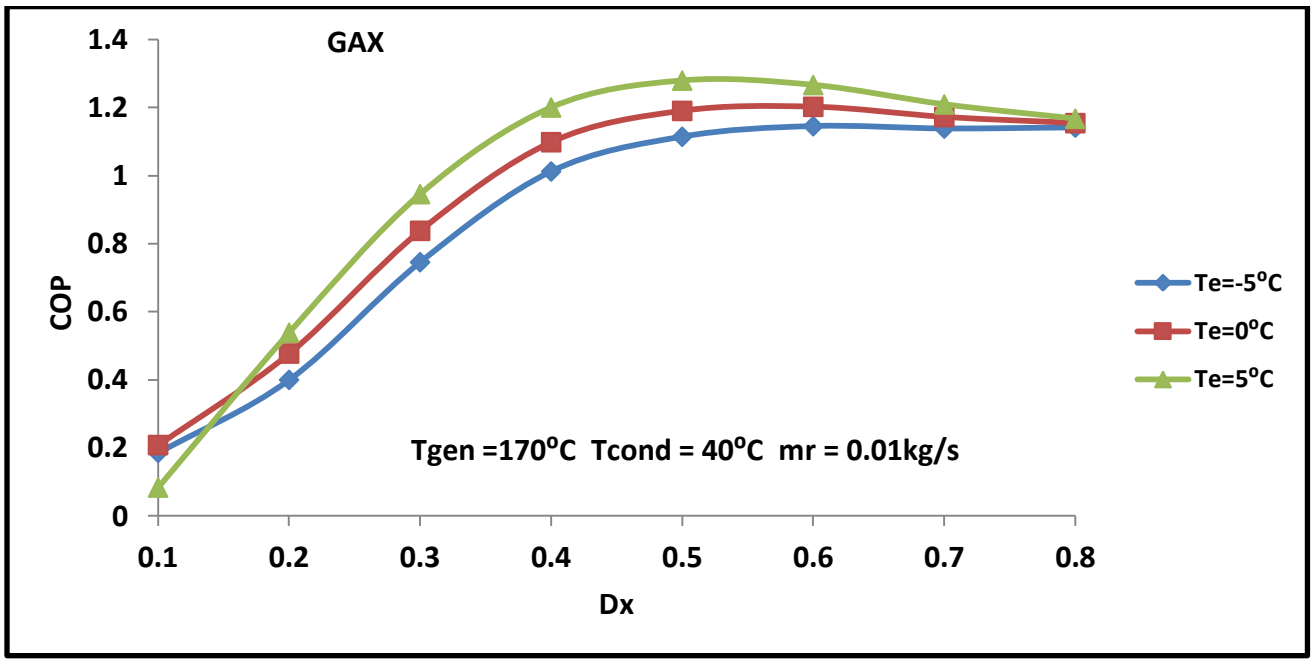

Fig.4.30. Variation of COP with degassing range for GAX cycle

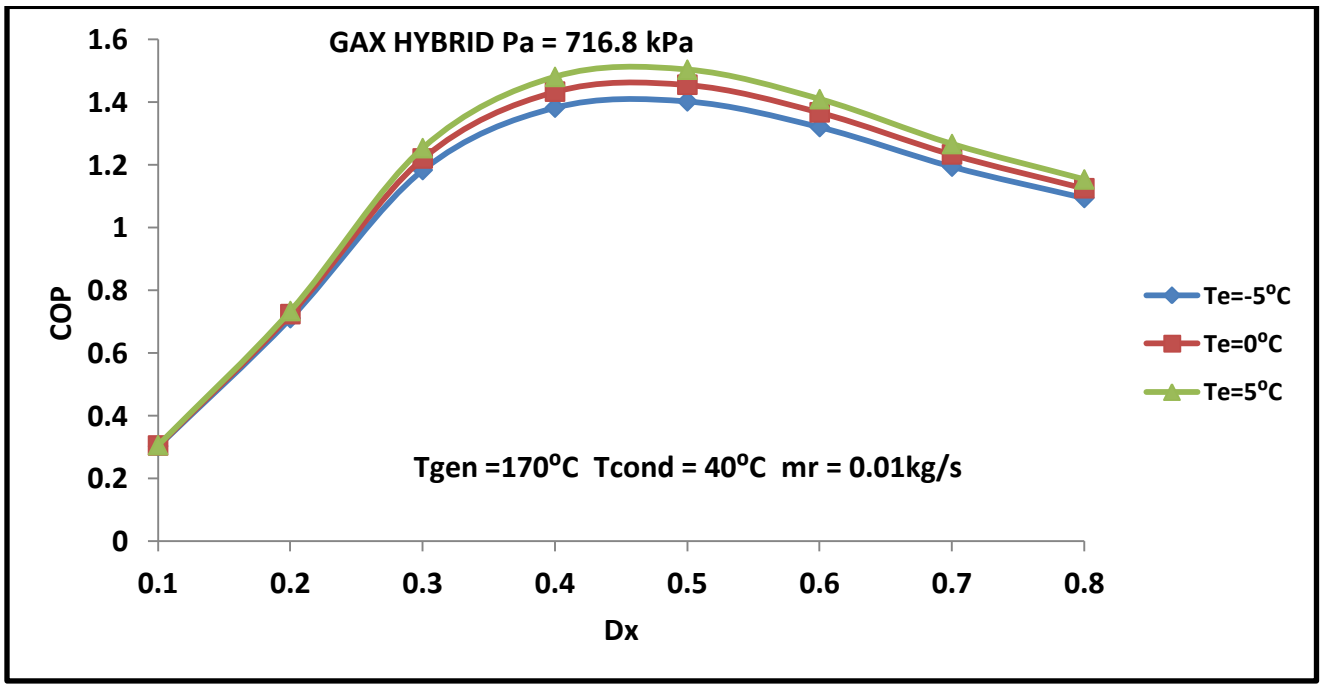

Fig.4.31. Variation of COP with degassing range for GAX hybrid cycle (Pa = 716.8 kPa)

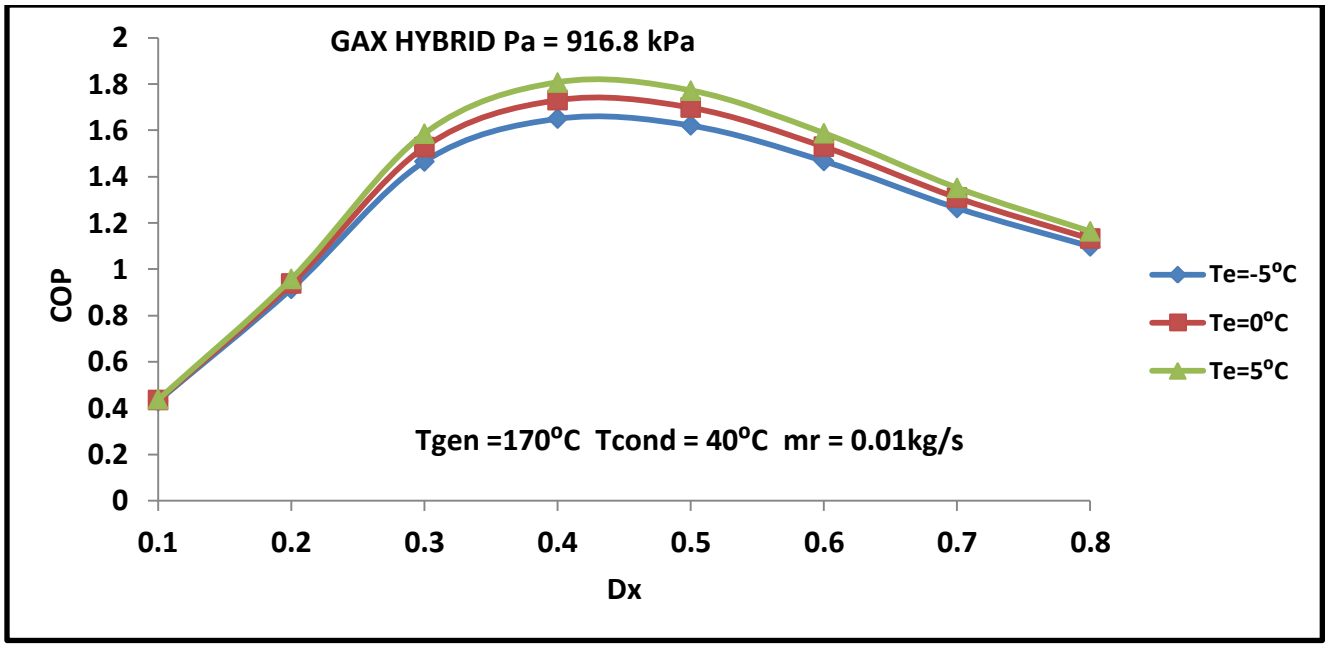

Fig.4.32. Variation of COP with degassing range for GAX hybrid cycle (Pa = 916.8 kPa)

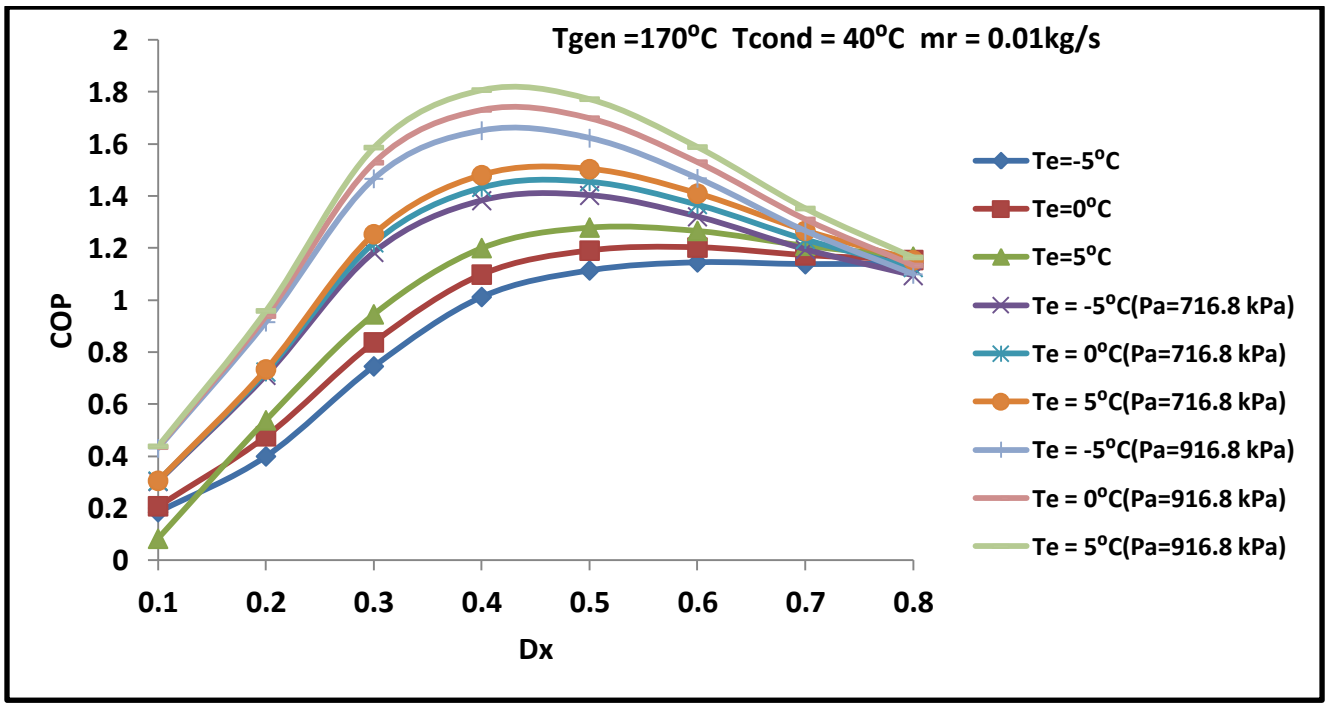

Fig.4.33. Variation of COP with degassing range for GAX and GAX hybrid cycles

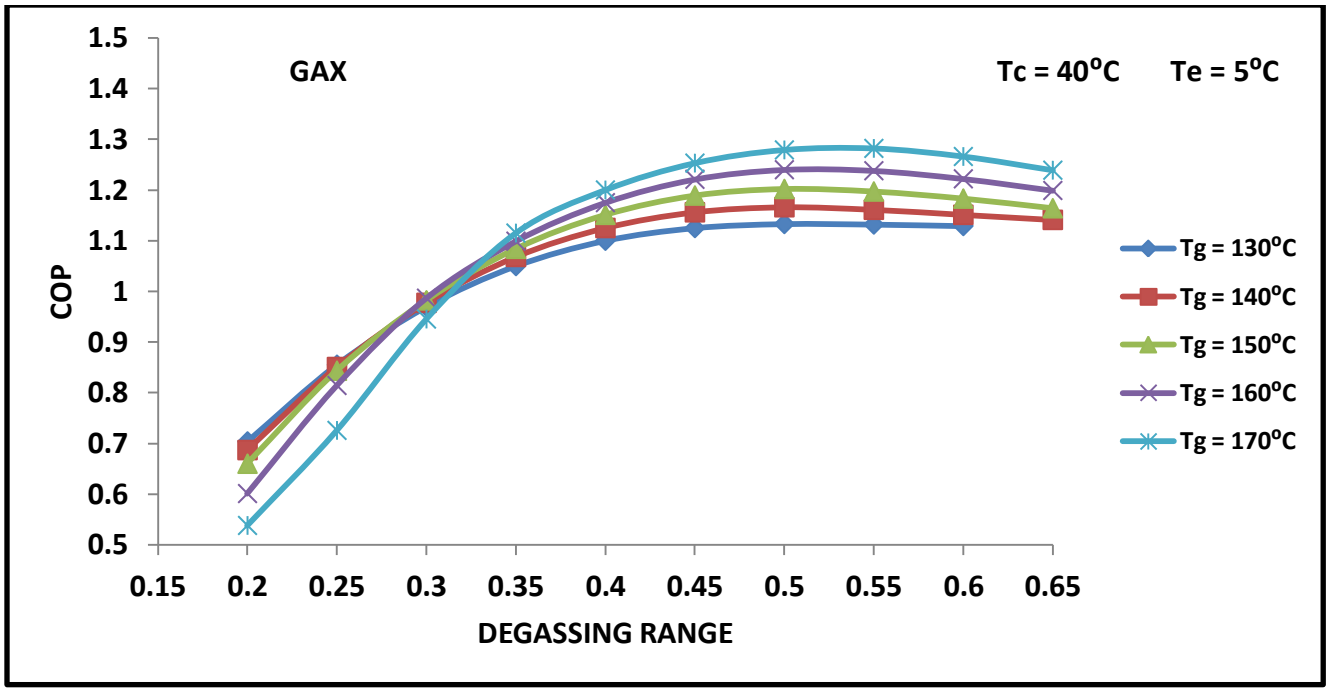

Fig.4.34. Variation of COP with degassing range for GAX cycle at different T_g

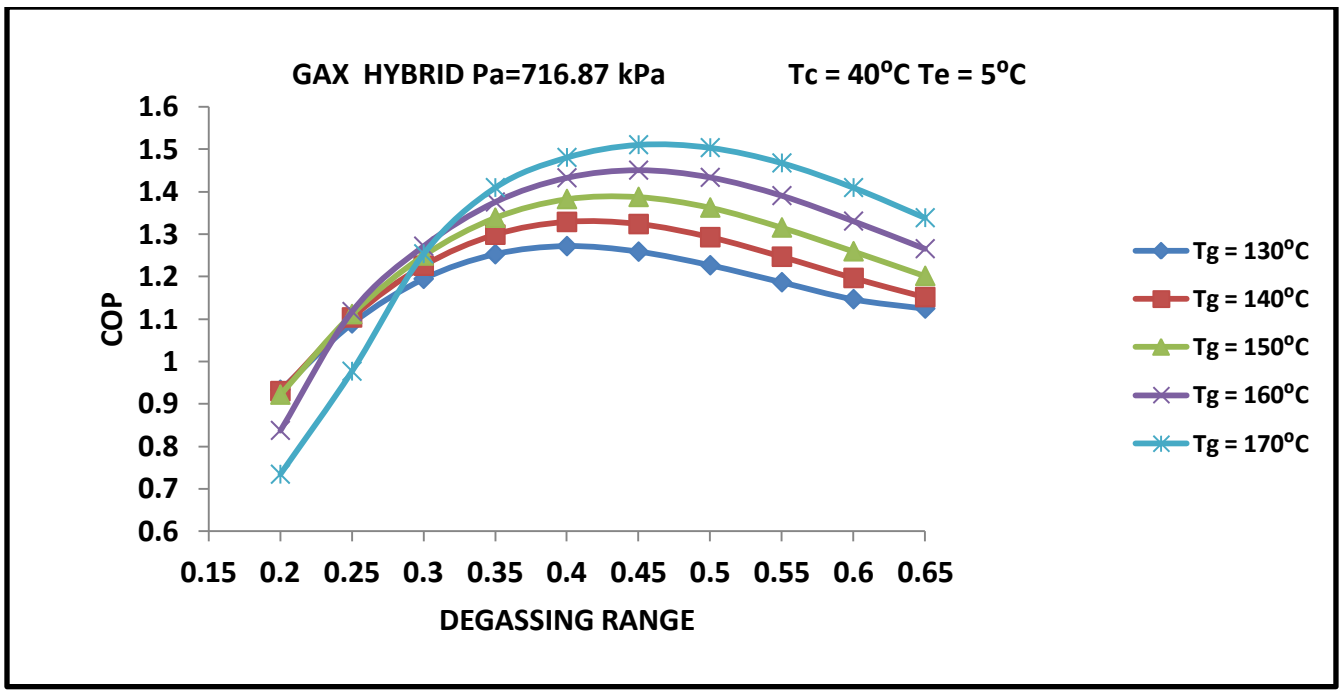

Fig.4.35. Variation of COP with degassing range for GAX hybrid cycle at different T_g

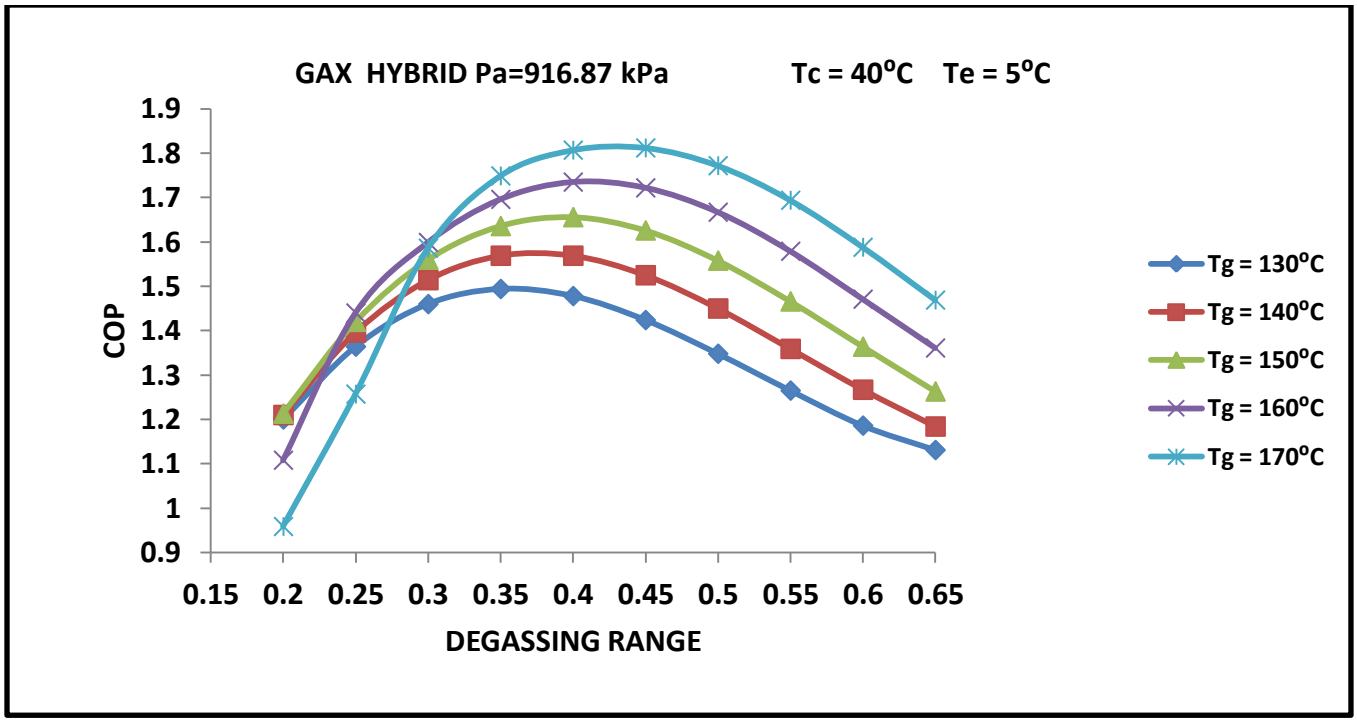

Fig.4.36. Variation of COP with degassing range for GAX hybrid cycle at different T_g

Figures 4.30 to 4.36 show the effects of varying degassing range on COP for GAX and GAX hybrid cycles. The degassing range at which COP attains the maximum value for a fixed value of generator, condenser and evaporator temperature is called the optimum degassing range. For a fixed condition of generator, absorber, condenser and evaporator, as the degassing range increases there is increase in COP. At a particular value of degassing range maximum COP is obtained. Further increment in degassing range causes reduction in COP. For a fixed value of degassing range, greater the generator temperature greater is the COP. It can also be deducted that increasing the absorber pressure in GAX hybrid cycle increases the COP for each degassing range.

Approximately 27%of the average increment in COP occurs within the degassing range of 0.2 to 0.5 when GAX and GAX hybrid (P_a = 716. 87 kPa) systems are compared. The COP of GAX hybrid system starts decreasing when the degassing range crosses the value of 0.4. This can be explained as follows. The required mass flow rate at state point 13_v in the cycle initially increases and then decreases with the increase in the degassing range; this in turn decreases the heat availability $\dot{Q}_{av}$. Further, as shown in fig.4.37 the rate of decrease in mass flow rate is much higher at higher degassing range. These two effects decrease the COP of the GAX hybrid cycle.

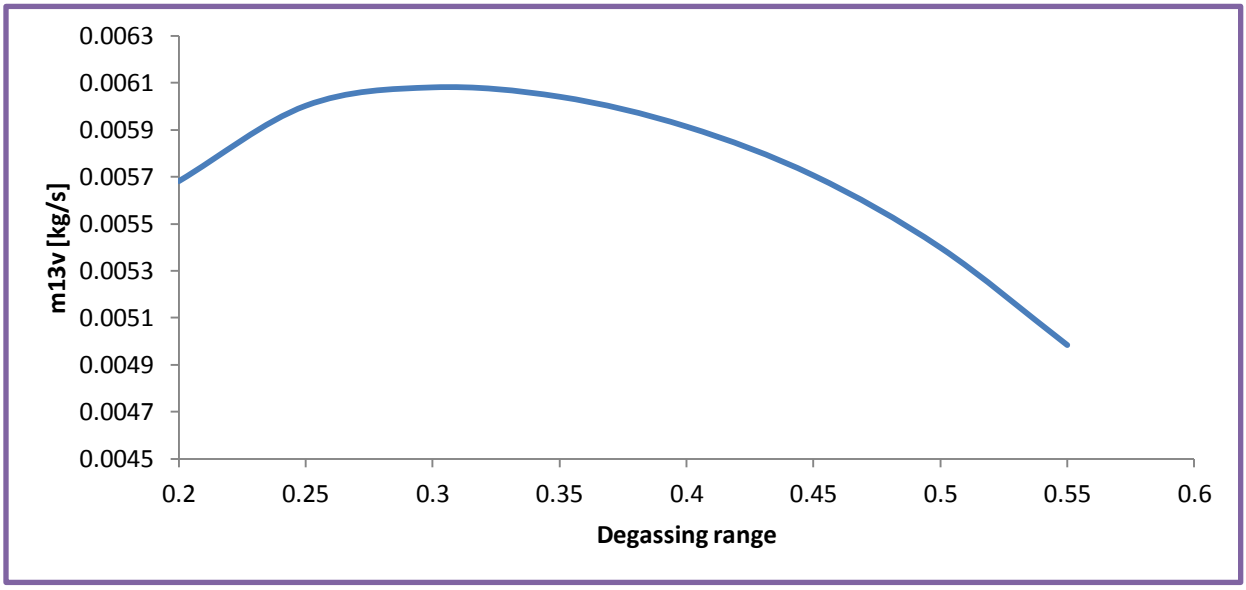

Fig.4.37. Variation of mass flow rate at state point 13_v with degassing range for GAX hybrid cycle (T_g=170ºC, T_c=40ºC, T_e=5ºC and P_a=916.87 kPa)

In the conventional GAX cycle, the value of COP of 1.253 is attained in the degassing range of 0.45. In GAX hybrid cycle (P_a=916.87 kPa) same COP of 1.253 is attained in the much lower degassing range of 0.25. This fact is very significant component of GAX hybrid cycle.

4.2.5. Effect of degassing range on heat duty

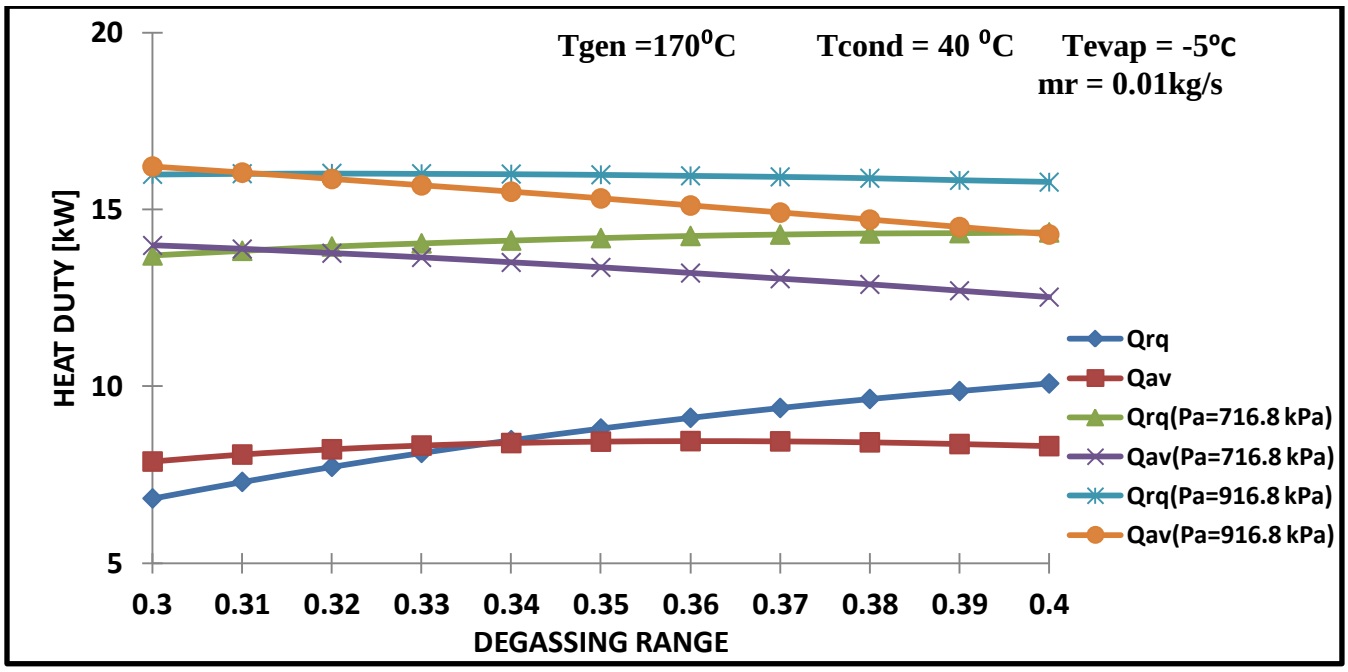

Fig.4.38 Variation of heat duty with degassing range

Fig.4.38 shows the dependence of $\dot{Q}_{av}$ and $\dot{Q}_{rq}$ on the degassing ranges for the conventional GAX and GAX hybrid cycles. It can be observed that at constant refrigerant flow rate, the $\dot{Q}_{av}$ in the GAX hybrid (P_a=916.87 kPa) is 8.34 kW higher than that in the GAX cycle when the degassing range is 0.3. For the values of degassing range from 0.3 to 0.4, it is apparent that $\dot{Q}_{av}$, for GAX cycle first increases and then decreases with the increasing degassing range. However, for GAX hybrid cycles there is continuous fall in these values.

4.2.6. Effect of degassing range on heat transfer rate

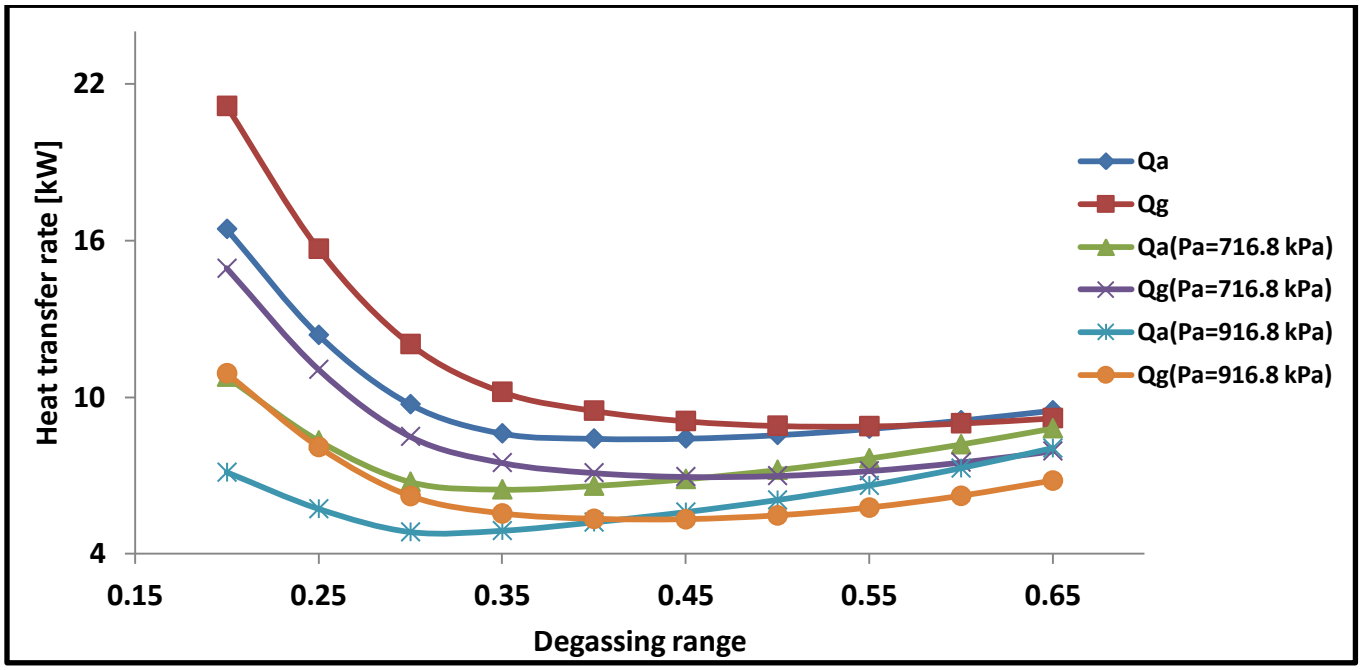

Fig.4.39. Variation of heat transfer rate with degassing ranges (T_g=170ºC, T_c=40ºC, T_e=5ºC)

Fig.4.39 represents the variation of heat transfer rate in the absorber and the generator with degassing ranges. It is apparent from the fig. that the rate of heat rejection in the absorber and the rate of heat supplied in the generator in the GAX cycle is higher as compared to both the GAX hybrid cycles at all degassing ranges. It is also clear from the fig. that the higher rate of rejection in the absorber at the higher degassing ranges causes the reduction in COP in the GAX hybrid cycles. It also indicates the requirement of higher degassing range for the GAX cycle as compared to GAX hybrid cycles. Heat transfer rate in the absorber and the generator decides the higher operating degassing range of the GAX hybrid cycle.

4.2.7. Effect of approach temperature on COP

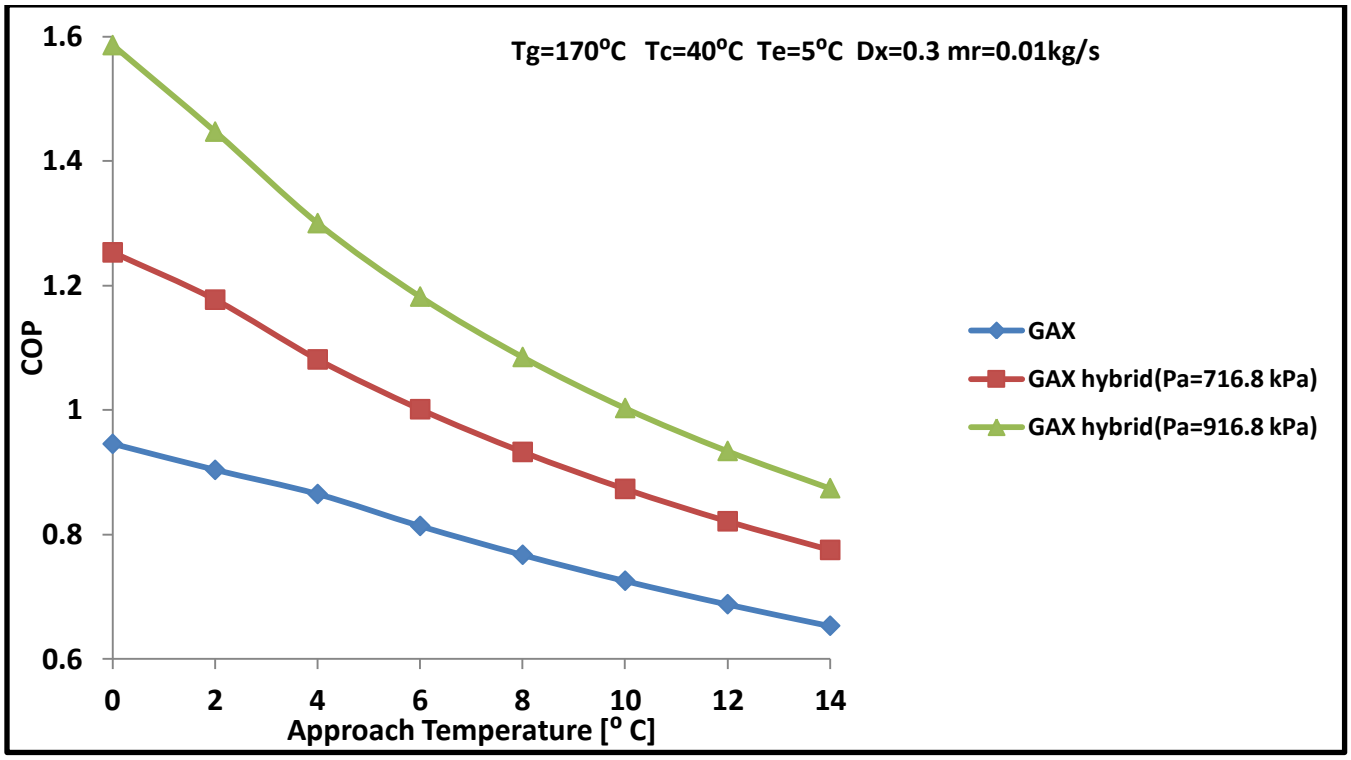

Fig.4.40. Variation of COP with approach temperature (T_g=170°C, T_c=40°C, T_e=5°C)

In fig. 4.40 the variation of COP with approach temperature difference is exhibited for GAX as well as GAX hybrid cycles. There is a dramatic decrease in the COP as the approach temperature difference increases. The approach temperature is varied up to 14ºC. Considering that possibly a hydronic heat transfer loop may be used to transfer heat from the absorber to the desorber, an approach temperature of 14ºC may not be unrealistic. For GAX cycle the COP has dropped from 0.9454 to 0.6532, a decrease of 30.91%. For GAX hybrid cycle (Pa = 716.8 kPa), this drop is 38.15%. Similarly drop in COP for GAX hybrid cycle (Pa = 916.8 kPa) is 44.88%. Hence it is apparent that the effect of approach temperature is more prominent on GAX hybrid cycle than on standard GAX cycle. Moreover, greater absorber pressure causes greater fall in the COP.

The reason for the decrease in the COP with the increase in the approach temperature can be understood as follows. An increase in the approach temperature decreases the temperature interval in which heat can be exchanged. This results in the decrease in the amount of heat available Q_{av} from the absorber as well as decrease in the heat required Q_{rq} in the desorber. Although both quantities decrease, the mismatch between the two increases. Since the amount of Q_{av} is already small, it decreases faster when limited by temperature constraints than the amount of Q_{rq} by the desorber. This decrease in the internal heat exchange at constant evaporator load leads to the increase in net heat input to the generator Q_{gen}. Similarly, heat rejection in the absorber Q_{abs} must increase. These considerations explain the decrease in the COP.

4.2.8. Effect of approach temperature on heat transfer rates

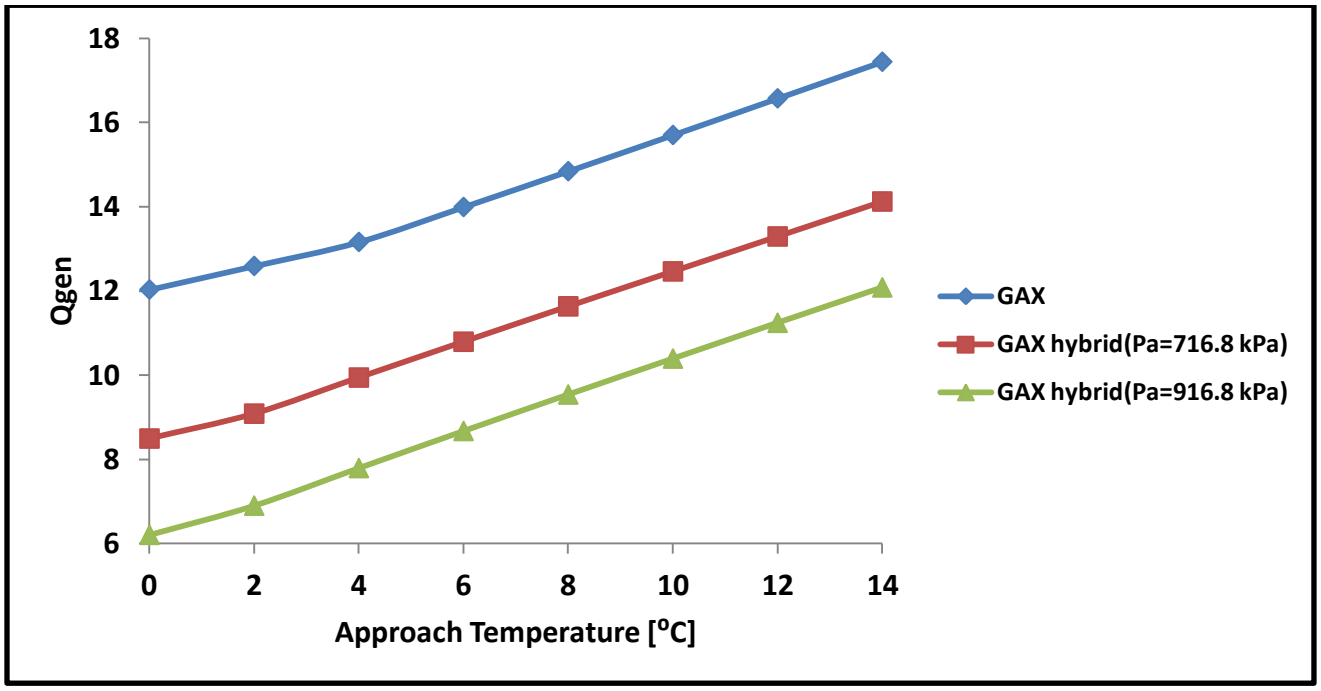

Fig.4.41. Variation of $\dot{Q}_{gen}$ with approach temperature (T_g=170°C, T_c=40°C, T_e=5°C)

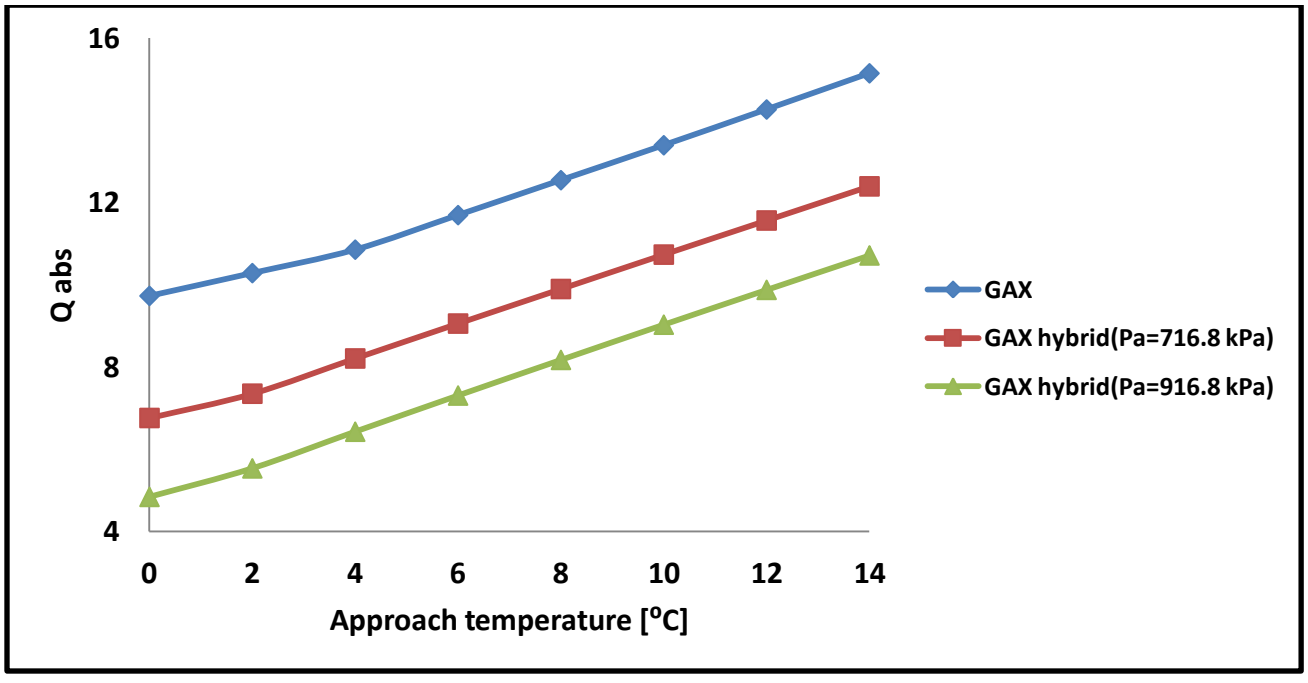

Fig.4.42. Variation of $\dot{Q}_{abs}$ with approach temperature (T_g=170°C, T_c=40°C, T_e=5°C)

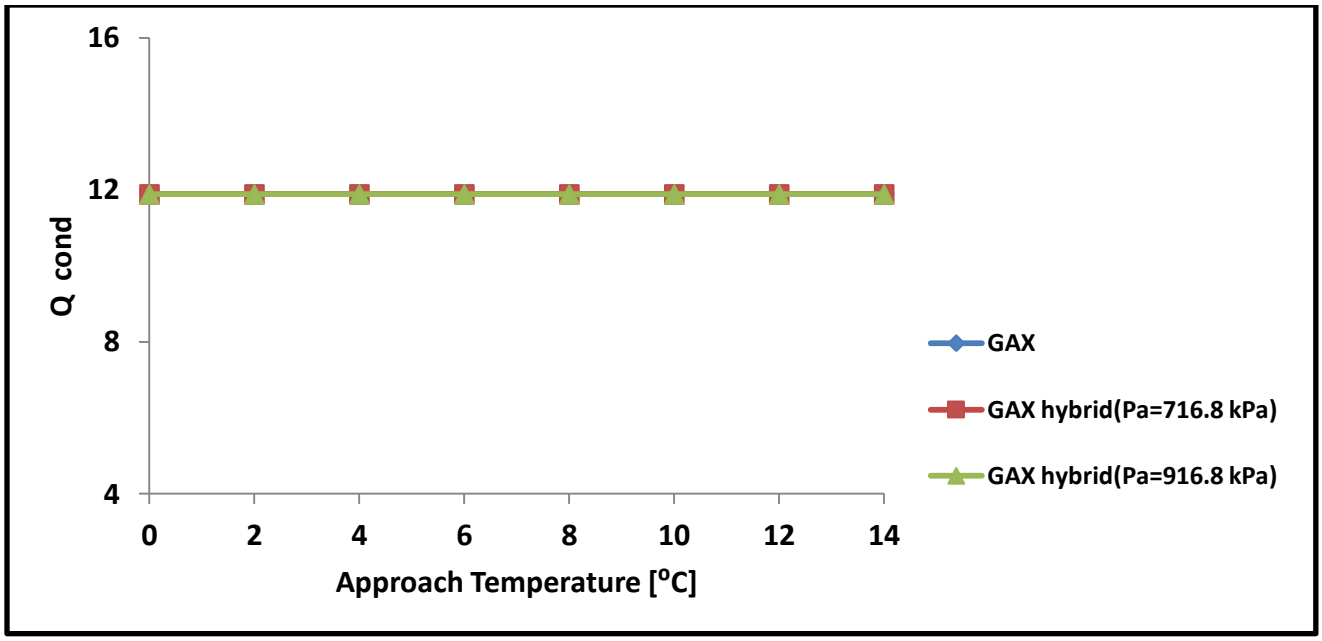

Fig.4.43. Variation of $\dot{Q}_{cond}$ with approach temperature (T_g=170°C, T_c=40°C, T_e=5°C)

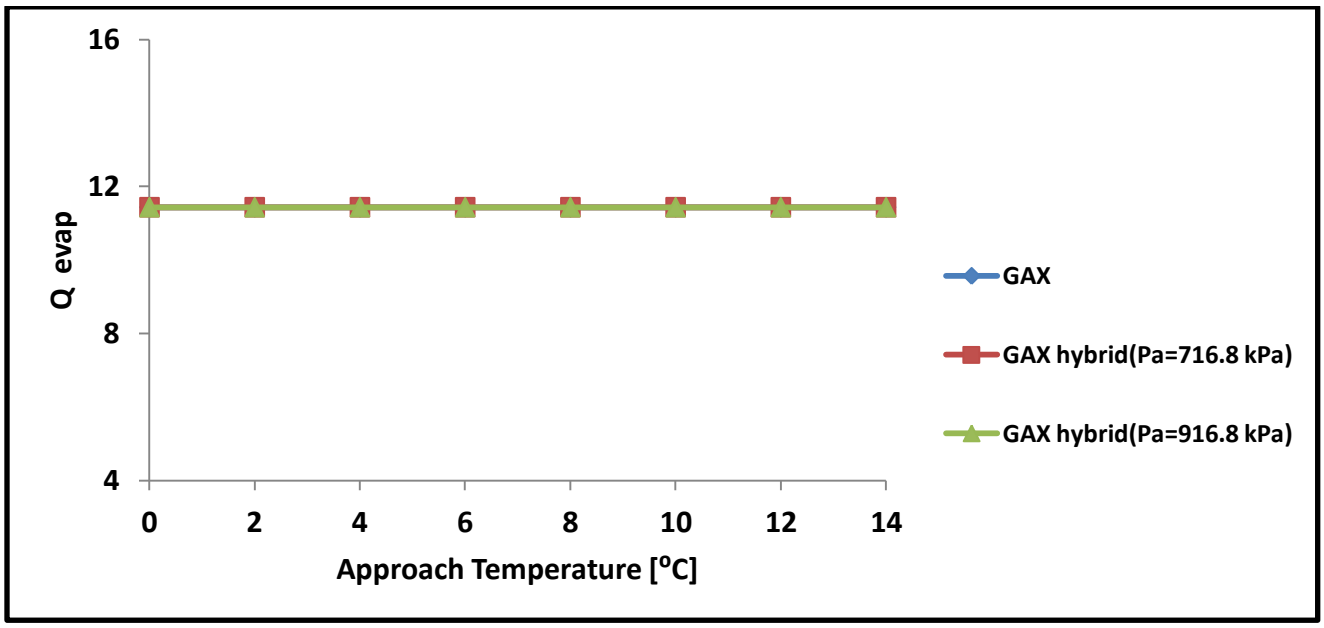

Fig.4.44. Variation of $\dot{Q}_{evap}$ with approach temperature (T_g=170°C, T_c=40°C, T_e=5°C)

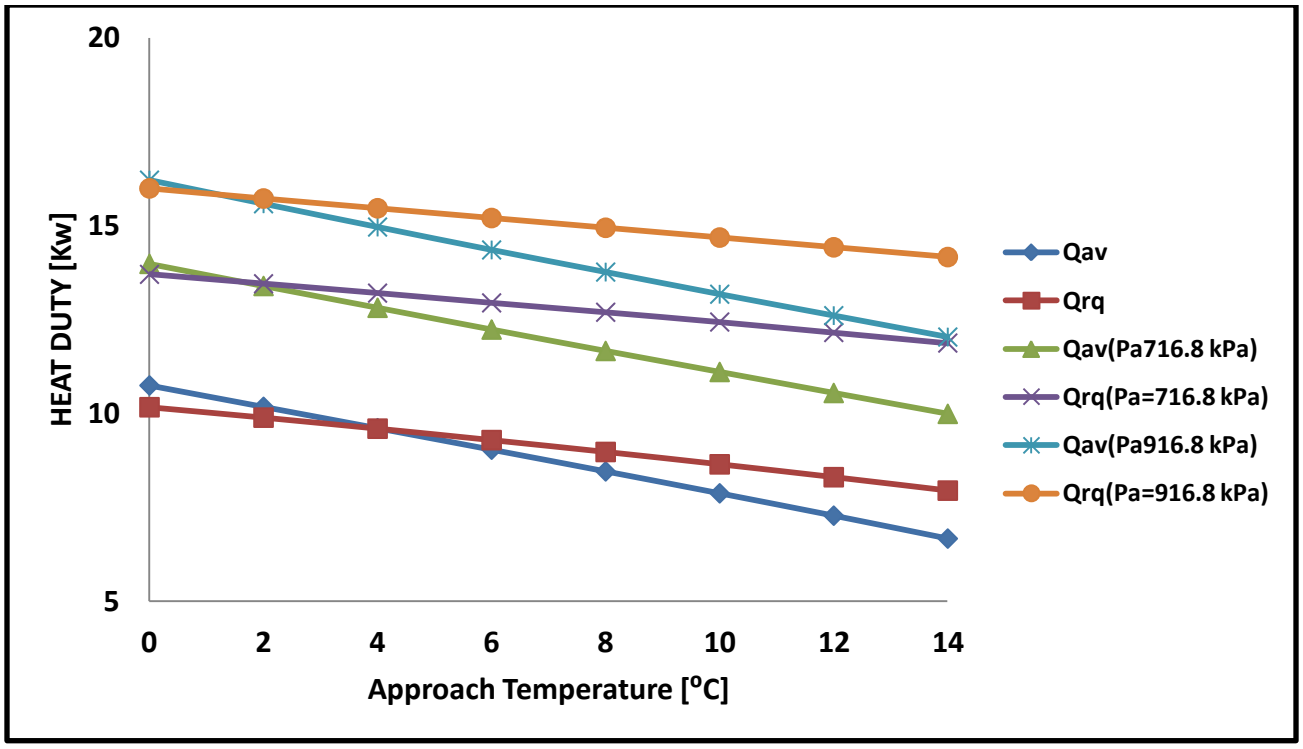

Fig.4.45. Variation of $\dot{Q}_{av}$ and $\dot{Q}_{rq}$ with approach temperature (T_g=170°C, T_c=40°C, T_e=5°C)

Fig.4.41 shows that $\dot{Q}_{gen}$ for GAX as well as GAX hybrid cycle increases with the increase in the approach temperature. Similarly, there is increase in $\dot{Q}_{abs}$ for GAX and GAX hybrid cycles as shown in fig.4.42. This happens because the amount of heat exchanged internally between absorber and desorber is decreasing with the approach temperature at constant evaporator capacity as shown in fig.4.44.Similar to evaporator capacity $\dot{Q}_{evap}$, the condenser load remains constant with approach temperature as depicted in fig.4.43. The increase in both $\dot{Q}_{gen}$ and $\dot{Q}_{abs}$ both with the approach temperature results in drop in COP with the increase in the approach temperature.

Fig.4.45 shows the variation of heat required in the desorber $\dot{Q}_{rq}$ and the heat available in the absorber $\dot{Q}_{av}$ with approach temperature. An increase in the approach temperature decreases the temperature interval in which heat can be exchanged. This results in the decrease in the amount of heat available Q_{av} from the absorber as well as decrease in the heat required Q_{rq} in the desorber.

4.3. Second Law Analysis

4.3.1. Effect of generator temperature on exegetic efficiency

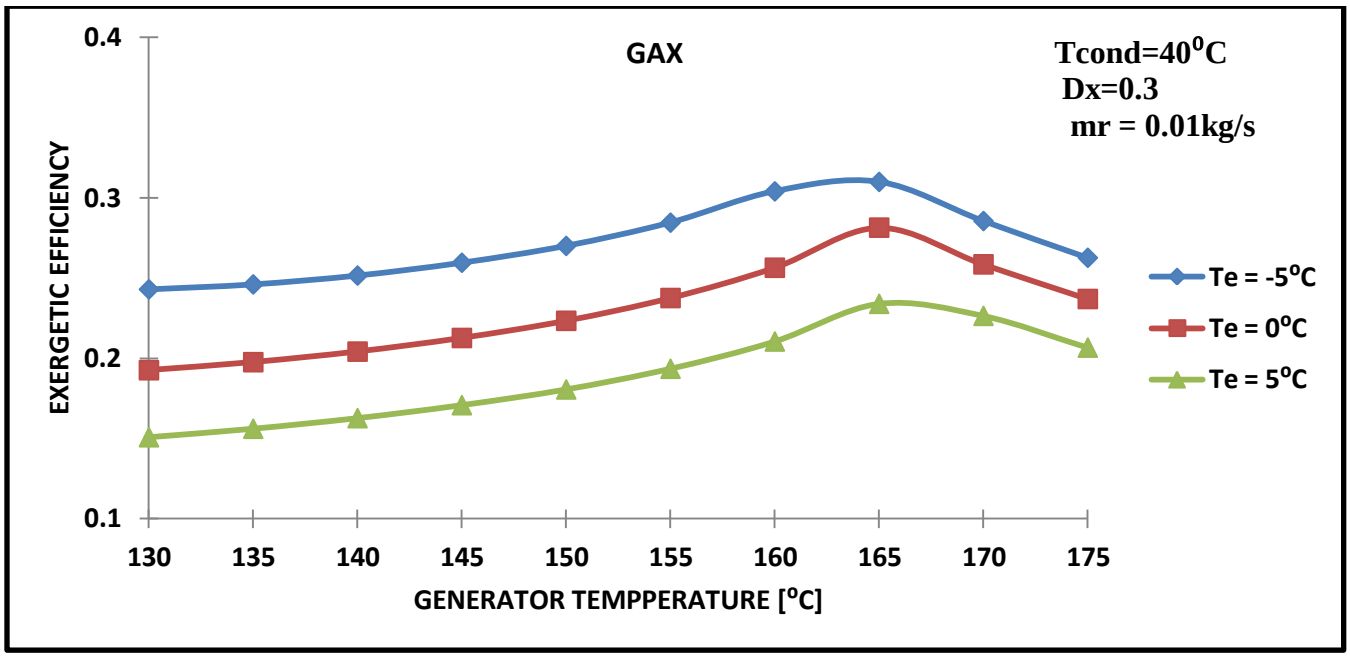

Fig.4.46. Variation of η_{II} with T_g for GAX cycle

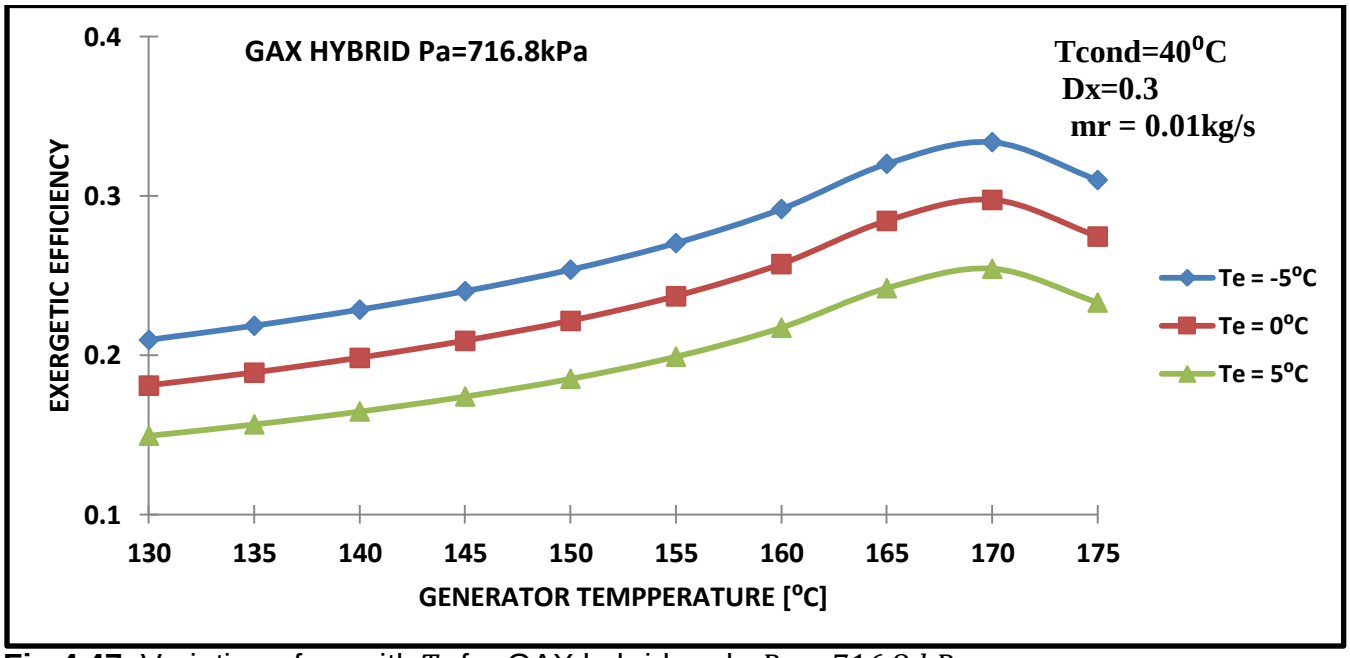

Fig.4.47. Variation of η_{II} with T_g for GAX hybrid cycle $P_a = 716.8\ kPa$

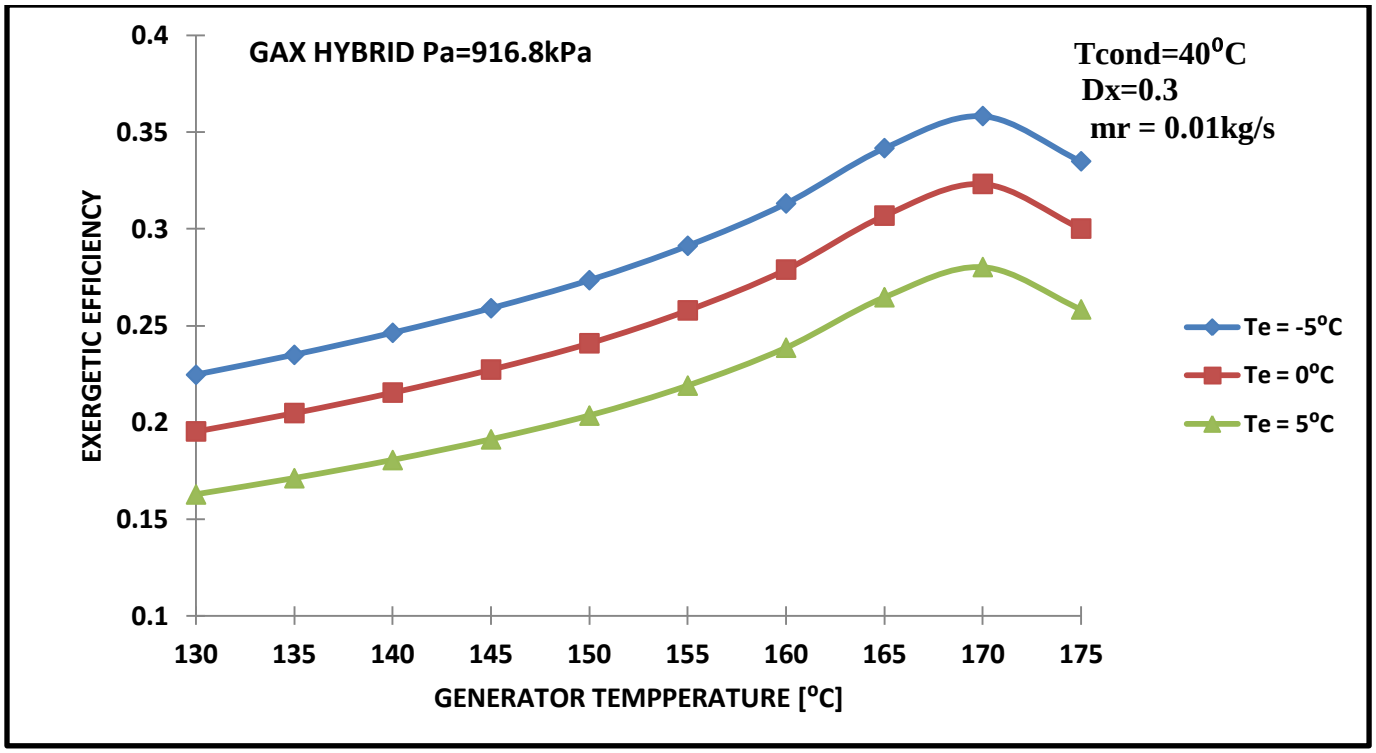

Fig.4.48. Variation of η_{II} with T_g for GAX hybrid cycle $P_a = 716.8\ kPa$

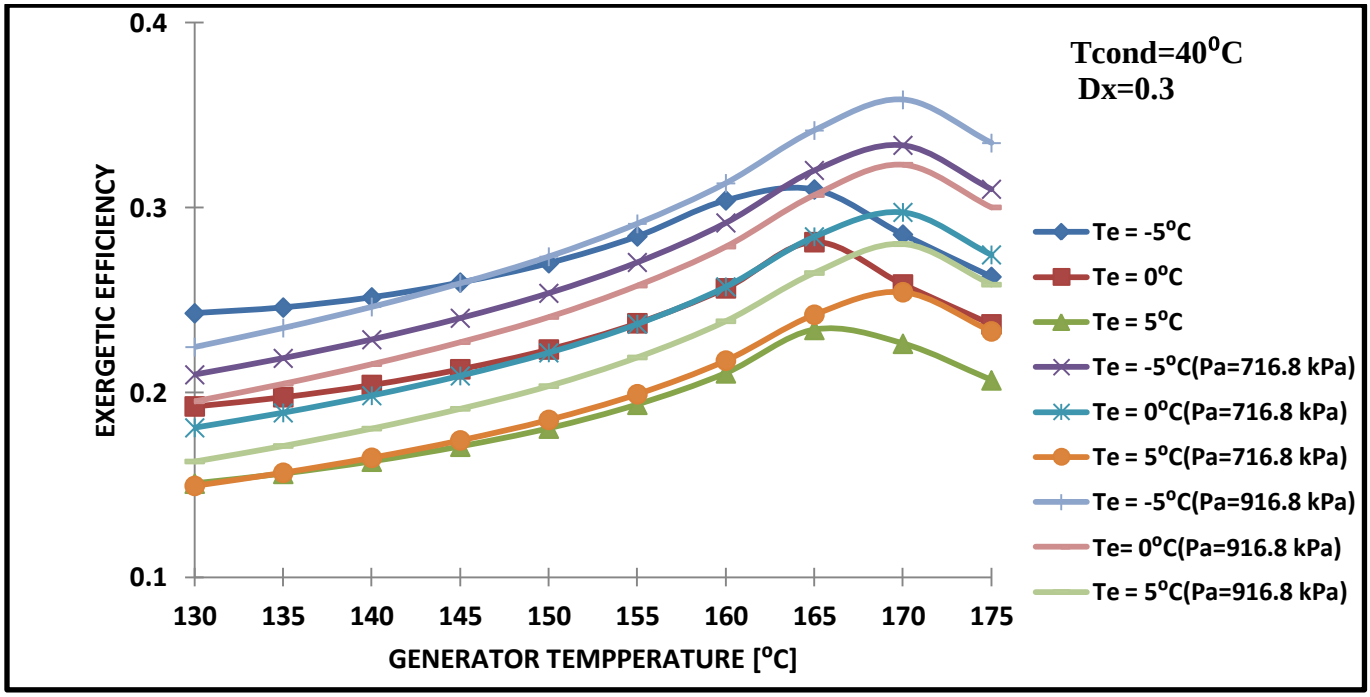

Fig.4.49. Variation of η_{II} with T_g for GAX and GAX hybrid cycles at T_c=40°C

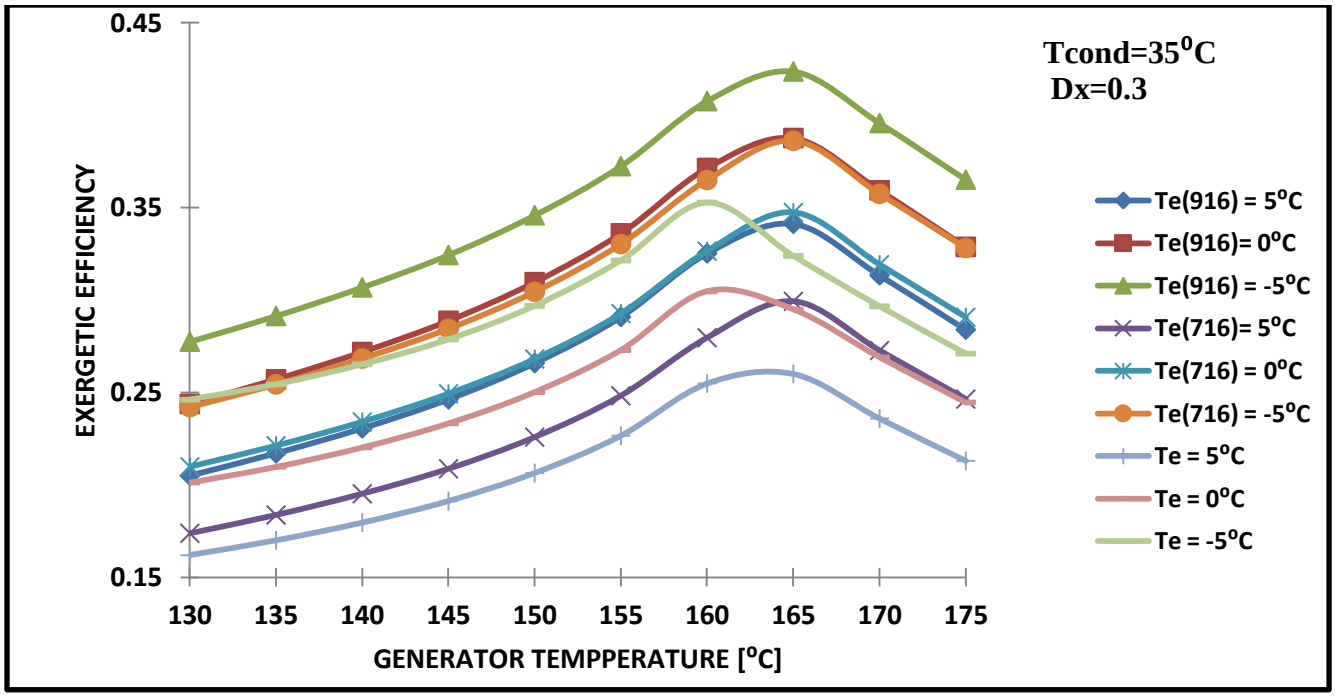

Fig.4.50. Variation of η_{II} with T_g for GAX and GAX hybrid cycles at T_c=35°C

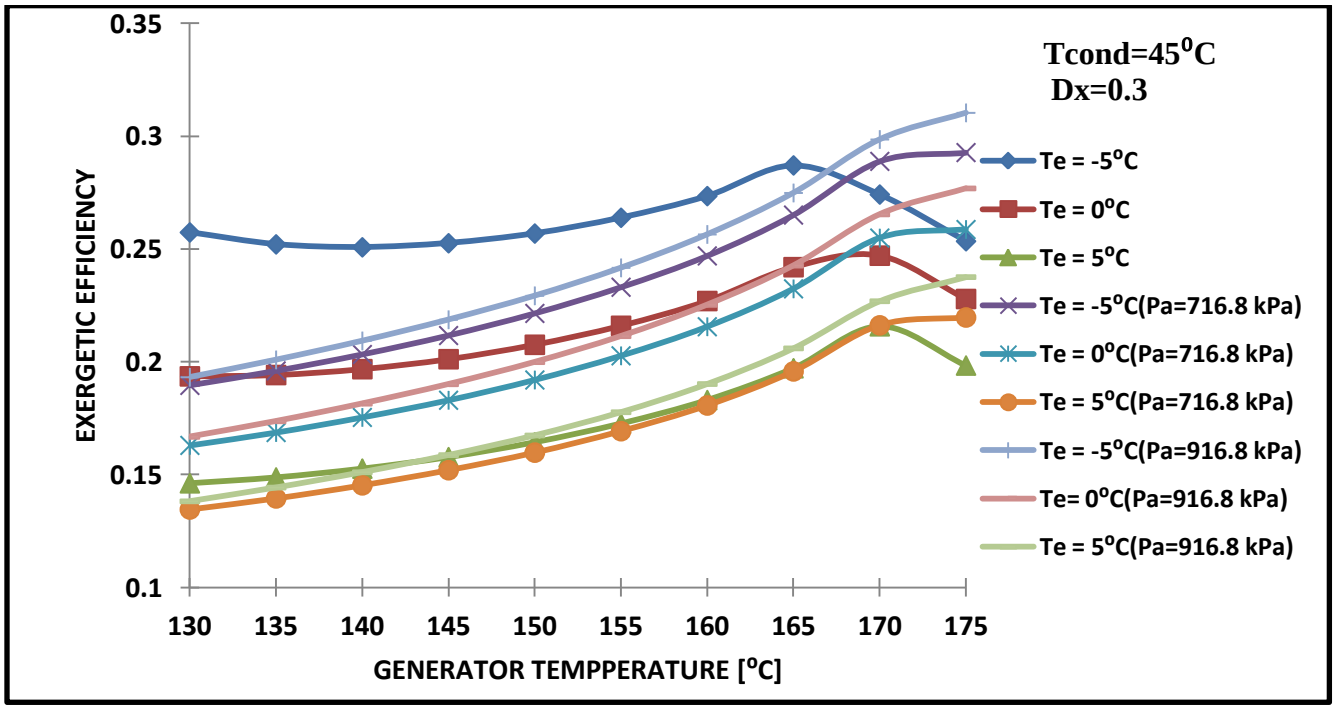

Fig.4.51. Variation of η_{II} with T_g for GAX and GAX hybrid cycles at T_c=45°C

Figures 4.46 to 4.51 indicate the variation exergetic efficiencies η_{II} with respect to generator temperature T_g for GAX and GAX hybrid cycles at different evaporator and condenser temperatures. At any specified values of T_{evap}, P_a and T_{cond}, there is a maximum value of exergetic efficiency at a particular generator temperature. First, exergetic efficiency η_{II} increases with the increase in the T_g, attains the maximum value at a particular generator temperature and then starts decreasing with the further increase in T_g.

The explanation for the second law efficiency behavior of GAX cycles is similar to that for the COP. However, the average temperature at which heat is added to the generator T_{avg} also influences the second law efficiencies. The slope of the exergetic efficiency graph is comparatively higher than that of the corresponding COP graph. This is due to the combined effect of the variation of $\dot{Q}_g$ and T_{avg} on the associated exergy.

As can be seen from the graphs, the maximum exergetic efficiency for GAX hybrid cycles occurs at higher generator temperature T_g as compared to that in the case of GAX cycle. Additionally, it can be observed that in case of GAX cycle at lower evaporator temperature T_{evap} , the T_g corresponding to maximum exergetic efficiency is lower. Similar results are reported in the literature [8].

4.3.2. Effect of generator temperature on exergy destruction rate

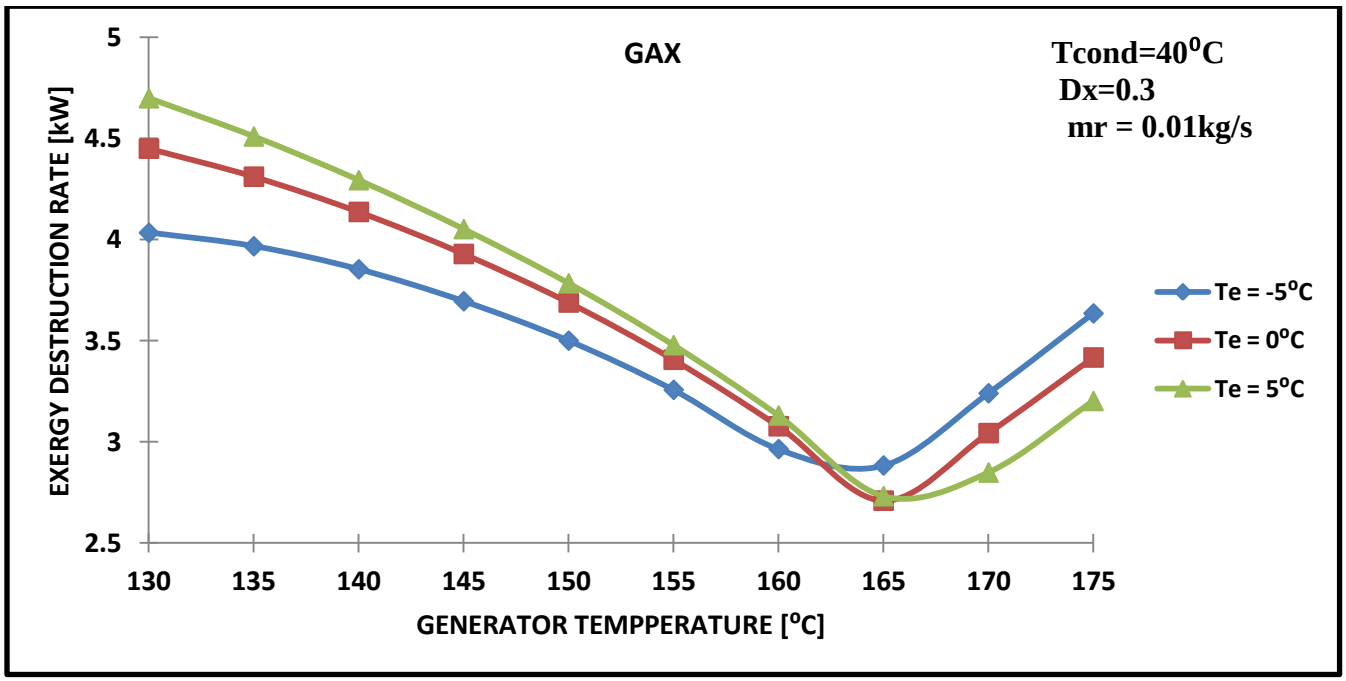

Fig.4.52. Variation of $\dot{E}_{d,total}$ with T_g for GAX cycle at T_c=40°C

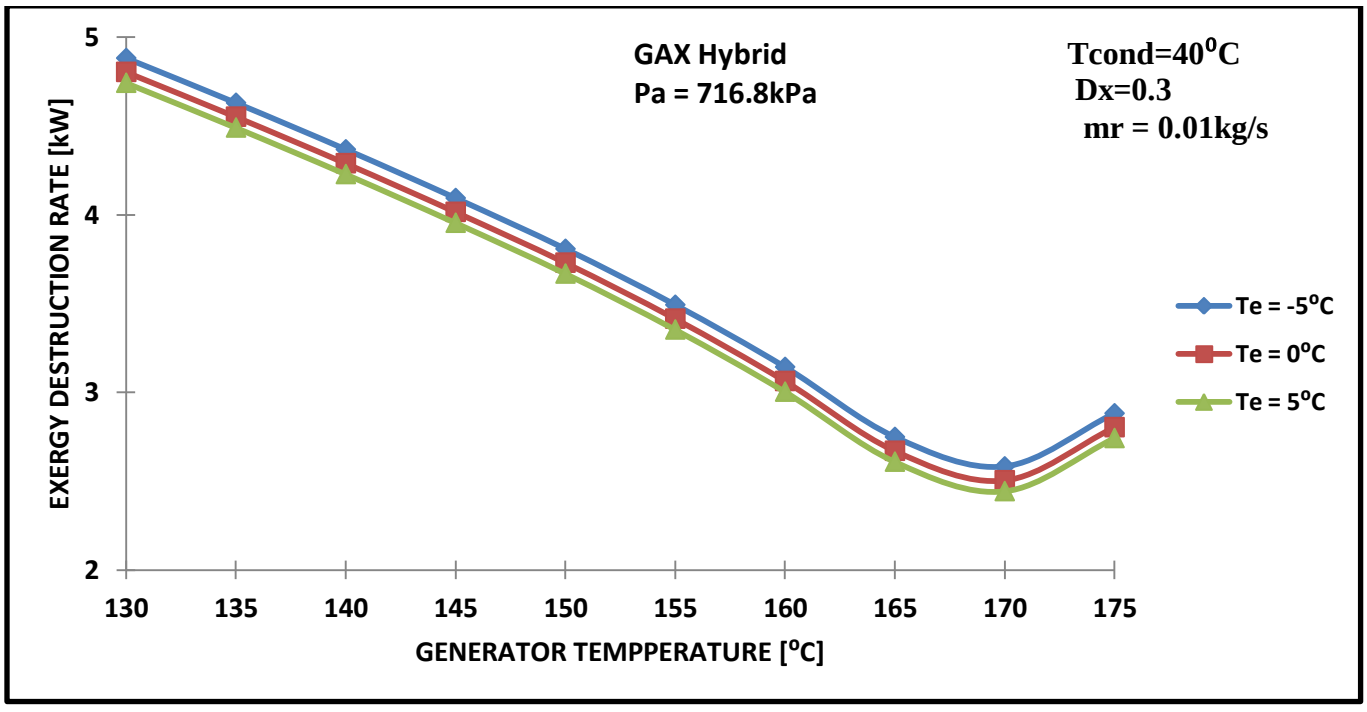

Fig.4.53. Variation of $\dot{E}_{d,total}$ with T_g for GAX hybrid cycle at T_c=40°C

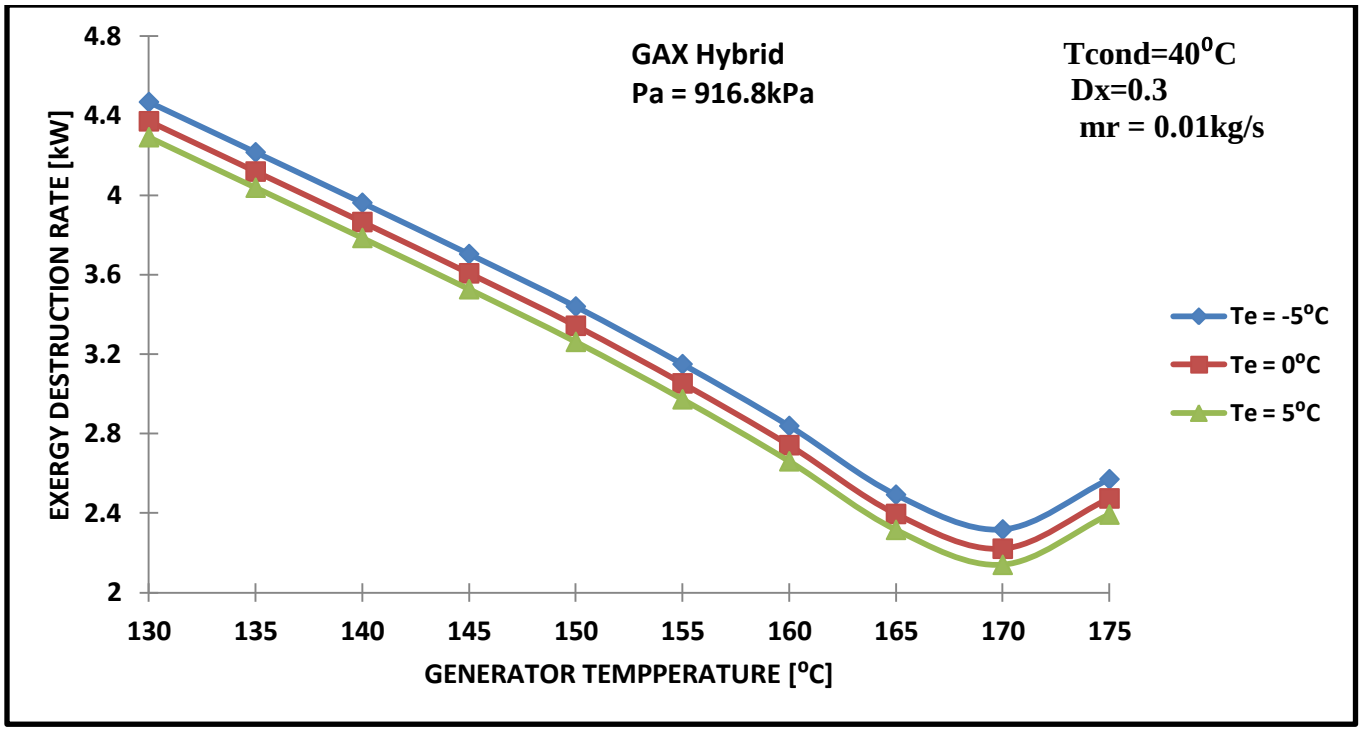

Fig.4.54. Variation of $\dot{E}_{d,total}$ with T_g for GAX hybrid cycle at T_c=40°C

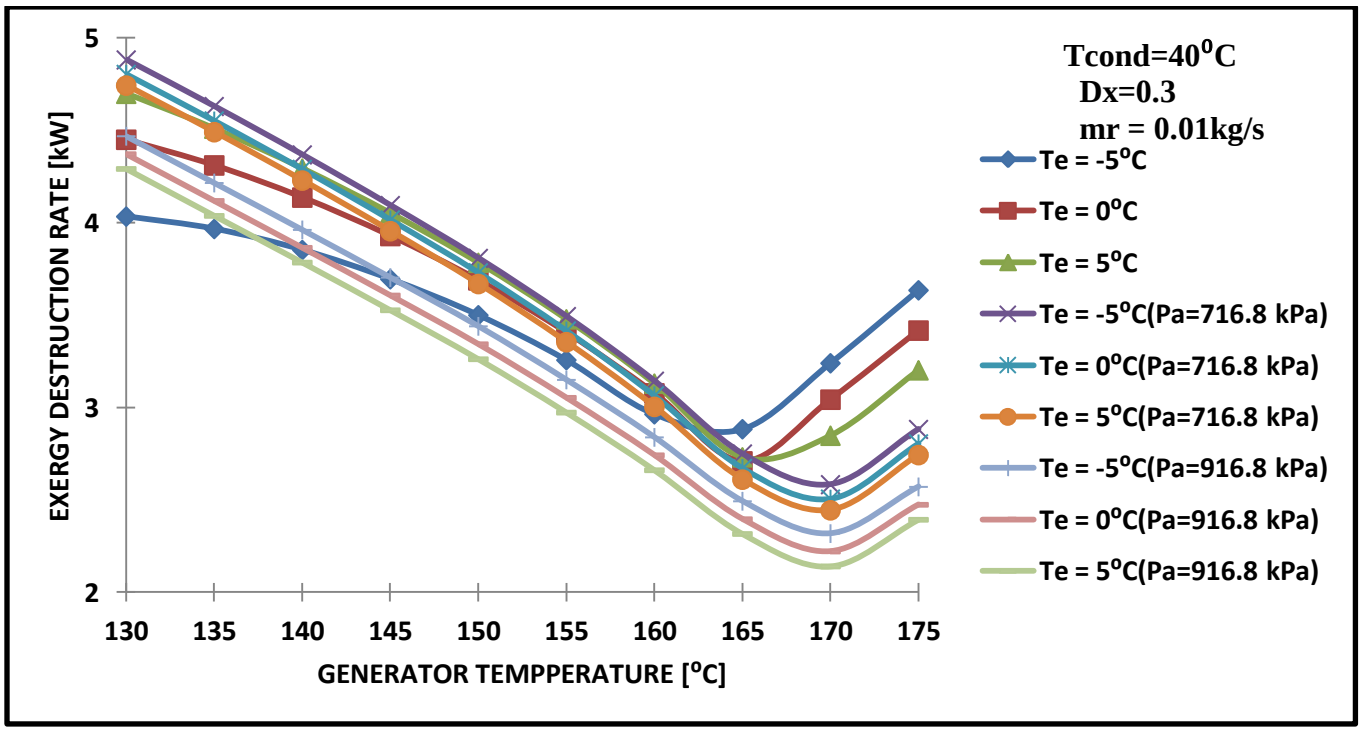

Fig.4.55. Variation of $\dot{E}_{d,total}$ with T_g for GAX and GAX hybrid cycles at T_c=40°C

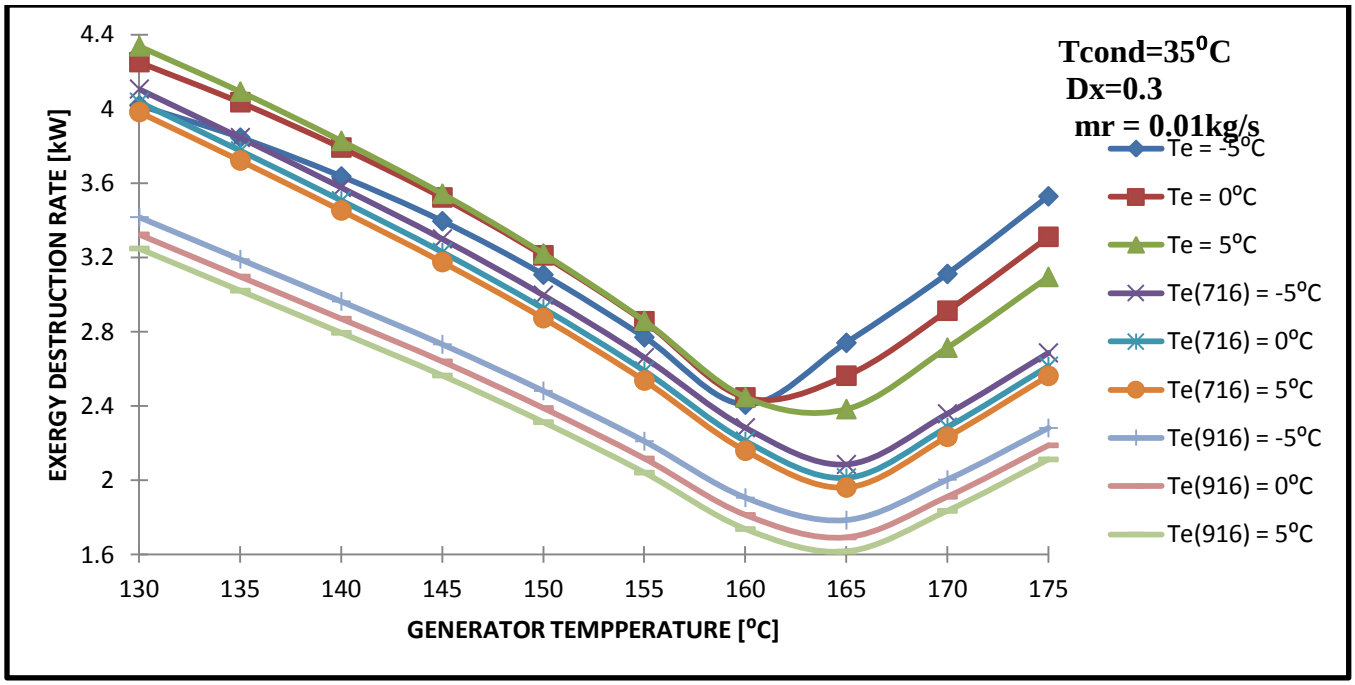

Fig.4.56. Variation of $\dot{E}_{d,total}$ with T_g for GAX and GAX hybrid cycles at T_c=35°C

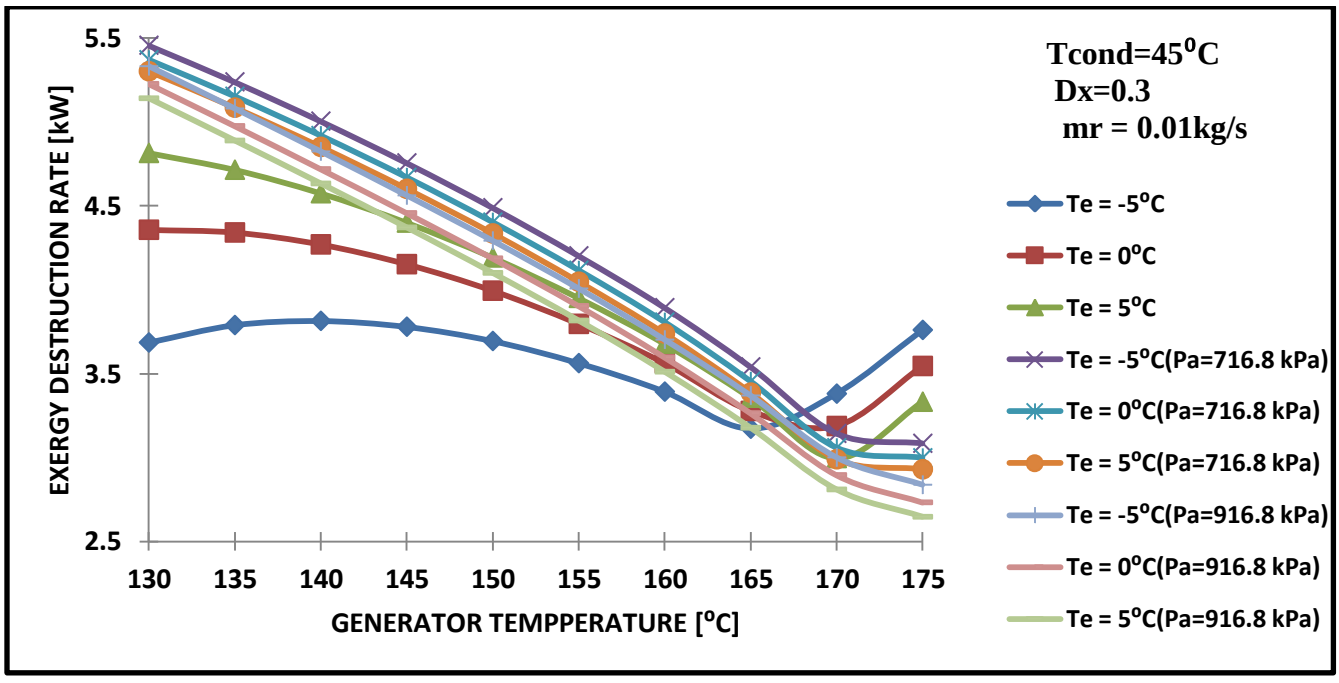

Fig.4.57. Variation of $\dot{E}_{d,total}$ with T_g for GAX and GAX hybrid cycles at T_c=45°C

Figures 4.53 to4.57 show the variation of total exergy destruction in both cycles with respect to T_g at different evaporator and condenser temperature. They reveal that the total exergy destruction rate is minimum at a particular value of generator temperature. It is the same temperature at which the COP is maximum for the specified conditions.

GAX and GAX hybrid, both cycles are studied in these figures. The total exergy destruction in the GAX hybrid cycle at any particular evaporator and condenser temperature is lower than that in the GAX cycle. For a particular generator temperature, as the evaporator temperature increases, the exergy destruction decreases. Similarly, reduction in condenser temperature at a given generator temperature causes decrease in the exergy destruction. The results are consistent with the Carnot principle.

4.3.3. Effect of degassing range on exergetic efficiency

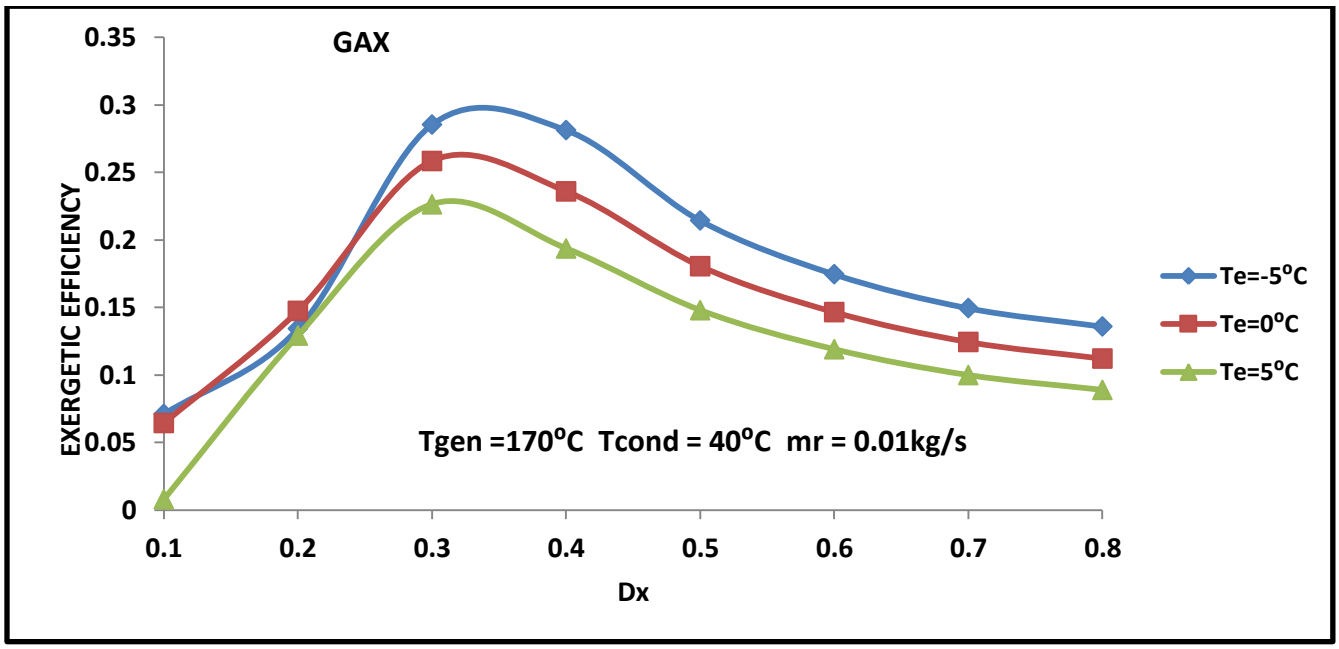

Fig.4.58. Variation of exergetic efficiency η_{II} with degassing range D_x for GAX cycle

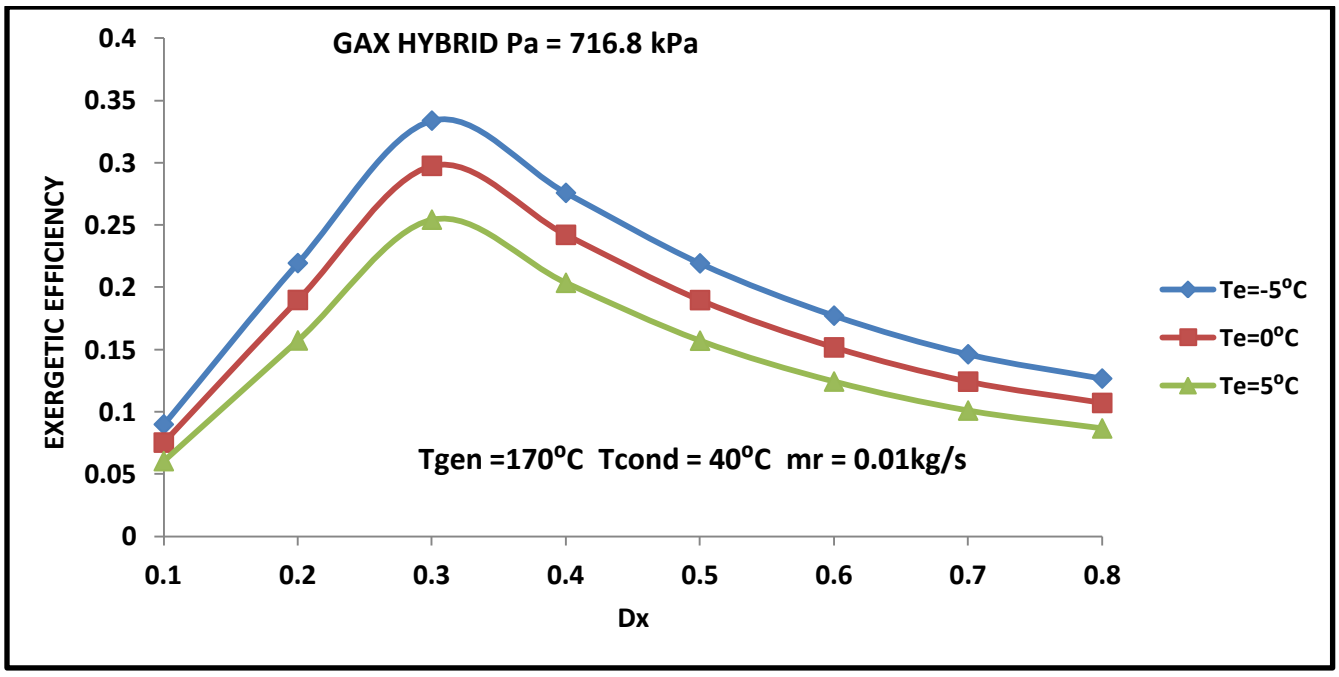

Fig.4.59. Variation of $\eta_{II}$with D_x for GAX hybrid cycle

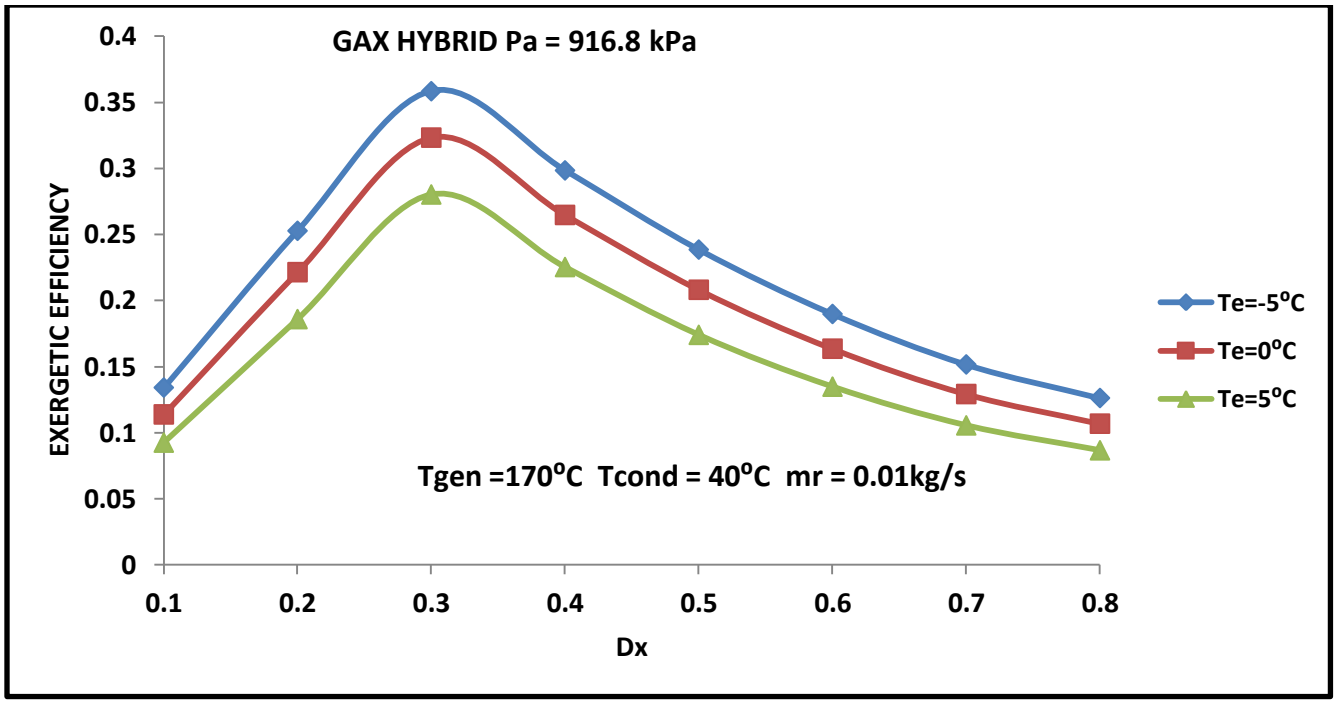

Fig.4.60. Variation of η_{II} with D_x for GAX hybrid cycle

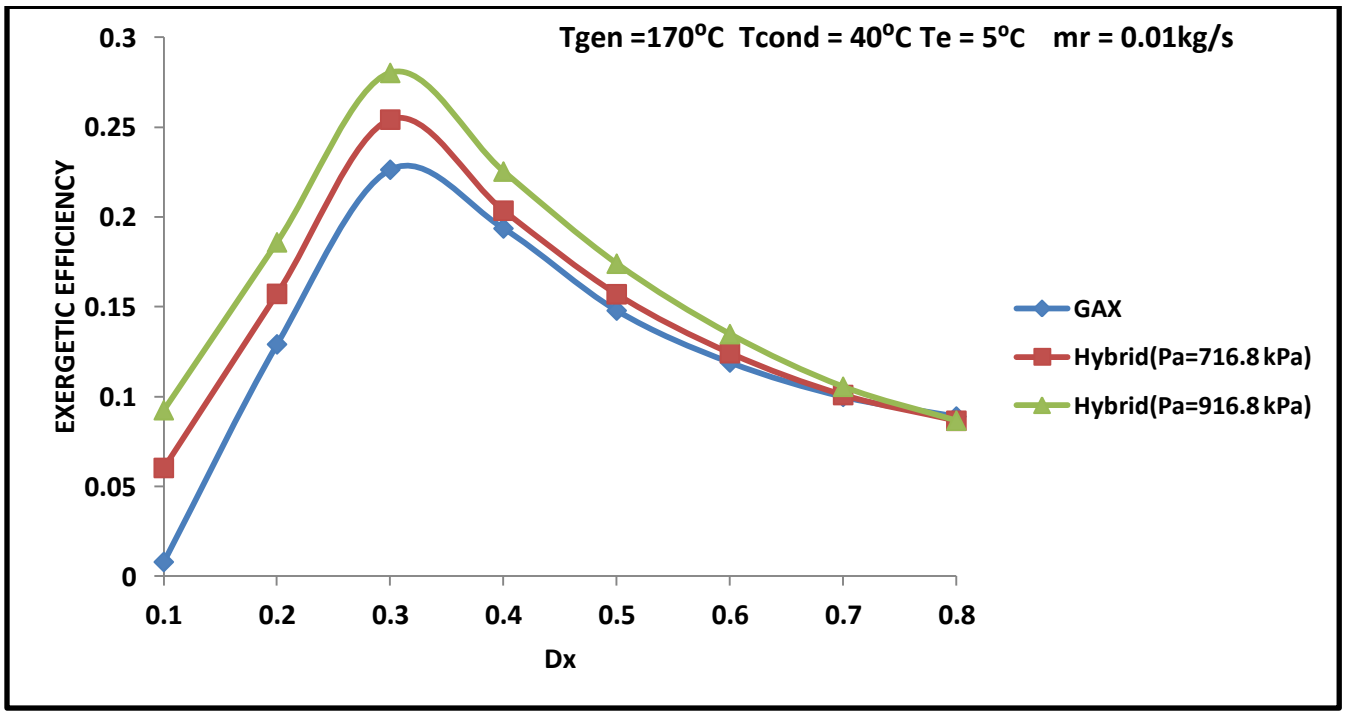

Fig.4.61. Variation of η_{II} with D_x for GAX and GAX hybrid cycles

Fig. 4.58 shows the variation of second law efficiency η_{II} with the degassing range D_x for GAX cycle. For a particular evaporator, generator and condenser temperature, as the degassing range is increased, exergetic efficiency also increases. It becomes maximum at a particular value of D_x and again starts decreasing with the increase in D_x. Similar trends are observed in fig.4.59 and fig.4.60 for GAX hybrid cycles.

The increase of mass flow rate at state point 13v ($\dot{m}_{13v}$) results in the increment of heat availability in the absorber (Q_{av}) and the decrease of mass flow rate at state point 14v ($\dot{m}_{14v}$) results in the increase of heat required in the generator (Q_{rq}). It may be seen here that the required $\dot{m}_{13v}$ in the cycles initially increases and then decreases with the increase of degassing range, and it, in turn, decreases the Q_{av}. Further, the rate of decrease of $\dot{m}_{13v}$ is much higher at the higher degassing range. The cumulative effect of these two phenomenons causes the reduction of η_{II} at higher degassing range.

Within the degassing range of 0.3 to 0.4, it is shown in fig.4.58 that the exergetic efficiency is higher for lower evaporator temperature for fixed condenser and generator temperatures. Similar results are shown for GAX hybrid cycles in fig.4.59 and fig.4.60. In fig.4.58 it is shown that for D_x=0.3, η_{II} at $T_e = 0°C$ is 14.18 % higher than at $T_e = 5°C$ and this increment becomes 26.10 % when $T_e = -5°C$. Similarly, for GAX hybrid cycle (P_a = 916.8 kPa), for D_x=0.3, η_{II} at $T_e = 0°C$ is 15.34 % higher than at $T_e = 5°C$ and this increase is 27.86 % for $T_e = -5°C$.

Fig.4.61 shows the comparison of GAX and GAX hybrid cycles at $T_g = 170°C$, $T_e = 40°C$ and $T_e = 5°C$. It is apparent from the figure that maximum η_{II} occurs at D_x=0.3 for GAX as well as GAX hybrid cycles. The increase in η_{II} for D_x=0.3 is 12.32 %for GAX hybrid

(P_a=716.8 kPa) and 23.81 % for GAX hybrid cycle (P_a=916.8 kPa) as compared to simple GAX cycle.

4.3.4. Exergy destruction in components

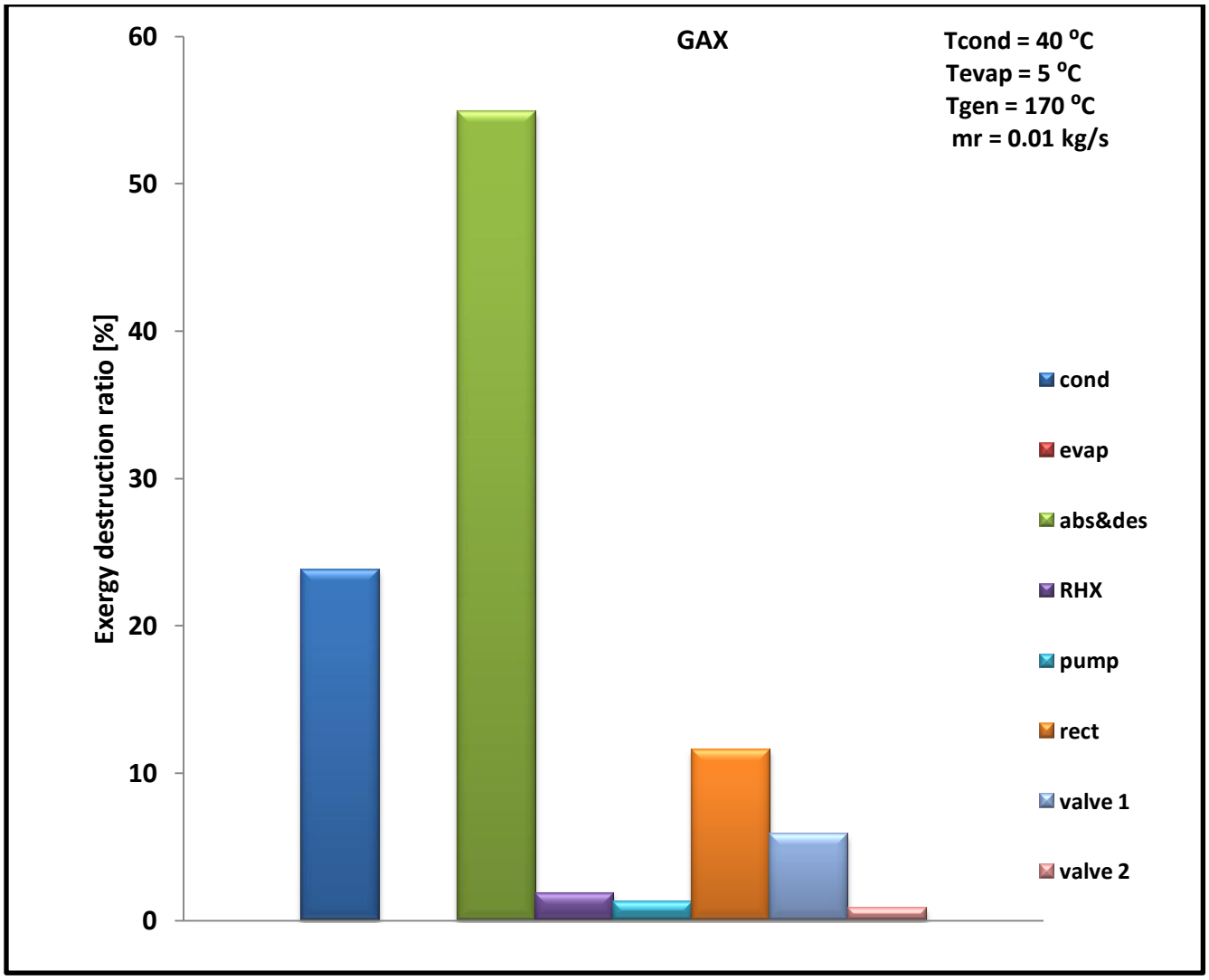

Fig.4.62. Exergy destruction in the components of GAX cycle

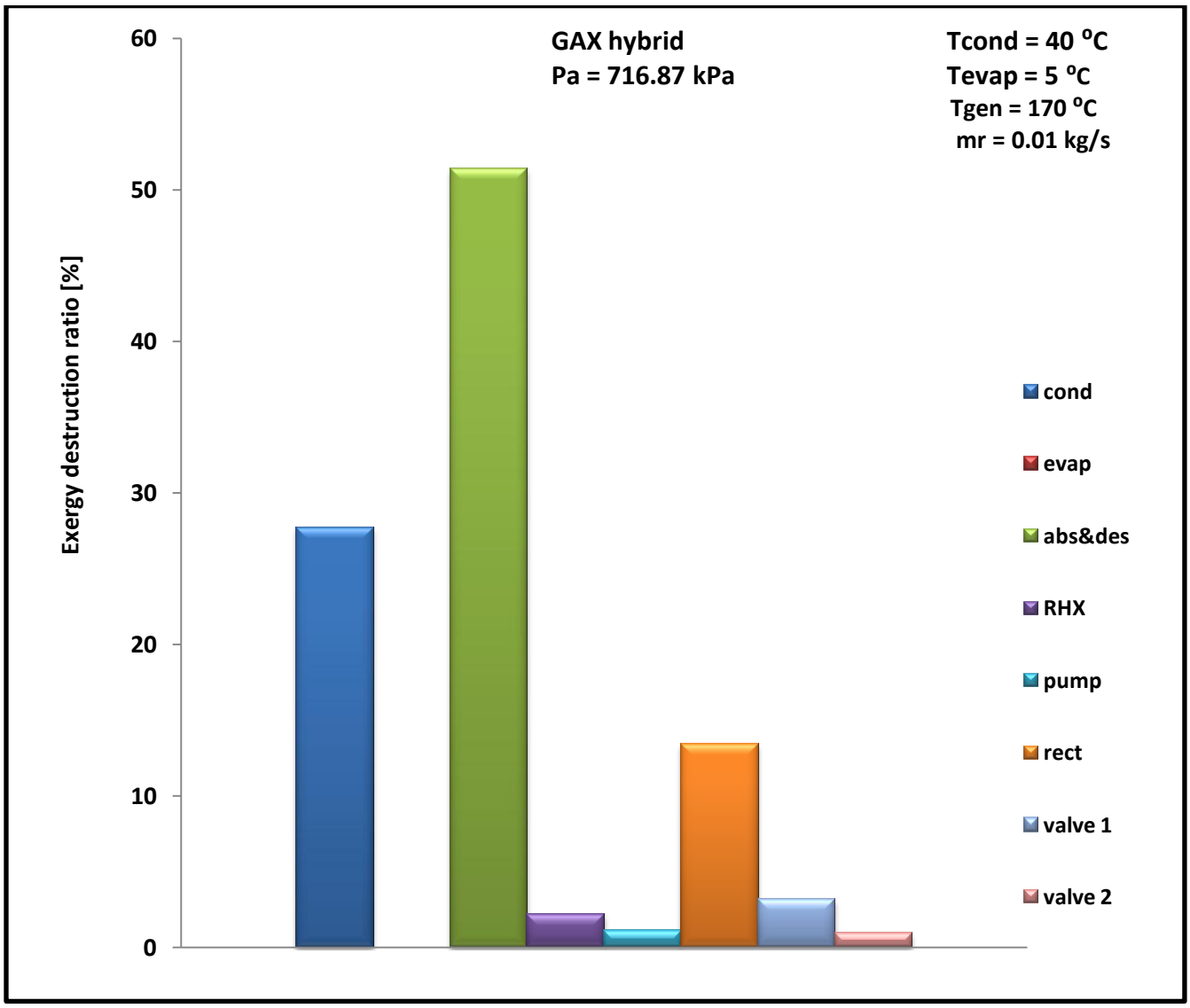

Fig.4.63. Exergy destruction in the components of GAX hybrid cycle $P_a = 716.8\ kPa$

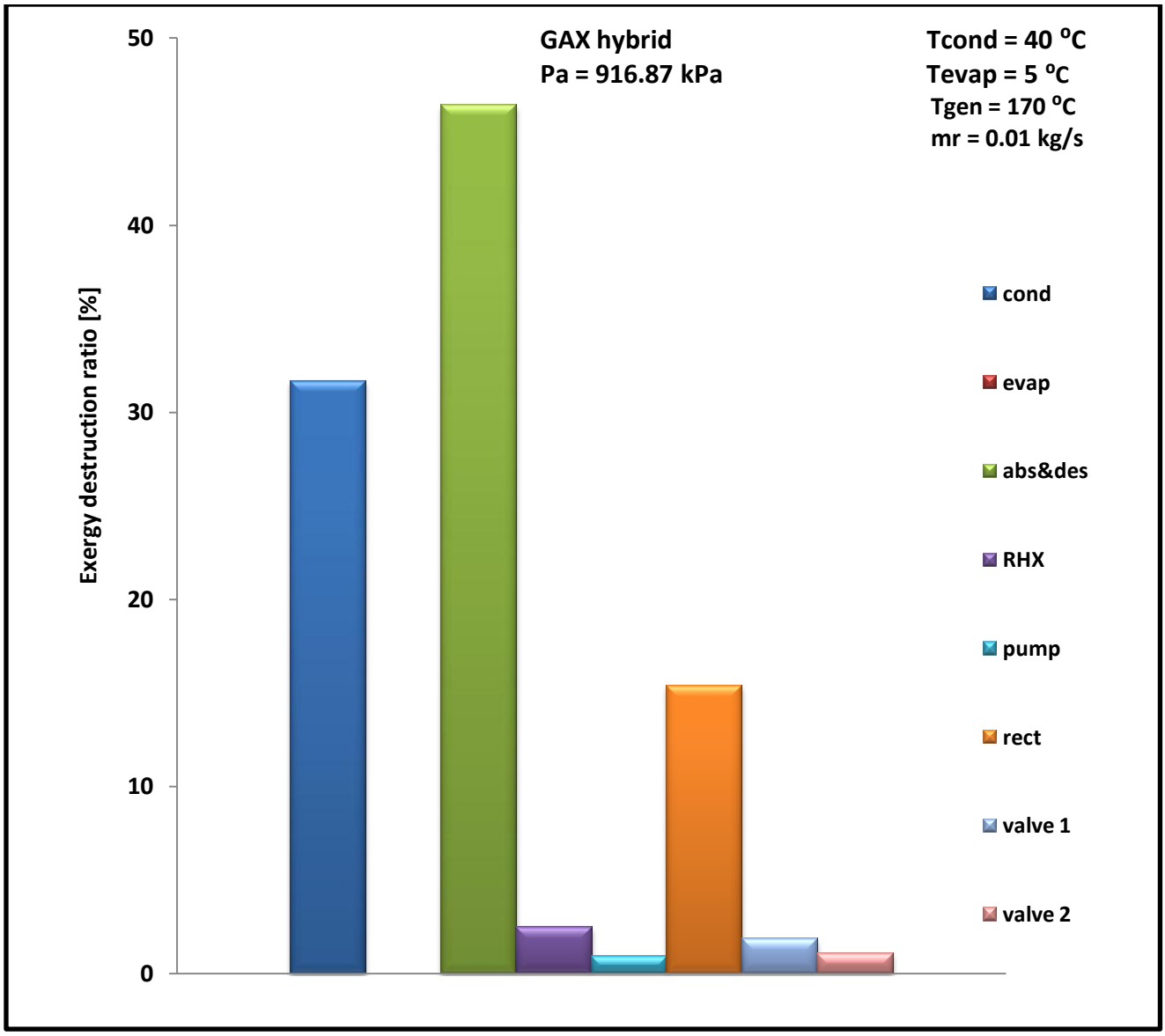

Fig.4.64. Exergy destruction in the components of GAX hybrid cycle $P_a = 916.8\ kPa$

Figures 4.62 to 4.64 show the exergy destruction in each component of the GAX and GAX hybrid cycles at given conditions. It is apparent from these figures that the maximum exergy destruction occur in absorber and desorber taken together. As the absorber pressure increases in the GAX hybrid cycle, the exergy destruction in absorber and desorber decreases. This decrease is also reported in the expansion valve 1. However, the increase in the absorber pressure causes increase in the exergy destruction in other components particularly rectifier and condenser. The total exergy destruction in the GAX hybrid cycles for all cases is lower than that in the GAX cycle.

CHAPTER – 5

CONCLUSIONS AND RECOMMENDATIONS

5.1 Conclusions

GAX and GAX hybrid aqua-ammonia absorption refrigeration cycles are theoretically analyzed. From the obtained results, the following conclusions are made.

1. COP as well as η_{II} for GAX and GAX hybrid cycles attains a maximum value at a particular generator temperature. Generator temperature T_g corresponding to maximum COP and maximum η_{II} lies between 160 ºC to 175 ºC depending upon the cycle and parameters considered. Maximum COP for GAX cycle varies within the range of 0.7 to 1.1 whereas for GAX hybrid cycles maximum COP lies in between 1 to 1.5 (for P_a =716.8 kPa) and 1.25 to 1.88 (for P_a = 916.8 kPa). Similarly, maximum η_{II} lies in between 21% to 35 % for GAX cycle, 22% to 39% for GAX hybrid cycle (P_a = 716.8 kPa) and 24% to 43 % for GAX hybrid cycle (P_a = 916.8 kPa)

2. The value of T_g corresponding to maximum exergetic efficiency is 5 ºC higher for GAX hybrid cycle as compared to GAX cycle.

3. The influence of generator temperature on η_{II} is more prominent than on COP. As T_g is varied from 130ºC to 175ºC, for GAX hybrid cycles, the increase in η_{II} is up to 72%, whereas, corresponding increase in COP is up to 10% only. Similarly, for GAX cycle the increase in η_{II} and COP is 60% and 4% respectively.

4. Degassing range corresponding to maximum COP lies in the interval of 0.5 to 0.6 for GAX cycle and 0.4 to 0.5 for GAX hybrid cycles at T_c= 40ºC, T_g= 170ºC and T_e= -5 to 5ºC.

5. Exergetic efficiency and COP both increase with the absorber pressure in case of GAX hybrid cycle. Exergetic efficiency and COP of hybrid cycle (P_a = 916.8 kPa) is about 8% and 35 % respectively higher than that of the hybrid cycle (P_a = 716.8 kPa).

6. The required COP can be obtained in lower degassing range in the GAX hybrid cycle as compared to the simple GAX cycle. Therefore, GAX hybrid cycle can operate successfully utilizing low temperature energy sources.

7. The increase in approach temperature from 0 ºC to 14 ºC causes decrease in COP of GAX cycle by 30% and of GAX hybrid cycles by 40% to 45%.

8. The maximum exergy destruction occurs in desorber and absorber (as a unit component) of both the cycles, while the lowest contribution belongs to the expansion valve 2. Exergy destruction in desorber and absorber accounts for around 45% to 55% of the total exergy destruction.

5.2 Limitations and Recommendations for Future Work

In this work the results are obtained at specified conditions and valid for the assumptions considered. Assumptions other than these could bring about different results. In the present work, the approach temperature is assumed as 0 K which is not possible in reality. Similarly the isentropic efficiency is also assumed to be 100 percent which is not a real case.

So, in order to design the GAX and GAX hybrid absorption refrigeration systems for real utility, the approach temperature and compressor efficiency of suitable value can be considered. Similarly, compressor can be replaced by ejector to improve the standard GAX cycle. Therefore, the application of an ejector in the GAX cycle can be investigated to study its effect on cycle's performance.

REFERENCES

[1] Sun D.W., 1996, Thermodynamic design data and optimum design maps for absorption refrigeration systems, Appl. Therm. Engg, **17(3)**, 211-221.

[2] Gomri R., Hakimi R., 2008, Second law analysis of double effect vapour absorption cooler system, Energy Convers. Manag, **49**, 3343-3348.

[3] Kang Y.T., Kunugi Y., Kashiwagi T., 2000, Review of advanced absorption cycles, performance improvement and temperature lift enhancement. Int. J. Refrigeration. **23(5)**, 378-387

[4] Altenkirch E., 1913, Reversible absorptionmaschinen, zeitschrift for die gesamte Kalte-industrie, Jahrgang. Heft 1:1-19, Heft 6, 114-119.

[5] Scharfe J., Ziegler F., Radermacher R., 1986, Analysis of advantages and limitations of absorber generator heat exchange. Int. J. Refrigeration, **9**, 326-333.

[6] Velazquez N., Best R., 2002, Methodology for the energy analysis of an air cooled GAX absorption heat pump operated by natural gas and solar energy. Appl. Therm. Engg, **22**, 1089 – 1103.

[7] Kang Y.T., Hong H., Park K.S., 2004, Performance analysis of advanced hybrid GAX cycles, HGAX. Int. J. Refrigeration, **27(4)**, 442-448.

[8] Yari M., Zarin A., Mahmoudi S.M.S., 2011, Energy and exergy analysis of GAX and GAX hybrid absorption refrigeration cycles, Renewable Energy, **36**, 2011-2020.

[9] Kang Y.T., Akisawa A., Kashiwagi T., 1999, An advanced GAX cycle for waste heat recovery: WGAX cycle, Appl. Therm. Engg, **19**, 933-947.

[10] Pongsid S., Satha A., Supachart C., 2001, A review of absorption refrigeration technologies, Renew Sustain Energy Rev, **5(4)**, 343-72.

[11] Aphornratana S., Eames I.W., 1998, Experimental investigation of a combined ejector-absorption refrigerator. Int. J. of Energy Res, **22**, 195–207.

[12] Velazquez N., Best R., 2002, Methodology for the energy analysis of an air cooled GAX absorption heat pump operated by natural gas and solar energy, Appl. Therm. Engg, **22**, 1089 – 1103.

[13] Park C.W., Koo J., Kang Y.T., 2008, Performance analysis of ammonia absorption GAX cycle for combined cooling and hot water supply modes, Int. J. Refrigeration, **31**, 727 – 733.

[14] Gomez V.H., Vida A, Best R., Garcia O., Velazquez N., 2008, Theoretical and Experimental evaluation of an indirect – fired GAX cycle cooling system, Appl. Therm. Engg, **28**, 975 – 987.

[15] Kang Y.T., Kashiwagi T., 2000, An environmentally friendly GAX cycle for panel heating, PGAX cycle, Int. J. Refrigeration, **23**, 378-387.

[16] Garimella S., Christensen R.N., Lacy D., 1996, Performance evaluation of a generator-absorber heat-exchange heat pump, Appl. Therm. Engg, **16(7)**, 591-604.

[17] Sabir H.M., Chretienneau R., Elhag Y.B.M., 2004, Analytical study of a novel GAX-R heat driven refrigeration cycle, Appl. Therm. Engg, **24**, 2083-2099.

[18] Kumar R. A., Udayakumar M., 2007, Simulation studies on absorption compression cooler, Energy Convers. Manag, **48**, 2604-2610.

[19] Jawahar C.P., Saravanan R., 2011, Experimental studies on air-cooled $NH_3 - H_2O$ based modified GAX absorption cooling system, Int. J. Refrigeration. **34,** 658-666.

[20] Kaushik S.C., Arora A., 2009, Energy and exergy analysis of single effect and series flow double effect water-lithium bromide absorption refrigeration systems, Int. J. Refrigeration, **32(6),** 1247-1258.

[21] Gomri R., 2009, Second law comparison of single effect and double effect vapour absorption refrigeration systems, Energy Convers. Manag, **50,** 1279-87.

[22] Kumar R. A., Udayakumar M., 2008, Studies of compressor pressure ratio effect on GAX absorption compression cooler, Appl. Therm. Engg, **85(12)**, 1163-1172.

[23] Herold K.E., Radermacher R., Klein S.A., 1995, Absorption chillers and heat pumps, New York, CRC Press.

[24] Patek J., Klomfar J., 1995, Simple functions for fast calculations of selected thermodynamic properties of the ammonia-water system, Int. J. Refrigeration, **18(4),** 228-34.

[25] Klein S.A., Alvarado F., 2007, Engineering Equation Solver (EES). WI: F-chart software.